ΕΘΝΙΚΟ ΜΕΤΣΟΒΙΟ ΠΟΛΥΤΕΧΝΕΙΟ
ΣΧΟΛΗ ΗΛΕΚΤΡΟΛΟΓΩΝ ΜΗΧΑΝΙΚΩΝ ΚΑΙ ΜΗΧΑΝΙΚΩΝ ΥΠΟΛΟΓΙΣΤΩΝ
ΤΟΜΕΑΣ ΣΥΣΤΗΜΑΤΩΝ ΜΕΤΑΔΟΣΗΣ ΠΛΗΡΟΦΟΡΙΑΣ ΚΑΙ ΤΕΧΝΟΛΟΓΙΑΣ ΥΛΙΚΩΝ

Επίδραση των Συστημάτων Πολλαπλών Κεραιών στον Σχεδιασμό των Ασυρμάτων Δικτύων WiMAX

Impact of Advanced Antenna Technologies in Planning of WIMAX Access Networks

ΔΙΠΛΩΜΑΤΙΚΗ ΕΡΓΑΣΙΑ

Ελένη Θ. Καρασούλα

Επιβλέπων : Φίλιππος Κωνσταντίνου
Καθηγητής Ε.Μ.Π.

Αθήνα, Απρίλιος 2009

ΕΘΝΙΚΟ ΜΕΤΣΟΒΙΟ ΠΟΛΥΤΕΧΝΕΙΟ
ΣΧΟΛΗ ΗΛΕΚΤΡΟΛΟΓΩΝ ΜΗΧΑΝΙΚΩΝ ΚΑΙ ΜΗΧΑΝΙΚΩΝ ΥΠΟΛΟΓΙΣΤΩΝ
ΤΟΜΕΑΣ ΣΥΣΤΗΜΑΤΩΝ ΜΕΤΑΔΟΣΗΣ ΠΛΗΡΟΦΟΡΙΑΣ ΚΑΙ ΤΕΧΝΟΛΟΓΙΑΣ ΥΛΙΚΩΝ

Επίδραση των Ευφυών Κεραιών στον Σχεδιασμό των Ασυρμάτων Δικτύων WiMAX
Impact of Advanced Antenna Technologies in Planning of WIMAX Access Networks

ΔΙΠΛΩΜΑΤΙΚΗ ΕΡΓΑΣΙΑ

Ελένη Θ. Καρασούλα

Επιβλέπων :Φίλιππος Κωνσταντίνου
Καθηγητής Ε.Μ.Π

Εγκρίθηκε από την τριμελή εξεταστική επιτροπή την 30η Απριλίου 2009.

.....	.....	.....
Φ.Κωνσταντίνου	Γ. Φικιώρης	Α. Παναγόπουλος
Καθηγητής Ε.Μ.Π.	Καθηγητής Ε.Μ.Π.	Καθηγητής Ε.Μ.Π.

Αθήνα, Απρίλιος 2009

.....
Ελένη Θ. Καρασούλα

Διπλωματούχος Ηλεκτρολόγος Μηχανικός και Μηχανικός Υπολογιστών Ε.Μ.Π.

Περίληψη

Σκοπός της παρούσας διπλωματικής εργασίας είναι η μελέτη των πλεονεκτημάτων που εισάγονται από την χρήση των συστημάτων πολλαπλών κεραιών στα νεας γενιάς ασύρματα ευρυζωνικά δίκτυα όπως το WiMAX, το οποίο βασίζεται στο πρότυπο IEEE 802.16e. Βασικό αντικείμενο είναι ο συσχετισμός των βελτιωμένων επιδόσεων με τις διαδικασίες σχεδιασμού ραδιοδικτύων, καθώς αναμένεται ότι η αναθεώρηση των παραδοσιακών διαδικασιών θα κριθεί απαραίτητη.

Ο σχεδιασμός του ραδιοστρώματος των συστημάτων πολλαπλών κεραιών μπορεί να επιδράσει θετικά στο κέρδος και την χωρητικότητα του συστήματος. Το αυξημένο κέρδος, επιτρέπει την επίτευξη κυψελών με μεγαλύτερη ακτίνα κάλυψης, κάτι που επιτυγχάνεται με χρήση συστημάτων χωροκρονικών κωδικών ή συστημάτων ευφυϊών κεραιών. Σε αστικές περιοχές όπου η πυκνότητα των συνδρομητών είναι αυξημένη, με την μετάβαση σε χωρική πολυπλεξία είναι δυνατό να πολλαπλασιαστεί η χωρητικότητα του δικτύου. Η απόκλιση μεταξύ των αποτελεσμάτων των εργαστηριακών μελετών ή των προσομοιώσεων με τις επιδόσεις των πραγματικών δικτύων οφείλεται στην παρουσία παρεμβολών απο την χρήση κοινού ραδιοδιαύλου από πολλούς σταθμούς βάσης. Με την χρήση προηγμένου λογισμικού για τον σχεδιασμό των ραδιοδικτύων, είναι δυνατή η προσομοίωση της συμπεριφοράς ενός πραγματικού δικτύου ώστε να μελετηθούν με μεγαλύτερη ακρίβεια οι επιδόσεις των συστημάτων πολλαπλών κεραιών.

Κατα την ανάλυση που πραγματοποιήθηκε με το λογισμικό σχεδιασμου ραδιοδικτύων ICS Telecom nG, βρέθηκε οτι τα συστήματα MIMO χωροχρονικών κωδικών είναι σε θέση να επιτύχουν αυξημένη κάλυψη σε συνδιασμό με βελτιωμένη φασματική απόδοση. Τα συστήματα ευφυϊών κεραιών, τα οποία συγκεντρώνουν περισσότερα πλεονεκτήματα, παρουσιάζουν βελτιωμένες δυνατότητες κάλυψης ενώ συγχρόνως παρατηρήθηκε μεγιστοποιήση της φασματικής αποδοτικότητας.

Η παρούσα μελέτη είναι διαρθωμένη σε τρια μέρη: Στο πρώτο μέρος, παρουσιάζονται οι βασικές αρχές του προτύπου IEEE 802.16e με ιδιαίτερη έμφαση σε ό,τι αφορά τις τεχνικές και τους αλγορίθμους υλοποίησης συστημάτων πολλαπλών κεραιών. Στο δεύτερο μέρος, παρουσιάζονται τα οφέλη απο τη χρήσης των συστημάτων πολλαπλών κεραιών σύμφωνα με την υπάρχουσα βιβλιογραφία και με τις προδιαγραφές των προϊόντων που υπάρχουν στην αγορά. Ενω το τρίτο και τελευταίο μέρος της μελέτης εστιάζει στην προσωμοίωση των συστημάτων πολλαπλών κεραιών με την χρήση του λογισμικού σχεδιασμού ραδιοδικτυων ICS Telecom nG.

Λέξεις Κλειδιά

WiMAX, 802.16e, Συστήματα Πολλαπλών Κεραιών, AAS, MIMO, STBC, Beam-forming, Matrix-A, Matrix-B.

Abstract

The main scope of this study is to identify and quantify the advantages that emerge from the utilization of Advanced Antenna Systems (AAS) in next generation broadband wireless networks such as WiMAX based on IEEE 802.16e standard. The analysis of AAS techniques and algorithms is concentrated mainly on those included within the IEEE 802.16e standard. An important objective is to relate the performance enhancements by AAS with the RF planning procedures. It is expected that AAS will impose changes on the traditional RF planning methodologies, as the air-interface operational flexibility presented in WiMAX systems requires more detailed studies.

The RF configuration of AAS may provide benefits in system gain and/or system capacity. The higher system gain allows WiMAX cells to achieve greater operational ranges, and this can be achieved by using Beam-forming and MIMO Matrix-A technologies. In urban areas where the high subscriber density imposes higher cell capacities, AAS can switch to MIMO Matrix-B to ideally expand the cell capacity. A great differentiation between lab tests and simulations and the performance of real networks, is the appearance of co-channel interference due to frequency re-use. Through the use of advanced RF planning software the advantages and capabilities of AAS technologies are investigated through the perspective of a real network.

Based on the analysis performed with ICS Telecom nG RF planning software, Matrix-A systems, which benefit from high system gain and satisfactory interference rejection capabilities, are capable to achieve high coverage performance and at the same time improve the spectral efficiency of the network. Beam-forming systems, which are the most beneficial among the systems simulated, experience higher system gain resulting in extended coverage, while at the same time the spectral efficiency is maximized through the significant interference rejection during the traffic transmission.

The thesis is separated into three sections: In the first part, the basic technical characteristics of IEEE 802.16e standard are presented with emphasis on the AAS techniques and algorithms. The second part provides an analysis of the AAS performance based on bibliographical resources and product specifications. The analysis is focused on the enhancements in system gain, capacity and interference mitigation. The final part of this thesis focuses on the simulation of the AAS technologies with the ICS Telecom nG RF planning software.

Keywords

WiMAX, 802.16e, MIMO, AAS, Beam-forming, STBC, Matrix-A, Matrix-B.

Table of Contents:

Index of Tables:

Index of Figures:

List of Abbreviations:

AAS	Advanced Antenna Systems
AGL	Above Ground Level
AMC	Adaptive Modulation and Coding
AMS	Adaptive MIMO Switch
BAA	Beam-forming Antenna Arrays
BE	Best Effort
BF	Beam-Forming
BLAST	Bell Labs layered Space/Time
BS	Base Station
CDD	Cyclic Delay Diversity
CPE	Customer Premises Equipment
CSI	Channel State Information
DL	Downlink
DSTTD	Double Space Time Transmit Diversity
EGC	Equal Gain Combining
EIRP	Equivalent Isotropic Radiated Power
FCH	Frame Control Header
FDD	Frequency Division Duplexing
FFT	Fast Fourier Transform
H-ARQ	Hybrid Automatic Repeat Request
IC	Interference Canceller
ISI	Inter Symbol Interference
LDPC	Low Density Parity Check
MCS	Modulation and Coding Scheme
MIMO	Multiple Input Multiple Output
MISO	Multiple Input Single Output
MRC	Maximal Ratio Combining
OC	Optimal Combiner
OFDM	Orthogonal Frequency Division Multiplexing
OFDMA	Orthogonal Frequency Division Multiple Access
OSTBC	Orthogonal Space Time Block Codes
PAA	Phased Antenna Arrays
PCG	Power Combining Gain
PL	Path-Loss
PUSC	Partial Usage of Sub-Carriers
QoS	Quality of Service
SAA	Switched Antenna Arrays
SIMO	Single Input Multiple Output

SINR	Signal to Interference plus Noise Ratio
SISO	Single Input Single Output
SNR	Signal to Noise Ratio
STBC	Space Time Block Codes
STC	Space Time Codes
STCG	Space Time Coding Gain
STTC	Space Time Trellis Codes
TDD	Time Division Duplexing
TS	Terminal Station
UL	Uplink
WD	Waveform Diversity
WiMAX	Worldwide Interoperability for Microwave Access

1. Worldwide Interoperability for Microwave Access

Worldwide Interoperability for Microwave Access (WiMAX) is the acronym for Institute of Electrical and Electronics Engineers (IEEE) 802.16 set of standards governing Air Interface for Fixed Broadband Wireless Access Systems. In the history of wireless systems, WiMAX is revolutionary technology as affords its users the Wi-Fi grade throughput and cellular system level of mobility. With WiMAX, broadband technology (traditionally ADSL and Fiber) goes wireless and WiMAX users can basically enjoy triple-play application, and split-second download and upload rates.

For the operator, WiMAX is a welcome development because it merges traditional cellular networks with broadband technology thus opening them to more business offerings and a larger client base and all this at a reduced cost of deployment.

WiMAX supports fixed, nomadic, portable and mobile access. To meet the requirements of different types of access, two version of WiMAX have been defined. The first is based on IEEE 802.16-2004, also known as Revision D, is optimized for fixed and nomadic access. The second version is designed to support portability and mobility and is based on the IEEE 802.16e amendment to the standard.

In the course of this literature, the term WiMAX and 802.16e will be used interchangeably, where a distinction is to be made between the 802.16 standards, the appropriate numbering will be applied.

Features of 802.16e

WiMAX is a wireless broadband solution that offers a rich set of features with a lot of flexibility in terms of deployment options and potential service offerings. Some of the more salient features that deserve highlighting are as follows:

- *OFDMA*; facilitates the exploitation of frequency diversity and multi-user diversity to offer multiple access and significantly improve the system capacity. It allows user devices to transmit only through the sub-channels allocated to them, thus offers the capability of minimizing the effect of interference on user devices with omni-directional elements. The method for allocating sub-channels to the users is named Sub-channelization, [2][5][8].

- *Scalable and high data rates*; in OFDMA mode the fast Fourier transform (FFT) size may be scalable based on the available channel bandwidth. OFDMA combined with Adaptive Modulation and Coding (AMC) enables users to be apportioned spectrum based on bandwidth/data rate requirement, [8].

- *Sub-channelization gain*, when only one sub-channel is allocated to a device, all the transmit power will be concentrated in only one of the available sub-channels, [3][7][8].

- *Greater flexibility in managing spectrum resources*. Sub-channelization also offers the ability to use network intelligence to allocate resources to user devices as needed, as more sub-channels will be allocated to users that need more resources, [6][7].

- *Support for mobility*, 802.16e products are optimized for mobility and support handoffs, power-saving and sleep modes which extend the battery life of mobile user devices. Physical-layer enhancements, such as more frequent channel estimation, uplink sub-channelization, and power control, are also specified in support of mobile applications, [6].

- Both *fix and mobile users* accommodation,[6].

- *Support of Advanced Antenna Techniques (AAS)*,[2].

- *Better indoor coverage* achieved through sub-channelization and AAS option benefits both fixed and mobile applications with higher EIRP levels,[6].

- *Link layer retransmission*, using Hybrid Automatic Repeat Request (H-ARQ),[3].

- Supports both *time division duplexing (TDD) and frequency division duplexing (FDD)* including variable DL/UL ratios,[2] [11].

- Embedded *Quality of Service (QoS)* scheduling, [3].

WiMAX PHY Layer

The 802.16-2004 physical layer is based on orthogonal frequency division multiplexing (OFDM), which is a multi-carrier modulation transmission scheme that enables high-speed data, video, and multimedia communications,[1]. OFDM is based on the idea of dividing a high-bit-rate data stream into several lower bit-rate streams and modulation each stream on separate carrier (sub-carriers). By making the symbol time duration enough in means of delay spread minimization, OFDM eliminates or minimizes inter-symbol interference (ISI). Moreover the sub-carriers are selected in a way that they are all orthogonal to one another of the symbol duration, thus avoiding the need of inter-carrier interference elimination through selection of non-overlapping sub-carriers. Moreover, in order to completely avoid ISI, guard intervals are used between OFDM symbols, which are larger than the multi-path delay spread, on the cost of power and bandwidth wastage. The number of sub-carriers that are available in a symbol depends on the FFT size. For OFDM-PHY the FFT size is fixed at 256, where 192 sub-carriers are carrying data, 8 are pilot sub-carrier for channel estimation and synchronization purposes and the rest are guard band sub-carriers. Since the number of sub-carriers is fixed, the sub-carrier spacing varies with the channel bandwidth. When larger bandwidths are used, the sub-carrier spacing increases and the symbol time decreases; as a result larger guard time allocation is needed in order to overcome delay spread

As mentioned before, in 802.16e orthogonal frequency division multiple access (OFDMA) is used, where the FFT size is scalable from 128 to 2048,[2],[6]. In contrast to OFDM where the FFT size is fix for any channel bandwidth, in OFDMA the FFT size increases when the available bandwidth increases. This keeps the OFDM symbol duration fixed, while the sub-carrier spacing of 10.94 KHz that is chosen, offers a good balance between delay spread and Doppler spread requirements in mixed fixed and mobile users accommodation.

The available sub-carriers are divided into groups of sub-carriers called sub-channels, [3]. The number of sub-channels depends on the FFT size. Combinations of 1, 2, 4, 8,… or all sub-carriers can be allocated to a user in both downlink (DL) and uplink (UL) direction in OFDMA-PHY. UL sub-channelization allows user device to transmit using only a fraction of the bandwidth allocated to it by the base station (BS), which provide link budget improvement that can be used to enhance range performance and/or improve battery life of the mobile user devices. The sub-channels may be constituted either by contiguous sub-carriers or by pseudo-randomly distributed sub-carriers across the frequency spectrum. The second way of sub-carrier allocation provides more frequency diversity, which is particularly useful in mobile applications. The number and the exact distribution of the sub-carriers that constitute a sub-channel depend on the sub-carrier permutation scheme.

The WiMAX PHY layer is also responsible for slot allocation and framing over the air, [2]. The minimum time-frequency resource that can be allocated by a WiMAX system to a given link is called a slot. Each slot consists of one sub-channel over one, two or three OFDM symbols depending on the sub-channelization scheme used.

One sub-channelization scheme that is based on distributed sub-carriers is called partial usage of sub-carriers (PUSC) and is mandatory for all 802.16e implementations in both directions (DL and UL),[2].

In DL PUSC permutation scheme all the sub-carriers are first divided into clusters which consist of 14 adjacent sub-carriers over two symbols. In each cluster, 24 sub-carriers are assigned for data transmission and the remaining 4 are pilot sub-carriers as it presented in Figure 1. The clusters are then renumbered using a pseudorandom numbering scheme. Following the renumbering of the clusters, the clusters are divided into six groups, with the first one-sixth of the clusters belonging to group 0, the second to group 1 and so on as it can be seen in Figure 2. A sub-channel is created by using two clusters from the same group. Thus in DL PUSC the slot consists of 2 clusters in other words 56 sub-carriers where 48 of them are used for data transmission and 8 are pilot sub-carriers. [3]

In UL PUSC permutation scheme, the sub-carriers are first divided into various tiles. Each tile consists of 4 sub-carriers over 3 symbols as it is presented in Figure 3. The sub-carriers within a tile are divided into 8 data sub-carriers and 4 pilot sub-carriers. The tiles are then renumbered, using a pseudorandom numbering sequence and divided into six groups. Each sub-channel is created using six tiles from a single group. Consequently, the minimum allocation for UL PUSC is a sub-channel that consists of 3 tiles over 2 symbols or in other words 72 sub-subcarriers where 48 are assigned for data transmission and 24 are pilot subcarriers. [3]

It should be noted that the number of sub-channels and groups shown in Figure 1 to Figure 4 refer to 5 MHz channel. In a 10 MHz channel these numbers are doubled resulting in 12 groups for DL PUSC and in 30 sub-channels of UL PUSC. Moreover, the constitution of 15 sub-channels in UL PUSC results in 360 used sub-carriers for the 5 MHz channel, the remaining 60 sub-carriers are used for signaling.

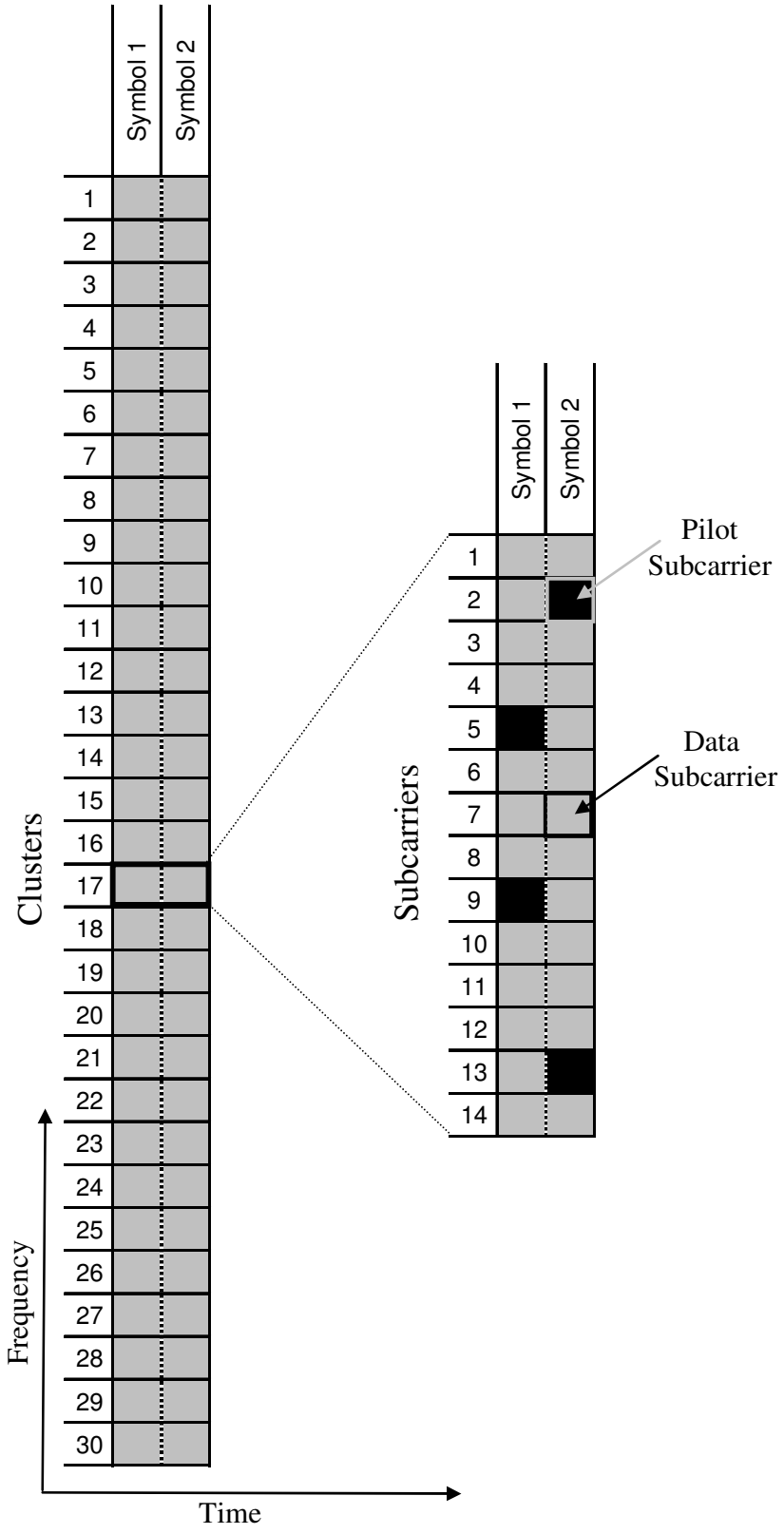

Figure 1: PUSC – Clusters and Sub-carriers

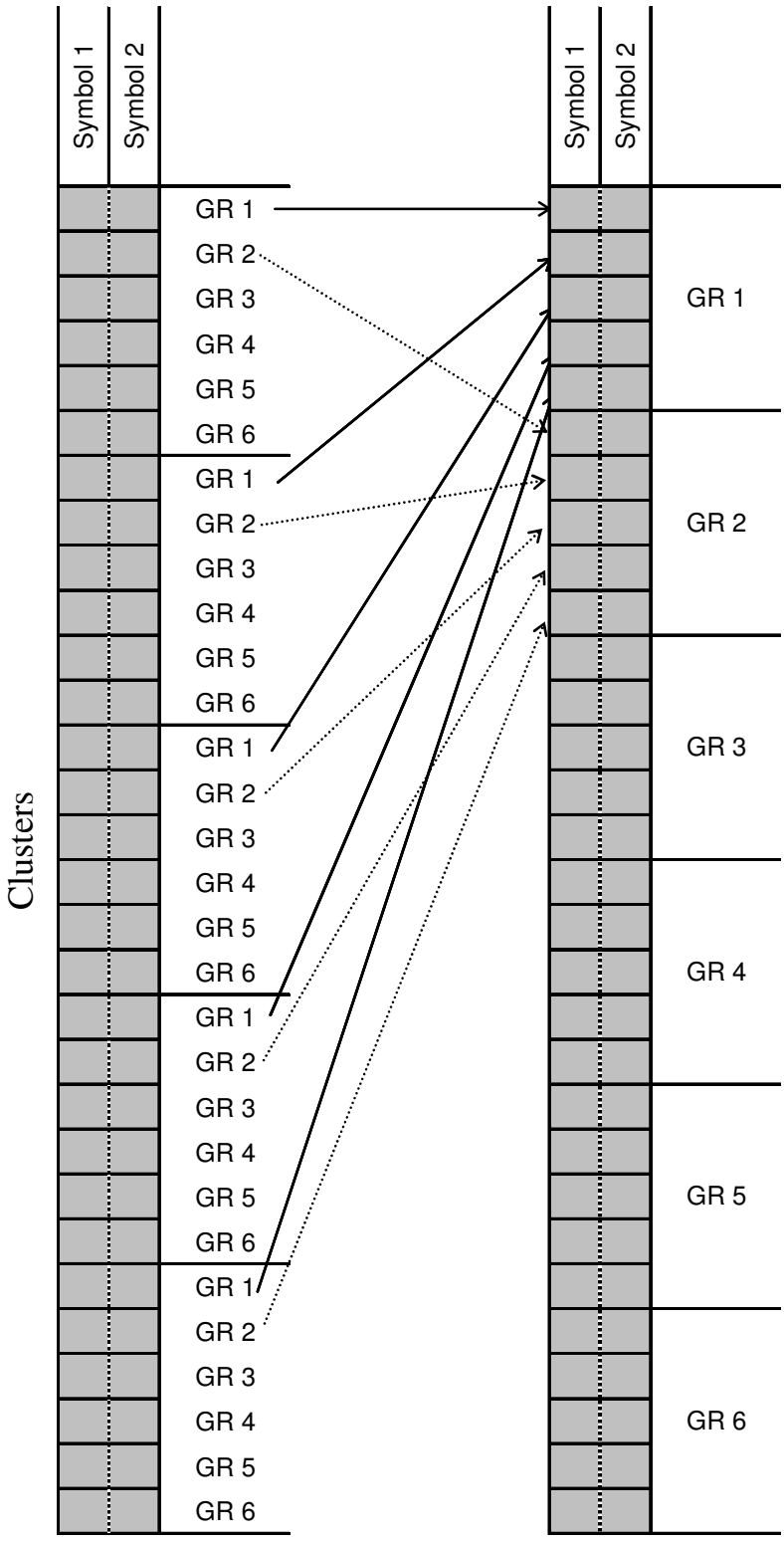

Figure 2: DL PUSC – Clusters Grouping in GR1-GR6

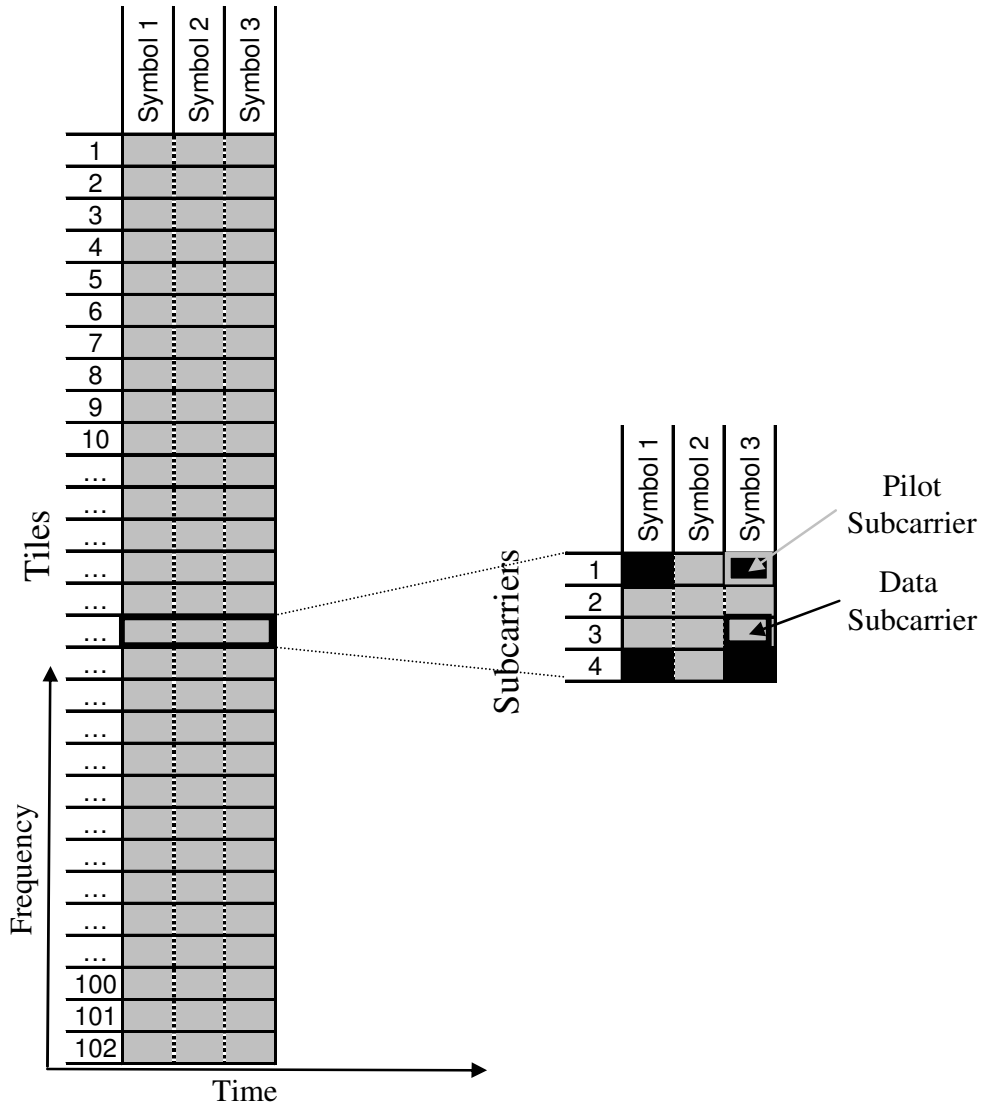

Figure 3: UL PUSC – Tiles and Sub-carriers

.

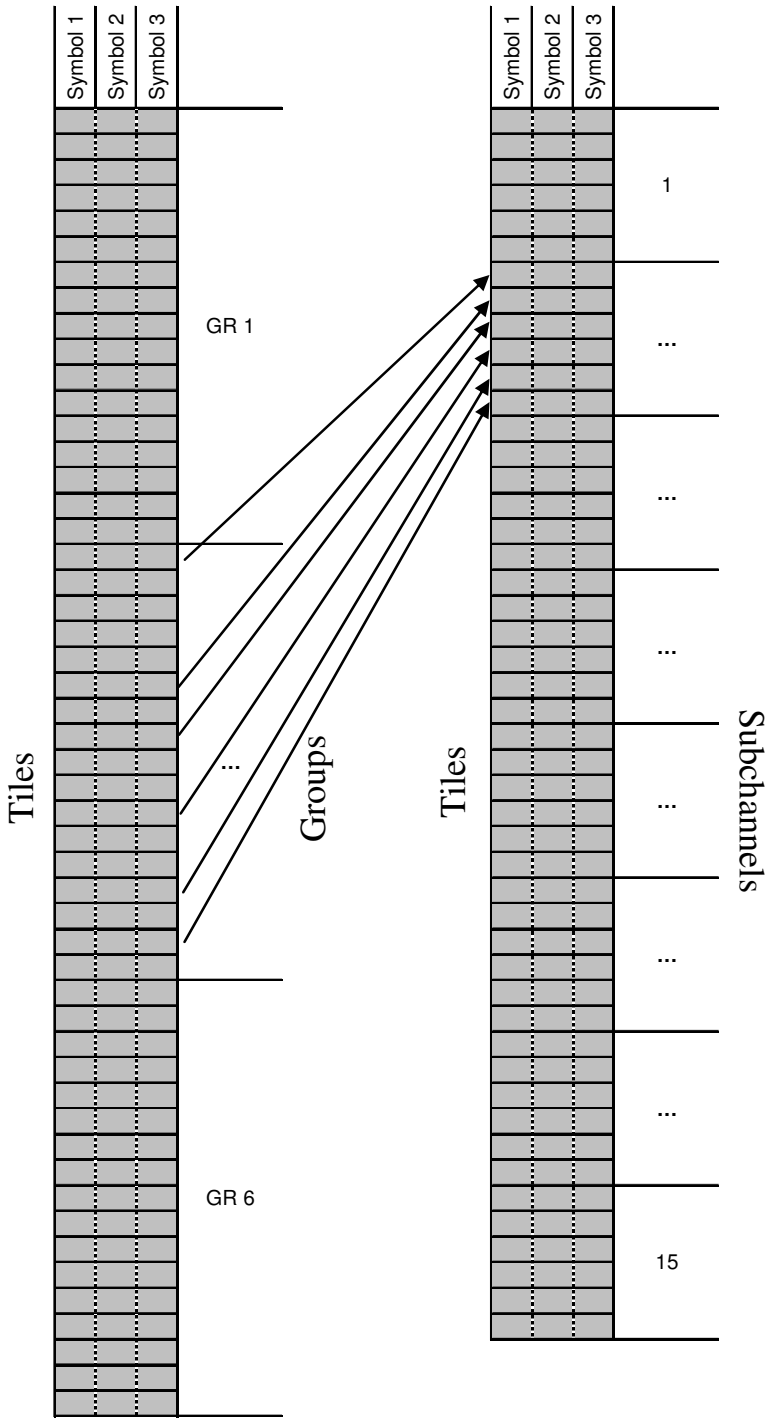

Figure 4: UL PUSC – Tiles Grouping

When PUSC permutation scheme is applied, it is possible to allocate either all or only a subset of the six groups in the DL direction. By allocating disjoint subsets of the six available groups to collocated BSs; it is possible to separate their signals in the sub-carrier space. Consequently i.e. in a three sector BS, all the sectors can use the same RF channel, while maintaining their orthogoniality among sub-carriers, thus enabling a tighter frequency reuse at the cost of data rate. The usage of a subset of the available groups is referred to as segmentation. [3]

Regarding the OFDMA frame, both TDD and FDD mode are available, [11]. Most WiMAX deployments are likely to be in TDD mode because it allows a more flexible sharing of bandwidth between DL and UL, it doesn't require paired spectrum and it offers a reciprocal channel that can be exploited for spatial processing in addition to a simpler transceiver design. In TDD mode the frame is divided into two sub-frames, the DL and the UL sub-frame. The DL/UL sub-frame ratio may vary in order to support different traffic profiles. In FDD format the frame structure is the same except from the fact that DL and UL are transmitted simultaneously over different channels.

The downlink sub-frame begins with a downlink preamble that is used for PHY layer procedures, such as time and frequency synchronization and initial channel estimation. The downlink preamble is followed by a frame control header (FCH), which provides the frame configuration information, such as the MAP message length, the modulation and coding scheme and the usable sub-carriers. Multiple users are allocated data regions within the frame, and these allocations are specified in the uplink and downlink MAP messages (DL-MAP and UL-MAP) that are broadcasted following the FCH in the downlink sub-frame. MAP contains critical information that needs to reach all users, for that reason it is sent over a very reliable link (BPSK ½). The MAP messages import a significant overhead, thus reduce the available bandwidth of the frame. In 802.16e the system can optionally use multiple sub-MAP messages where the dedicated control messages to different users are transmitted at higher rates, based on their individual SINR conditions, or they may also optionally be compressed for additional efficiency.[2]

In Figure 5 the frame structure of 802.16e is presented. As it can be seen one symbol of the DL sub-frame is allocated to the preamble, while the FCH and DL/UL MAP are transmitted over two symbols, this number may vary with the number of users served by the BS, thus the representation in Figure 5 is indicative.

Moreover there is the option that the DL and UL sub-frame is transmitted with repetition. The available repetition schemes are 2x, 4x and 6x where the channel is transmitted 2, 4 or 6 times respectively, wasting more symbols of each sub-frame. This technique offers robustness to these channels but on the other hand the wastage of symbols results in lower available bandwidth for data transmition.

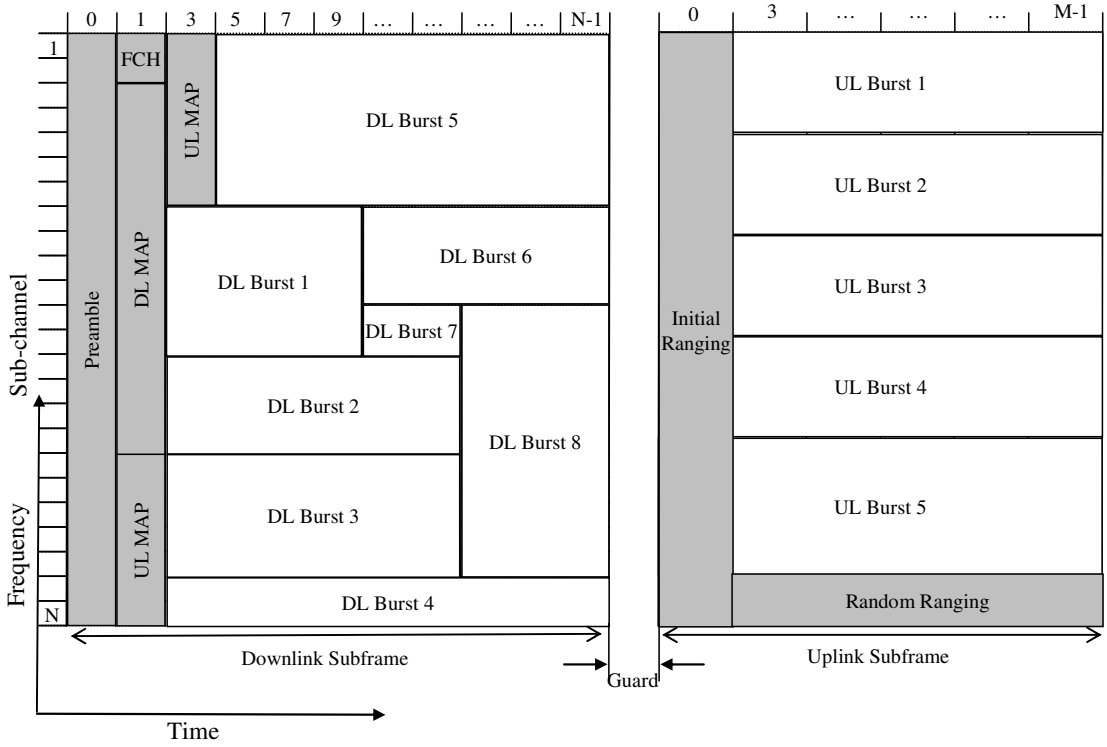

Figure 5: Frame Structure

The DL sub-frame may contain multiple bursts of varying size and type carrying data for several users, while the UL sub-frame is made up of several UL bursts from different user. Three classes of bursts can be transmitted in the UL sub-frame. The first one refers to transmission for performing closed-loop frequency, time and power adjustments which compose the Initial Ranging channel. The second class refers to those that are transmitted in contention opportunities defined by Request Intervals reserved for response to multicast and broadcast polls – Random Ranging. This channel may also be used by the user device for best effort (BE) data transmission, particularly when the amount of data to send is too small to justify requesting a dedicated channel. The third class contains the UL data bursts that are transmitted according to the UL MAP information provided to each terminal station (TS) in the DL sub-frame. [2]

There are 6 possible modulation and coding combinations which are supported by WiMAX, that allow the scheme to change on a burst-by-burst basis per link depending on the channel condition, an information that is provided by the ranging channels for the DL direction and by the received signal strength for the UL. Based on this information the scheduler assigns a modulation and coding scheme (MCS) that maximizes the throughput for the available signal-to-noise-and-interference ratio. In specific the modulation schemes are QPSK with coding scheme ½ or ¾, 16 QAM with coding scheme ½ or ¾ and 64 QAM with coding scheme 2/3 or ¾; the SINR thresholds for each combination of modulation and coding rate are shown in Table 1 . [2]

Table 1: 802.16e SINR Thresholds

MCS	SINR Threshold
QPSK-1/2	4
QPSK-3/4	6.8
16 QAM-1/2	10
16 QAM-3/4	13
64 QAM-2/3	17.8
64 QAM-3/4	19

.

In order to estimate the receiver sensitivity threshold, the noise floor of the system shall be calculated first. The noise floor for a WiMAX system is:

$$N = -174 + 10 * \log(BW * F_s * C_{used} / C_{total}) + NF$$

, where BW is the channel bandwidth in Hz, F_s is the over-sampling rate, C_{used} are the sum of the pilot and data sub-carriers, or in other words the number of the powered sub-carriers and C_{total} and NF is the noise figure of the receiver [9]. The over-sampling rate, as well as the number of sub-carriers (used and total) depend on the channel bandwidth as shown in Table 2, [3]

Table 2: 802.16e OFDMA Mode Parameters

Parameter	Channel Bandwidth	
	5 MHz	10 MHz
FFT Size/Total Subcarriers	512	1024
Data Subcarriers	360	720
Pilot Subcarriers	60	120
Oversampling Rate	28/25	28/25

The receiver sensitivity threshold per MSC arises by adding the thresholds shown in Table 1 to the noise floor of the system. It should be noted that when repetition is applied to the system (i.e. DL/UL Map channel) an additional component is added to the receiver sensitivity threshold estimation, which is equal to $10 * \log(R)$ where R is the repetition coding rate. [9]

The WiMAX receivers have specific interference rejection capabilities, [2]. According to the standard, the receiver is able to achieve a 10^{-6} BER performance when for an interferer at the first adjacent channel, the C/I ratio is equal or lower than -4 dB while the received signal of the wanted signal (C) is 3 dB higher than the receiver sensitivity threshold for 64 QAM ¾. The corresponding C/I ratio for the 2nd adjacent channel is -23 dB. Consequently, if it is taken into account that the 64 QAM ¾ threshold is 22 dB (3 dB higher than the threshold in Table 1) the WiMAX receiver is able to reduce the power of a possible interferer in the 1st adjacent channel by 26 dB and for an interferer in the 2nd adjacent channel by 45 dB.

The total available symbols for traffic have to be estimated in order to estimate the throughput that a BS can provide in a second per modulation and coding scheme. For a frame duration of 5 msec, given the fact that the symbol duration is 102.86 μsec there are 48 symbols in a frame. For a guard band of 1/16 the final numbers of symbols that are available for signaling and traffic are 45. In the DL sub-frame 1 symbol is used for the Preamble transmission while the FCH and DL/UL MAP use totally 2 slots in each frame. Moreover, 3 symbols are used for the transmission of the initial ranging channel, resulting in 37 available symbols for the DL and UL Traffic sub-frame. The symbol assignment for the 802.16e is summarized in Table 3.

Table 3: Symbol Assignment in 802.16e

802.16e	
Frame duration (msec)	5
Symbol duration (usec)	102.86
Available Symbols	48
Guard Band	1/16
Useful Symbols	45
Preamble Symbols	1
FCH and DL/UL MAP Symbols	2
Initial Ranging Symbols	3
Available Traffic Symbols	38

As mentioned above, the minimum allocation for the DL traffic is a slot, consisting of 2 clusters. Each cluster consists of 14 sub-carriers over 2 symbols. The total available sub-carriers for a 5MHz channel (512 FFT) are 420 subcarriers in each symbol, as long as 14 of them are assigned for each cluster in one symbol duration, there are 30 clusters available. For the UL Traffic 15 sub-channels are constructed that are available for traffic transmission.

As long as the transmission of one cluster in the DL PUSC needs 2 symbols and the transmission of on sub-channel in the UL PUSC 3 symbols, the DL/UL Ratio has to be selected in a way that the available symbols for each sub-frame will be multiples of 2 and 3 for the DL and UL Traffic. Given the 38 available symbols for a guard band of 1/16, for a DL/UL Ratio of 60/40, the resulting available symbols are 22 for the DL Traffic and 15 for the UL Traffic.

The 30 clusters that are available in the DL in 2 symbols duration, compose 15 DL slots. Given the fact that there are 22 symbols available for the DL traffic, totally 22/2*15=165 DL Traffic slots can be constructed in one frame. The 15 sub-channels in the UL use 3 symbols. Given the 15 available symbols for the UL Traffic 15/3*15=75 UL sub-channels are constructed in one frame.

The number of subcarriers that can be carried by one DL slot and on UL sub-channel is 48, resulting in 165*48=7920 available data sub-carriers for the DL traffic and 48*75=3600 available data subcarriers for the UL traffic in one frame.

In the duration of one second 200 frames can be transmitted given the duration of each frame as equal to 5msec. Consequently there are 7920*200=1584000 and 3600*200=720000 available data subcarriers per second for DL and UL traffic respectively.

Finally in order to estimate the total traffic that a BS is able to carry per second, the number of bits (N_{MCS}) that can be carried by one subcarrier has to be calculated. This number depends on the modulation and coding scheme (MCS). For each modulation (QPSK, 16 QAM and 64 QAM) the number of bits (N_M) is constant: a QPSK modulated sub-carrier can carry 2 bits ($N_{QPSK} = 2$ bits), a 16 QAM modulated can carry 4 bits ($N_{16QAM} = 4$ bits), and a 64 QAM can carry 6 bits ($N_{64QAM} = 6$ bits). In order to estimate the N_{MCS}, the N_M for each modulation is multiplied by the coding scheme (C), i.e. for QPSK ½, C is equal to ½. The resulting bits per MCS that a single sub-carrier can carry are presented in Table 4.

Table 4: Bits/sub-carrier per MCS

MCS	bits / sub-carrier
QPSK 1/2	1
QPSK 3/4	1.5
16QAM 1/2	2
16QAM 3/4	3
64QAM 2/3	4
64QAM 3/4	4.5

By multiplying the resulting total data subcarriers per second in the DL and UL, the total throughput per MCS of a BS can be estimated. The resulting throughput is presented in Table 5.

Table 5: TDD Ethernet Throughput per Modulation in 802.16e for 5 MHz Channel Bandwidth.

MCS	Data Rates (Mbps)	
	Downlink	Uplink
QPSK 1/2	1.584	0.72
QPSK 3/4	2.376	1.08
16QAM 1/2	3.168	1.44
16QAM 3/4	4.752	2.16
64QAM 2/3	6.336	2.88
64QAM 3/4	7.128	3.24

In WiMAX the symbol duration remains stable with the bandwidth, consequently when the FFT sizes is doubled, data and pilot sub-carriers are also doubled, resulting in double data rates for the same DL/UL ratio and guard band duration.

2.Advanced Antenna Systems

The continuously growing number of subscribers in addition to the fact that new high bandwidth services (VoIP, Video Streaming) entered the market pushed the evolution of the broadband wireless access. This evolution is strongly related to the development of Advanced Antenna Systems (AAS), which are able to offer better performance to the network in terms of coverage and capacity. The term AAS is referred to the techniques where more than one antenna elements are combined in arrays of different geometries at one or both ends of the communication link. Those arrays of antenna elements are able to transmit and receive at the same time. The increased performance of the system is obtained due to the algorithms that have been developed in order to be applied to the received and/or the transmitted signals of multiple receive and/or transmit antennas. Those techniques are able to achieve higher signal-to-noise-ratio and increase system capacity. Research on AAS gave last years several different solutions that can either stand alone or collaborate and give even better results to meet the demands of the modern system networks such as the Worldwide Interoperability for Microwave Access (WIMAX). The purpose of this chapter is to introduce the theoretical base of the schemes and the algorithms that are used in AAS.

AAS Technologies

One of the greatest challenges to traditional wireless systems has been managing multi-path fading environments, where signal degradation is caused due to obstacles between the transmitter and the receiver. With multi-antenna implementation the antenna system is able to benefit from multi-path propagation and offer robustness to the communication channel. This is the basic idea of all the AAS techniques that have been investigated.

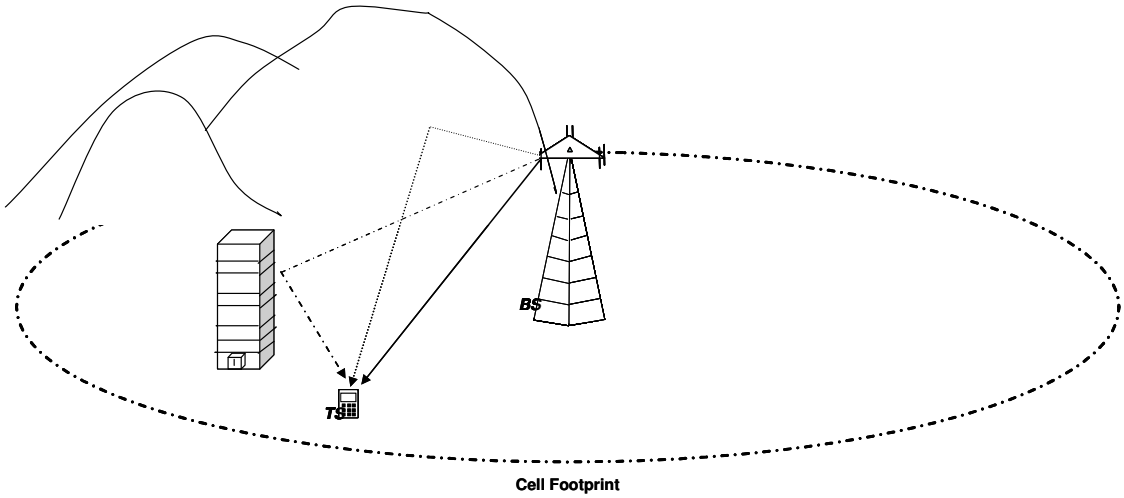

Figure 6: The signal of the user's antenna experiences multi-path propagation due to obstacles over the propagation direction between the user and the BS (BS).

In this paragraph a general overview of transmit and receive diversity, beam-forming and spatial multiplexing techniques will be introduced. Additionally the algorithms that have been developed for AAS will be presented, with a more extended reference to the algorithms that have been developed on the scope of WiMAX.

Diversity Schemes

Antenna diversity, or spatial diversity, can be obtained by placing multiple directional antenna elements at the transmitter and/or the receiver. If the antennas are placed sufficiently far apart, copies of the same signal are transmitted and/or received through channels with different characteristics. Each different channel is called diversity branch; even if some channels experience deep fades there will be at least one that will be received with a high signal-to-noise-ratio by the receiver antenna/antennas. In other words one branch may fail, but it is very unlikely that all branches will fail simultaneously. The basic idea of multiple-input-multiple-output (MIMO) antenna systems relies on diversity, which has been proved to be the best technique for overcoming multi-path fading in a wireless channel. [10]

In the case of a single-input-single-output (SISO) system, higher transmit power would be necessary in order to ensure the link margins and increase the reliability of the system. The same improvement could be achieved by implementing more antenna elements either at the transmitter or/and at the receiver without the negative effects that follow the increase of the transmit power.

Receive Diversity

Diversity in the receiver is the most predominant spatial diversity form to be implemented in AAS, also referred to as single-input-multiple output (SIMO) when no diversity is presented at the transmitter. The receive diversity scheme that is most often appointed is a two receive antenna elements scheme. An 1 x 2 and an 1 x N SIMO system are depicted in Figure 7.

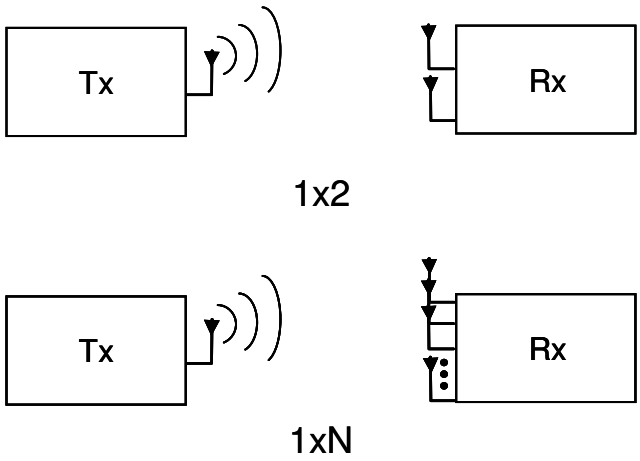

Figure 7: Receive Diversity

The N antenna elements of the receiver are turned on simultaneously the whole period of the downlink sub-frame and depending on the algorithm that is applied to the system, the N received signals are processed according to the procedure that is followed by the corresponding algorithm.[10]

Receive diversity places no particular requirements on the transmitter of a SIMO system but requires a receiver that processes the N signals that are received from its N different diversity branches.

Transmit Diversity

Receive diversity becomes unsuitable in deployments, such as mobile TS in the downlink direction. In such deployments the limiting factors are power consumption, size and also cost of multiple antenna deployments that would make the mobile terminals too expensive for the users and depending on the case due to the size of the terminals, it would be proved uncomfortable to carry them. On the other hand, implementation of antenna arrays at the BS doesn't raise such points. At the same time, in case the multiple antenna arrays are already implemented for receive diversity in the BS (BS) it is much more cost effective to use the same array for transmit diversity.

On this scope the other case of spatial diversity has been developed, known as transmit diversity. A two system with diversity only at the transmitter, multiple-input-single-output (MISO) system, are presented in Figure 8, the first one is a 2x1 system while the second a Nx1 as N antenna elements are implemented on the transmitter. The transmission of the signal operates in the following way: The same symbol is transmitted over the N different antenna elements, resulting in N different paths, [10]. The way those N paths are utilized in order to achieve higher performance depends on the signal processing that takes place at the transmitter. Consequently transmit diversity requires a signal process at the transmitter. There have been developed several algorithms on this scope but the most famous of them cause of implementation and diversity and capacity gains is the algorithm proposed of Alamouti. The most prevalent in WiMAX will be presented in following paragraph.

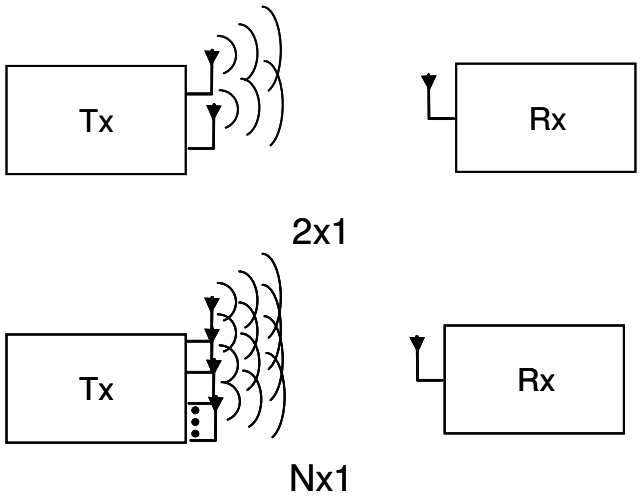

Figure 8: Transmit Diversity

Receive and Transmit Diversity

The combination of receive and transmit diversity results into a system with multiple antennas at both ends of the communication channel, a multiple-input-multiple-output (MIMO) system. A MIMO system combines the benefits of receive and transmit diversity and requires signal processing at both the received and transmitted signals.

Beam-forming Antenna Arrays

Main objective of this technique is to increase the antenna gain at the desired direction and simultaneously minimize it at the direction of un-desired terminal that acts as interferers; consequently the system performance is enhanced in means of coverage and interference mitigation at the same time. In other words, beam-forming acts as a spatial filter,[12][14]. This is obtained by using an array of antenna elements, fed with same signal at different time instances or provided with phase shifts.

In transmit diversity that has been introduced above, the N directional antenna elements are used in order to increase the total power of the system. In beam-forming instead, N omni-directional antenna elements are combined in order to simulate a directional antenna and steer its main lobe toward a particular direction. The formation of the antenna pattern depends on the antenna array geometry in means of beam-width and feeding amplitudes in means of direction, [13].

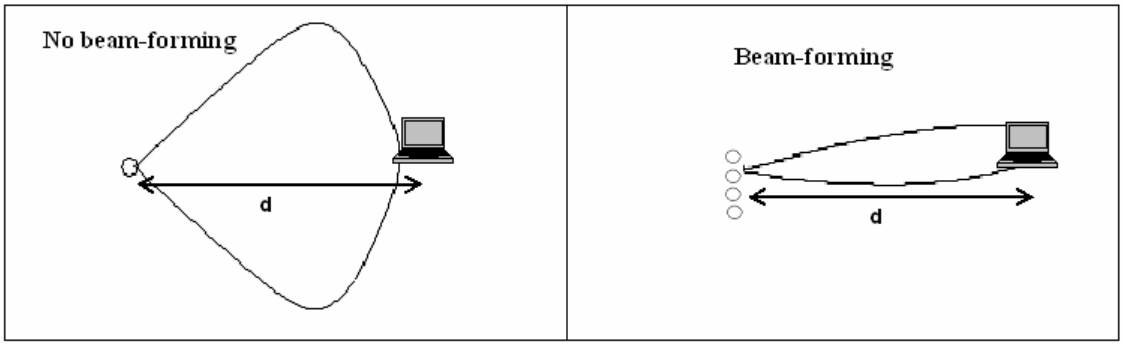

Figure 9: Sectoral Antenna Pattern without Beam-forming (a), 4- Elements Beam-forming Antenna Array (b).

Antenna Array Geometry

As stated before, the main objective of a beam-forming array is to form a narrow 3dB beam-width antenna pattern in order to point the radiation energy in one particular direction, and on the same time minimize it toward the direction of each possible interferer. The synthesis of the antenna pattern is highly dependent on the displacement, the number and the spacing between the antenna elements. The main phased and beam-forming array configurations, identified as Linear, Planar and Circular depending on the disposition of the antenna elements, are presented in Figure 10, [15].

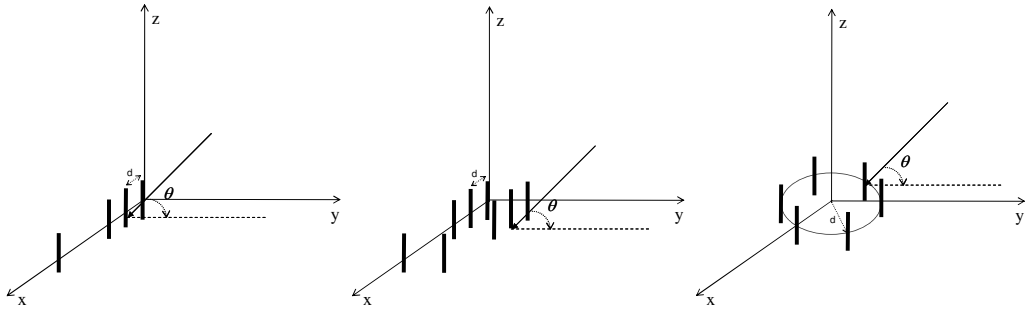

(a) (b) (c)

Figure 10: (a) Linear Array (b) Planar Array (c) Circular Array

The most basic property of an antenna array is that relative displacement of the antenna elements introduces relative space shifts in the radiation vectors, which can then add constructively in some directions or destructively in others, [13].

Considering, an array of several identical antennas as shown in Figure 11, where elements are located at positions $\vec{x}_0$, $\vec{x}_1$, $\vec{x}_2$,…, and the relative feed coefficients for each element are a_0, a_1, a_2,…, the corresponding radiation vector of the current for the nth element will be:

$$\vec{F}_n(\vec{k}) = a_n * e^{j\vec{k}\vec{d}_n} * \vec{F}(\vec{k})$$

,where $\vec{F}(\vec{k})$ is the three-dimensional Fourier transform of the current density $\vec{F}(\vec{k}) = \int e^{jkr'} * \vec{J}(r')d^3r'$. It can be observed that the factor $\vec{F}(\vec{k})$ will be common for all the elements of the array. So the total radiation vector of the array can be written:

$$\vec{F}_{tot}(\vec{k}) = (a_0 * e^{j\vec{k}\vec{d}_0} + a_1 * e^{j\vec{k}\vec{d}_1} + ... + a_n * e^{j\vec{k}\vec{d}_n}) * \vec{F}(\vec{k}) = \vec{A}(\vec{k}) * \vec{F}(\vec{k})$$

, where $\vec{A}(\vec{k})$ is identified as the Array Factor of the array.

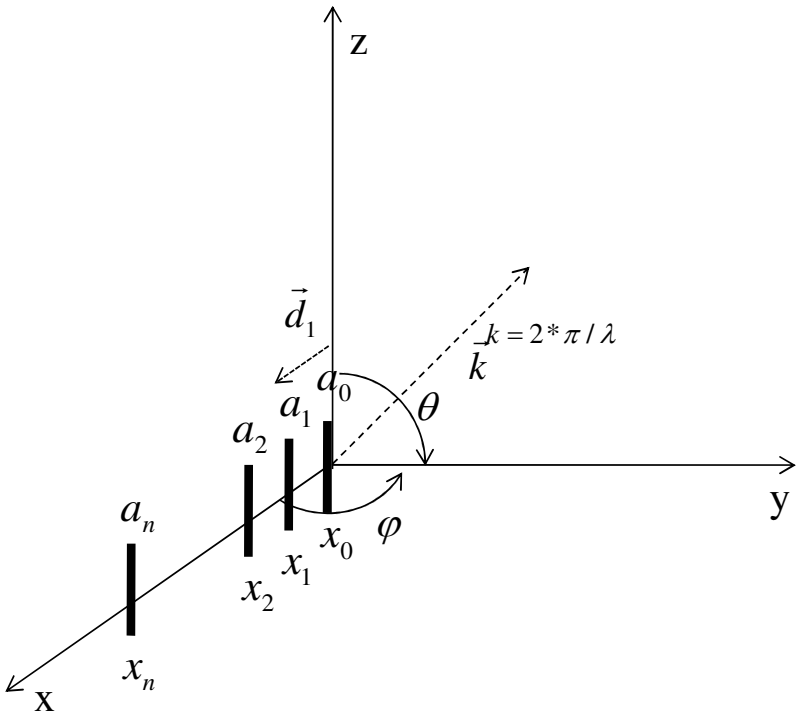

$$\vec{d}_n = x_n \hat{x} \qquad \vec{k} = k\hat{r} = k \sin\theta \cos\varphi \qquad k = 2*\pi / \lambda$$

Figure 11: Uniform Linear Antenna Array.

The total power gain is given by the equation:

$$G_{tot}(\vec{k}) = G_{tot}(\theta,\varphi) = \left|A(\theta,\varphi)\right|^2 G(\theta,\varphi)$$

, where $G(\theta,\phi)$ is the power gain of a single element.

As long as the all the antenna elements deployed on the array are omni-directional antennas with the same antenna gain, the gain $G(\theta,\phi)$ is equal toward each direction. In Figure 12 the antenna patterns, normalized to $G(90^o,\phi)$, for linear antenna arrays with different number of omni-directional elements N and spacing d are presented. It should be noted that the elements of this array are fed with equal relative amplitudes (equal weights). When the weights of an array are common for all the elements the array is identified as uniform.

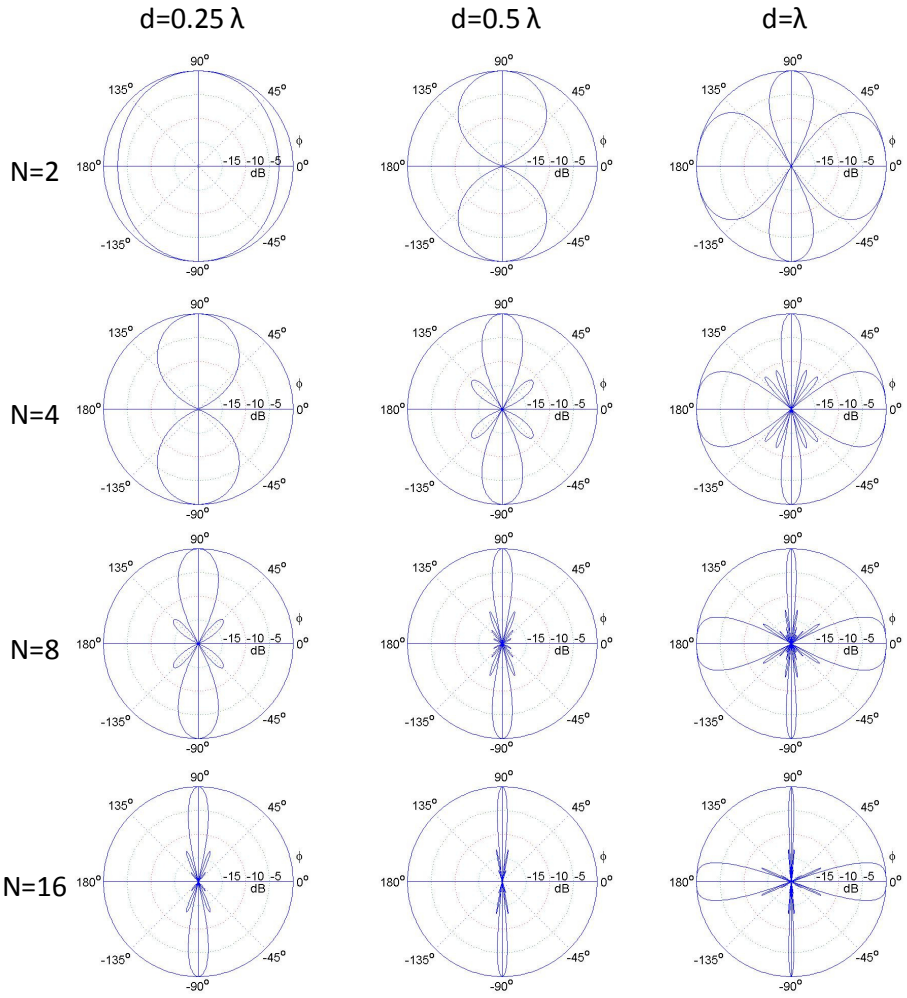

Figure 12: Beam-forming Antenna Patterns with Omni-directional Elements, normalized at θ=90o for Varying Number of Elements and Spacing.

In the case that directional elements are used instead of omni-directional, the $G(\theta,\phi)$ as mentioned before is added to the $G'(\theta,\phi)$ of the directional element.

As it can been observed in fig the main lobe width of the array depends on the number of antenna elements and the spacing between them, in specific the 3 dB beam-width of an array with N elements and fixed spacing d between them is $\Delta\phi_{3dB} = 0.886 * \lambda / N * d$.

In Table 6 the values of $\Delta\phi_{3dB}$ for the arrays presented in Figure 12 are shown.

Table 6: 3 dB Beam-width of Beam-forming Antenna Arrays for Varying Number of Elements and Spacing.

3-dB Beam-width	Spacing d		
	0.25 λ	**0.5 λ**	**λ**
N=2	101.53	50.76	25.38
N=4	50.76	25.38	12.69
N=8	25.38	12.69	6.35
N=12	12.69	6.35	3.17

It can be easily observed that as the number of antenna elements increases the 3dB beam-width decreases while for a specific number of elements the same observation can be made for the spacing between the elements. Although an array equipped with N elements and spacing equal to 0.5 λ could achieve the same antenna pattern with a second array with double elements and spacing equal to the half of the first array it is much more cost-effective to deploy the first array. That means that greater arrays could provide more directivity to the antenna radiation pattern for a specific spacing, however constructing large arrays is uncomfortable in means of cost and size.

Additionally the size of the side-lobes seems to be affected from the number of elements and the spacing between the elements. As it can be observed for any number of elements, the best choice is d=0.5 λ spacing between the elements as lower side-lobe levels are achieved and at the same time half the elements are needed in order to achieve the directivity a larger array with 0.25 λ spacing. Finally it should be noted that as the number of elements increases the side-lobes reach a constant level of about -13 dB for an array with uniform weights.

As it has been mentioned, the feeding of the antenna elements with different amplitudes results in beam-steering. In Figure 12 the main-lobe of the patterns presented is steered toward the broadside (y axis in Figure 11, φ=90o); in order to steer the main-lobe toward the direction that the desired TS is located, the antenna elements should be fed with different weights. This results to an 'electronic' rotation of the of the antenna array, without physically rotate it.

In contrast to the uniform array where all the elements are fed with equal weights, in order to steer the beam toward a desired direction, i.e. toward ϕ_0, the relative feed coefficients for the nth element shall be :

$$\alpha_n' = a_n * e^{-jkd_n \cos\phi_0}$$

Consequently in order to steer the main-lobe toward a particular direction the appropriate weight should be calculated and applied to each antenna element.

The corresponding array factor $A'(\phi)$ will be:

$$A'(\phi) = \sum_n a_n * e^{jkd_n \sin\theta \cos(\phi-\phi_0)}$$

In Figure 13 the steered antenna pattern for d=0.5 N=4 $\phi_0 = 60^o$ for omni-directional antenna elements.

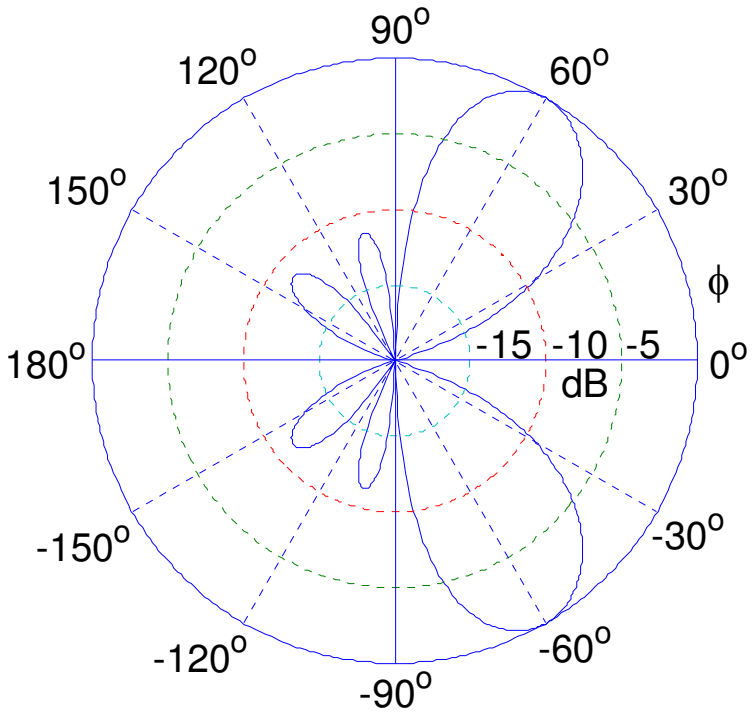

Figure 13: Beam-forming Antenna Pattern with Omni-directional Antenna Elements, Steered at φ=60°

Spatial Multiplexing

Spatial multiplexing is based on the idea of dividing the incoming high bit rate data streams into N independent data streams, [4]. Since those independent data streams are created, they are transmitted via N independent channels in space (independent spatial channels). It should be noted that no channel state information is required at the transmitter in order to create those independent data streams, but multiple antenna elements are required in both ends of the communication link. In contrast to receive and transmit diversity where the link quality in terms of signal-to-noise-ration is improved, with spatial multiplexing the systems benefits from a higher spectral efficiency, consequently higher capacity is obtained, [21].

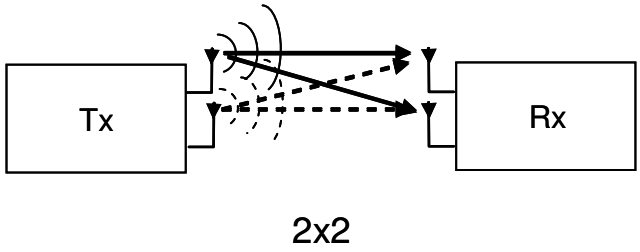

Figure 14: A spatial multiplexing MIMO system that transmits multiple data streams.

If the mobile station has only one antenna, WiMAX can still support spatial multiplexing by coding across multiple users in the uplink. This is called multi-user collaborative spatial multiplexing. Unlike transmit diversity and Beam-forming, spatial multiplexing works only under good SINR conditions.

AAS Algorithms

The basic schemes that have been developed for the AAS have been introduced in the paragraph above. In AAS implementations the transmitted and the received signals shall pass through a signal processing procedure. For each one of the technologies that have been introduced above, special algorithms have been developed in order to exploit the additional capabilities that are provided to the system. In the following paragraphs basic algorithms for each AAS technique are presented.

Transmit Diversity Algorithms

As mentioned before, transmit diversity is the most appropriate diversity scheme for mobile networks, where complexity is undesired especially at the mobile TS where in order to keep the size small implementation of multiple antennas is not efficient. Hence, in order to achieve higher performance at the system through diversity in both DL and UL direction, diversity is applied at the BS where more space, power and processing capability is available. There are two different approaches for transmit diversity, for the first one it is pre-supposed that the channel is known at the transmitter while for the other no such information is necessary at the transmitter, [3].

Space Time Transmit Diversity

Multiple-antenna transmit schemes utilize both transmit diversity and spatial multiplexing. While Spatial Multiplexing provides higher spectral efficiency, transmit diversity provides better link quality. In transmit diversity the signals sent from different transmit antennas interfere with one another. In order to avoid it, and achieve high link quality, signal processing is required at both the transmitter and the receiver in order to remove or at least attenuate the spatial interference that is produced and achieve diversity, [3].

Several algorithms have been developed in order to manipulate the benefits of AAS systems that utilize transmit diversity; those algorithms are known as space time codes (STC). The main idea is that for an input symbol sequence, Space-Time Encoder chooses constellation points in order to transmit simultaneously from all antennas so that coding and diversity gains can be maximized. STC may be split into two main types: Space-time Trellis Codes (STTC) that distribute a trellis code over multiple antennas and multiple time-slots and provide both coding gain and diversity gain and Space-time Block Codes (STBC) that act on a block of data at once and provide only diversity gain, but are much less complex in implementation terms than STTC,[16].

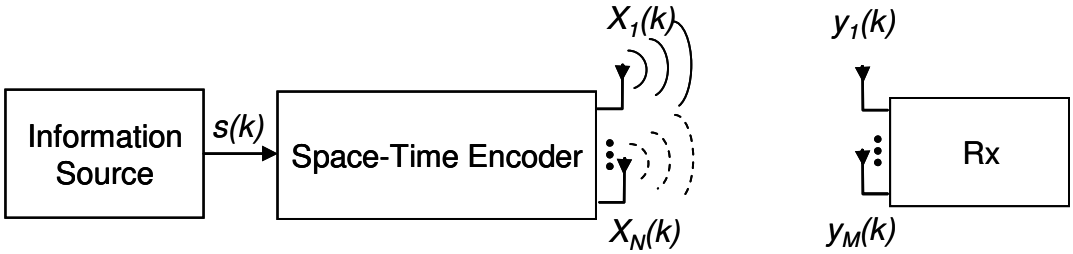

Figure 15: NxM System with Space – Time Block Coding at the Transmitter

Space-Time Trellis Coding

Space-Time Trellis Coding (STTC) was introduced as an effective transmit diversity technique to overcome fading. These codes have been designed to achieve maximum diversity gain. It is defined over a trellis structure where each input symbol has associated N symbols each one of them transmitted from each antenna. At the receiver signal processing is required with coding techniques appropriate to the coding scheme that has been utilized from the multiple antenna array at the transmitter, [18]. The performance of this type of STC is high in slow-fading environments as it is able to achieve both coding and diversity gains in MIMO channels and additionally provides a higher spectral efficiency due to modulation, [17]. However an important drawback of STTC is the high decoding complexity that they introduce to the system .Namely, for a fixed number of transmit antennas the complexity of the decoding at the receivers increases exponentially with the transmission rate.

Space-Time Block Coding

In access systems such as WiMAX where transmission rates are high, STTC becomes unsuitable due to high complexity. For this reason Space-Time Block Coding (STBC) were proposed as an attractive alternative to trellis coding. Despite the fact that STBC cannot provide coding gains like STTC they have been adopted by WiMAX due to low decoding complexity that they introduce to the system. In STBC the data stream to be transmitted is encoded into blocks. Those blocks are distributed among spaced antennas and across time. That means that in a Nx1 system, the data stream is transmitted N times, while in the duration of a symbol transmition only one antenna elements transmits,[3][25].

Assuming that the channel is known at the receiver, a simple Maximum Likelihood decoding algorithm is required, based only on a linear processing at the receiver.

To overcome the time penalty that STBC introduces to the radio link, Alamouti developed a transmit diversity scheme with 2 transmit antennas in 1998, that's why STBC is often referred to as Alamouti Scheme, [3]. The simplicity of Alamouti's Scheme lead to research on 'pseudo-Alamouti' schemes for more than two transmit antennas.

Alamouti Scheme - Matrix A

Alamouti Scheme or also known as Orthogonal Space Time Block Code (OSTBC) is the transmit diversity scheme that has been proposed in several third-generation cellular standards, also in WiMAX. It is designed mainly for 2 transmit antennas utilization. In a 2 transmit antennas - 1 receive antenna (2x1) case the received signal at the receiver will be:

$$y[n] = h_a[n] * x_a[n] + h_b[n] * x_b[n] + w_b[n]$$

, where $y[n]$ is the received signal at the receiver at symbol time n , $x_i[n]$ is the transmitted signal of the transmit antennas i (i=a or i=b) $h_i[n]$is the channel fading vector of for channel I and $w[n]$ is the noise at symbol time n, assuming that it follows $CN(0, N_0)$.

According to Alamouti scheme the two transmit antennas transmit 2 complex symbols u_a and u_b over two symbol times: at symbol time 1, $x_a[1] = u_a$ and $x_b[1] = u_b$ at symbol time 2, $x_a[2] = -u_b^*$ and $x_b[2] = u_a^*$. Assuming that the channel doesn't change over those two symbols time, $h_a[1] = h_a[2] = h_a$ and $h_b[1] = h_b[2] = h_b$, the received signal can be written in a matrix form as following:

$$\begin{bmatrix} y[1] & y[2] \end{bmatrix} = \begin{bmatrix} h_a & h_b \end{bmatrix} \begin{bmatrix} u_a & -u_b^* \\ u_b & u_a^* \end{bmatrix}$$

In order to detect the symbols u_a and u_b at the receiver, the conjugate of $y[2]$ has to be calculated:

$$y^*[2] = h_b^* * u_a - h_a^* * u_b$$

So the received signal at the receiver for the two symbols time can be written as,

$$\begin{bmatrix} y[1] \\ y[2] \end{bmatrix} = \begin{bmatrix} h_a & h_b \\ h_b^* & -h_a^* \end{bmatrix} + \begin{bmatrix} w_a \\ w_b \end{bmatrix}$$

As it can be seen the columns of the square matrix are orthogonal, hence the detection of u_a and u_b can be achieved by solving two separate, orthogonal, scalar problems. This technique results to a 2 symbols transmission over 2 symbol times with half the power consumption.

As it has been already mentioned, Alamouti Scheme has been developed for a 2x1 system but it can be further extended to systems with more transmit and/or receive antennas, [20]. It should be noticed that when more than 1 received antenna is used the system is not able to achieve higher data rates as 2 symbols are still transmitted over two symbol times but it can eliminate the spatial interference by combining the more received signals. In other words receive diversity is added to the system that is not able to offer higher transmission rates but can provide higher performance to the system in means of interference elimination. In the case of more than 2 transmit antennas in Alamouti Scheme can offer higher data rates. In a 4x2 Alamouti Scheme for example two data streams can be sent using a double space time transmit diversity (DSTTD) scheme that consists of two 2x1 parallel Alamouti Schemes, [3]. This scheme also known as stacked STBC combines receive and transmit diversity with some kind of spatial multiplexing.

Extended and Newer Transmit Diversity Schemes

The concatenation scheme of turbo codes and STBC (Turbo-STBC) was proposed and it has been shown that the Turbo-STBC can achieve good error rate performance, [4]. Recently, low-density parity-check (LDPC) codes have attracted much attention as the good error correcting codes achieving the near Shannon limit performance like turbo codes. The decoding algorithm of LDPC codes has less complexity than that of turbo codes. Furthermore, when the block length is large, the error rate performance of the LDPC codes is better than that of the turbo codes with almost identical code rate and block length. The error rate performance of the LDPC-STBC is almost identical to or better than that of the Turbo-STBC in a flat Rayleigh fading channel, [24].

Other newer diversity schemes are Cyclic Delay Diversity (CDD) and Waveform Diversity (WD), [21]. CDD is used in OFDM-based telecommunication systems, transforming spatial diversity into frequency diversity avoiding Inter-Symbol Interference (ISI), assuming that the

channel condition is known at the receiver while this information is not necessary at the receiver, [22]. Waveform diversity (WD) refers to the use of various waveforms (signals) in both transmitter and receiver design for improving the overall performance such as detection and/or identification of targets in interference and noise. Waveform diversity can be exploited spatially using a multiple set of sensors for both transmission and/or reception.

Receive Diversity Algorithms

For the implementation of the receive diversity algorithms, channel state information (CSI) is essential at the receiver in comparison to transmit diversity where such information is not necessary. There are three algorithms that have been developed: Selection Combining, Maximal Ratio Combining (MRC) and Equal Gain Combining (EGC). All of them are based on the technique of applying weights w at the signals received at each one of the receive antennas as it is shown in Figure 16,[10]. The technique that the receiver uses to estimate how the signal of each antenna will be weighted is presented in the following paragraphs for each on of those 3 techniques.

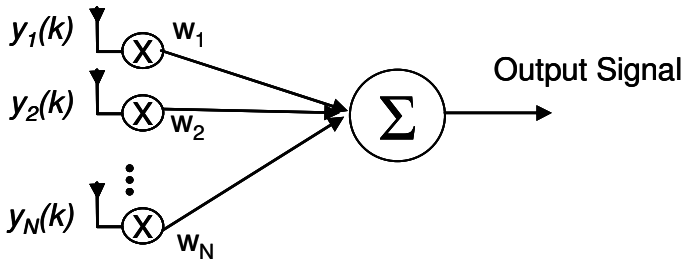

Figure 16: Receive Diversity is based on applying weights w at the received signal of each receive antenna element.

Selection Combining

Selection combining is based on the idea that, as long as each element experiences an independent sample of the fading process, the element with the greatest SNR is chosen for further processing. Therefore, in Selection Combining w_k is set equal to 1 for the element with the highest SNR, and 0 for all the remaining elements of the array.

Maximal Ratio Combining

A drawback of Selection Combining is that it ignores all the received signals of the N-1 elements of an N-element array. A more optimal solution is provided by Maximal Ratio Combining (MRC) where the weights of all the N elements are obtained on the scope of maximizing the output SNR.

Equal Gain Combining

In MRC technique, the weights w_k vary with the fading channel, in a heavy multi-path environment the magnitude of each signal fluctuates over several dB. That means that the diversity combiner has to obtain new weights for each element when such a fluctuation is observed. This process is not needed in Equal Gain Combining (EGC) where all the weights are set equal to unity.

All the combining techniques described above are capable to maximize the SNR at the combiner output based on the SNR of each element. However, in wireless systems, maximizing the SNR doesn't always offer higher performance to the system, due to interference. For that reason a more general technique called optimal combing that follows the same principle for system with both interference and fading to maximize the average signal-to-interference-plus-noise ratio (SINR) is more suitable for interference environments, i.e. urban areas where BSs are positioned with high overlapping. The extreme cases for this diversity technique are either to operate as an MRC receiver in the absence of interference or to operate as an interference chancellor based on the assumption that the receiver knows all the desired and interferer channel gains at each antenna element, a fact that adds high complexity at the receiver side.

Spatial Multiplexing Algorithms

When spatial multiplexing is applied on a multiple antenna elements system (N elements at both ends of the radio link) in a rich scattering environment, the impact on the system can be parallelized to a higher channel bandwidth adaptation. That results to a significant increase at the channel capacity. Several receivers have been developed for enhancing the capacity of the system through spatial multiplexing technique such as: linear receivers (zero forcing receiver, minimum mean squared error receiver), non-linear receivers (maximum likelihood receiver) and spatial interference canceling receivers (Bell Labs layered space/time (BLAST)),[3].

Adaptive MIMO

Adaptive MIMO switch (AMS) adopts both STBC and spatial multiplexing on the same system, and optimally the most suitable technique is selected based on the best throughput performance. When SINR conditions and antenna correlation is such that transmission of 2 symbols over two uncorrelated paths with high SINR is achieved, spatial multiplexing is selected, otherwise STBC is selecting offering better signal strength, [28].

Beam-forming Algorithms

In beam-forming, both the weight and phase of each antenna element are controlled. Combined amplitude and phase control can be used to adjust side lobe levels and steer nulls better than can be achieved by phase control alone. A beam-former radio transmitter applies the complex weight to the transmit signal for each element of the antenna array, while the receiver applies the complex weight to the signal from each antenna element and then sums all of the signal into one that has the desired directional pattern,[29].

There are three principal classes of beam-forming antenna arrays according to the method that the system utilizes in order to synthesize the appropriate antenna pattern:

Switched Antenna Arrays

In Switched Antenna Arrays (SAA), the antenna array generates overlapping beams that cover the surrounding area, by predefining the feeding phases that correspond to each beam. When an incoming signal is detected, the BS determines the beam that is best aligned in the wanted direction and the by applying the predefined weights and phases on the antenna elements of the array, “switches” to that beam in order to communicate with the terminal.

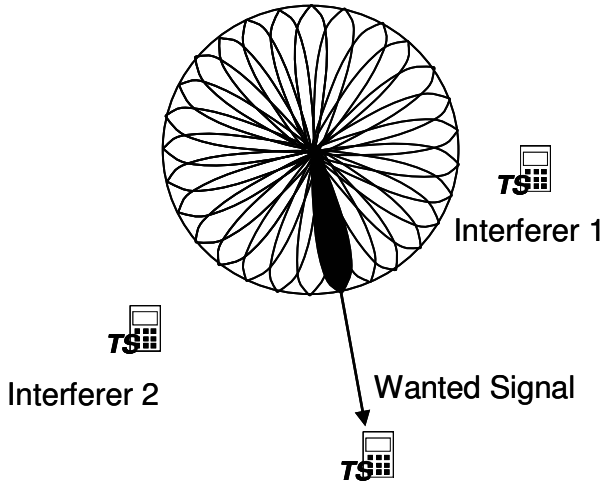

Figure 17: Switched Antenna Array, the antenna element with the best aligned main lobe is highlighted.

Phased Antenna Arrays

In Phased Antenna Arrays (PAA) the antenna pattern is generated by estimating the suitable feeding phase for each antenna element based on the direction of the terminal. When the exact direction of the terminal is known the PAA can achieve maximum system gain.

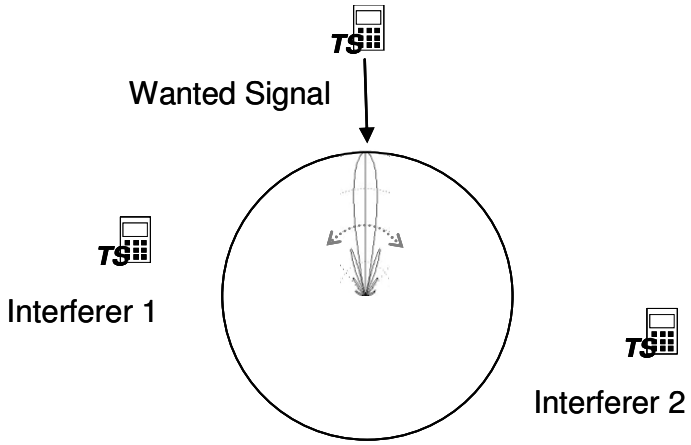

Figure 18: Phased Antenna Array, the main lobe is orientated to the direction of the wanted signal.

Beam-forming Antenna Arrays

In Beam-forming Antenna Arrays (BAA) the antenna pattern is generated by applying complex weights to the received signal of each element. The complex weights wk for the antenna elements are carefully chosen to give the desired peaks and nulls in the radiation pattern of the antenna array. In a simple case, the weights may be chosen to give one central beam in some direction. The weights could then be slowly changed to steer the beam until maximum signal occurs and the direction to the signal source is found. Moreover, the weights are chosen to give a radiation pattern that maximizes the quality of the received signal also in means of interference. Usually, a peak in the pattern is pointed to the signal source and signal reflections and nulls are created in the directions of interfering sources.

The process of altering the weights w_k of each element on-the-fly, in order to maximize the quality of the communication channel is called adaptive beam-forming. The most common methods for estimating the weights w_k are:

The process of altering the weights w_k of each element on-the-fly, in order to maximize the quality of the communication channel is called adaptive beam-forming. The most common methods for estimating the weights w_k are:

Minimum Mean-Square Error, where the shape of the desired received signal waveform is known by the receiver. Complex weights are adjusted to minimize the mean-square error between the beam-former output and the expected signal waveform.

Maximum Signal-to-Interference Ratio, where the receiver can estimate the strengths of the desired signal and of an interfering signal, weights are adjusted to maximize the ratio.

Minimum Variance, where the signal shape and source direction are both known, choose the weights to minimize the noise on the beam-former output.

Often, constraints are placed on the adaptive beam-former so that the complex weights do not vary randomly in poor signal conditions. Some radio signals include “training sequences” so that an adaptive beam-former may quickly optimize its radiation pattern before the useful information is transmitted.

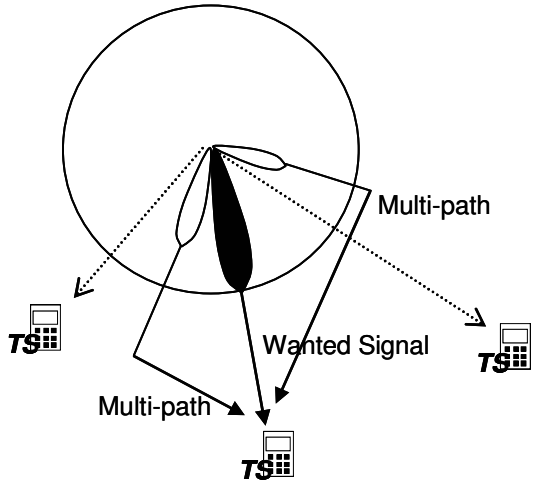

Figure 19: Beam-forming Antenna Array, the non-zero weighted beams are those that are aligned to the direction of the TS or aligned to direction of multi-path.

In addition, the synthesis of the array beam in PAA and BAA is highly dependent on the geometry of the antenna elements. The main phased and beam-forming arrays configurations are identified as Linear, Planar or Circular. When the spacing between the elements is identical, the array can be characterized as uniform.

3.AAS SNR Improvements

The AAS techniques presented in the previous section have been developed in order to offer specific gains to the wireless technologies. There are 3 types of improvement that these technologies are able to offer:

- *Link Gain Budget Improvement*, by additional gains that can be applied on one or both sides of a radio link

- *Capacity Improvement*, by offering higher spectral efficiency on the channel.

- *Interference Mitigation Improvement*, by lowering the threshold degradation issues.

It should be noted that these three type of improvements are not independent to one another, i.e. the range of a system is improved through coverage gains that a specific AAS technique is able to offer to the transmitter, and has as a result that more TS are capable to operate in higher PHY modes and provide higher spectral efficiency to the channel. In the following paragraphs the specific gains of each technology are investigated, based on measurements and literature references, without taking into account further entailed gains.

Diversity Gains

As it has been mentioned, diversity techniques offer the capability of selecting the diversity branch that provides the higher SNR levels. The gain that a Nx1,1XN or NxM system is able to provide, depends on the number of elements N as well as on the algorithm that is used to select the branch that offers better propagation conditions.

Transmit Diversity

The fade margin of a link is reduced through spatial diversity. In all orthogonal STBC techniques the gain that can be achieved by the transmission of a symbol N times is equal to the gain of a 1xN system with MRC implemented at the receiver.

The throughput in STBC is 1/N times less in a Nx1 system due to the fact during the symbol time duration, only one antenna elements transmit, and as a result in order to achieve a gain of 3 dB, the symbol is transmitted two times, wasting time equal to two symbols transmission, thus the throughput is reduced to the half of a SISO system. On the other hand, in Alamouti scheme which is proposed for WiMAX, the 2 antenna elements transmit 2 different symbols at the same time twice. For that reason the 3 dB gain is achieved without waste of time as finally 2 symbols are transmitted in a time slot equal to the duration of two symbols transmition of a SISO system, [3].

Space time trellis codes achieve better performance than orthogonal STBCs which in some cases reach a 2 dB better performance but as already mentioned they are uncomfortable for high bit rate transmissions,[17].

Receive Diversity

The gain of each technique depends on the algorithm that is implemented. Regarding receive diversity algorithms, three algorithms have been investigated as the most widely used in mobile networks.

Selection Combining

In Selection Combining, only the weight of the element with the better SNR is set equal to 1 and all the rest weights are set equal to zero, the outage probability decreases exponentially with the number of elements, while the improvement that is achieved on the average SNR is

of order of ln(N) over the average SNR of a single element reception. Consequently, selection combining can offer significant gains for relatively large number of elements (N),[4][10].

Maximal Ratio Combining

In Maximal Ratio Combining, the weights of each element are obtained on the scope of maximizing the SNR, the output SNR is the sum of the SNR at each element and as a result the average SNR improves by a factor of N. The best a diversity combiner can do is to choose the weights to be the fading of each channel. The MRC receiver, does not act as a receiver that simply receives in N times higher SNR values, but also as the number of elements increases the fluctuation in the output SNR reduces,[4][10].

Equal Gain Combining

In Equal Gain Combining the weights of each element are set equal to one, the average SNR improvement is comparable to that of the maximal ratio combining technique, despite being significantly simpler to implement it, [10].

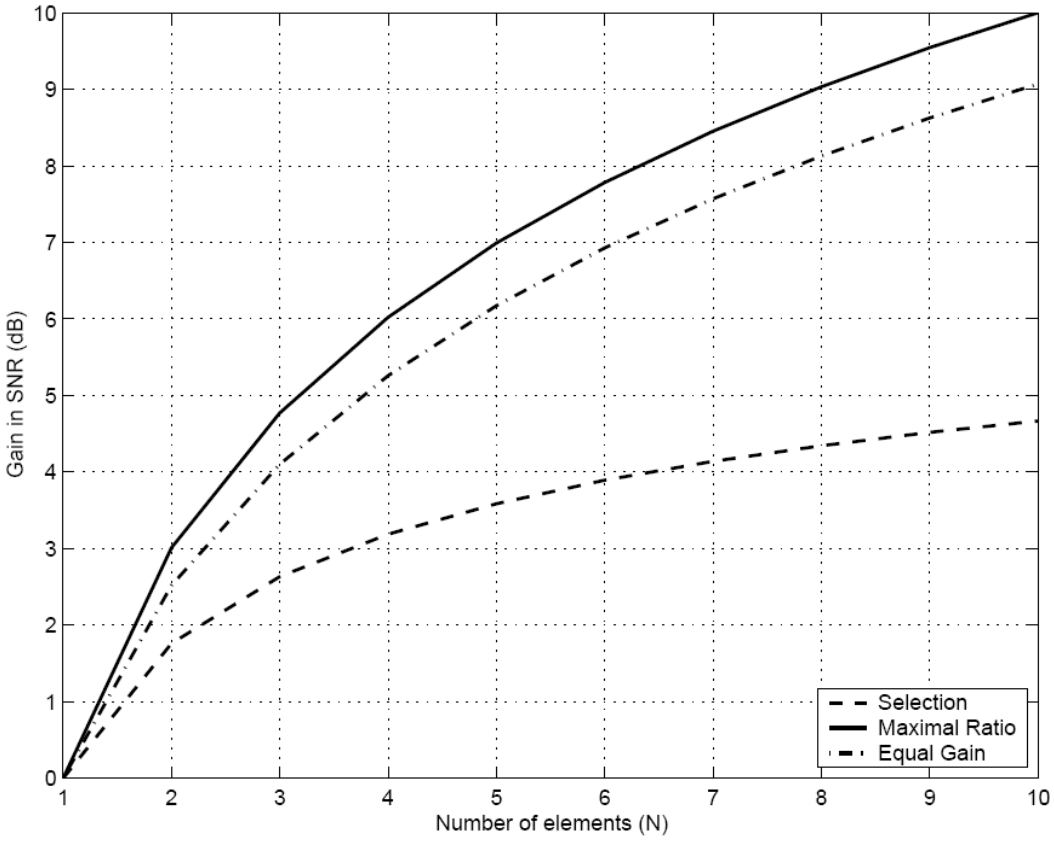

Figure 20: Average SNR Improvement of the 3 Types of Receive Diversity Algorithms

In Figure 20 the performance of the three algorithms in terms of improvement in SNR is presented. As expected the best improvement is observed in maximal ratio combining, while the worst is observed in selection combining and the performance of equal gain combining is comparable to that of maximal ratio combining.

In terms of the required processing the selection combiner is the easiest as it requires only a measurement of the SNR at each element. Both the maximal ratio and equal gain combiners require phase information while the former requires accurate measurement of the gain too. Such an implementation can become too complicated, as in a fading channel the dynamic range of a signal may be quite large, but for this cost maximal ratio combiner improves the performance of the system by about 0.6 dB over the equal gain combiner.

Optimal Combiner

Regarding optimal combiner, where the weights of each antenna element at the receiver is selected based on the SINR level, it is possible to achieve 2 dB higher SINR gain than the

SNR gain that an MRC receiver with N elements can achieve. It can be seen in fig where a performance comparison between an optimal combiner (OC), a MRC and an interference canceller (IC) receiver with 2, 3 and 4 antenna elements is presented. The measurements have been taken into an interference-dominated environment where noise is negligible. As expected, OC has the best performance since it generalizes both MRC and IC. Moreover, IC does worse than MRC except at low SIR, where interference dominates performance degradation and hence canceling interference is the correct strategy, while at high SIRs, performance degradation due to multi-path fading causes more degradation than interference and hence MRC leads to better performance than IC, [30].

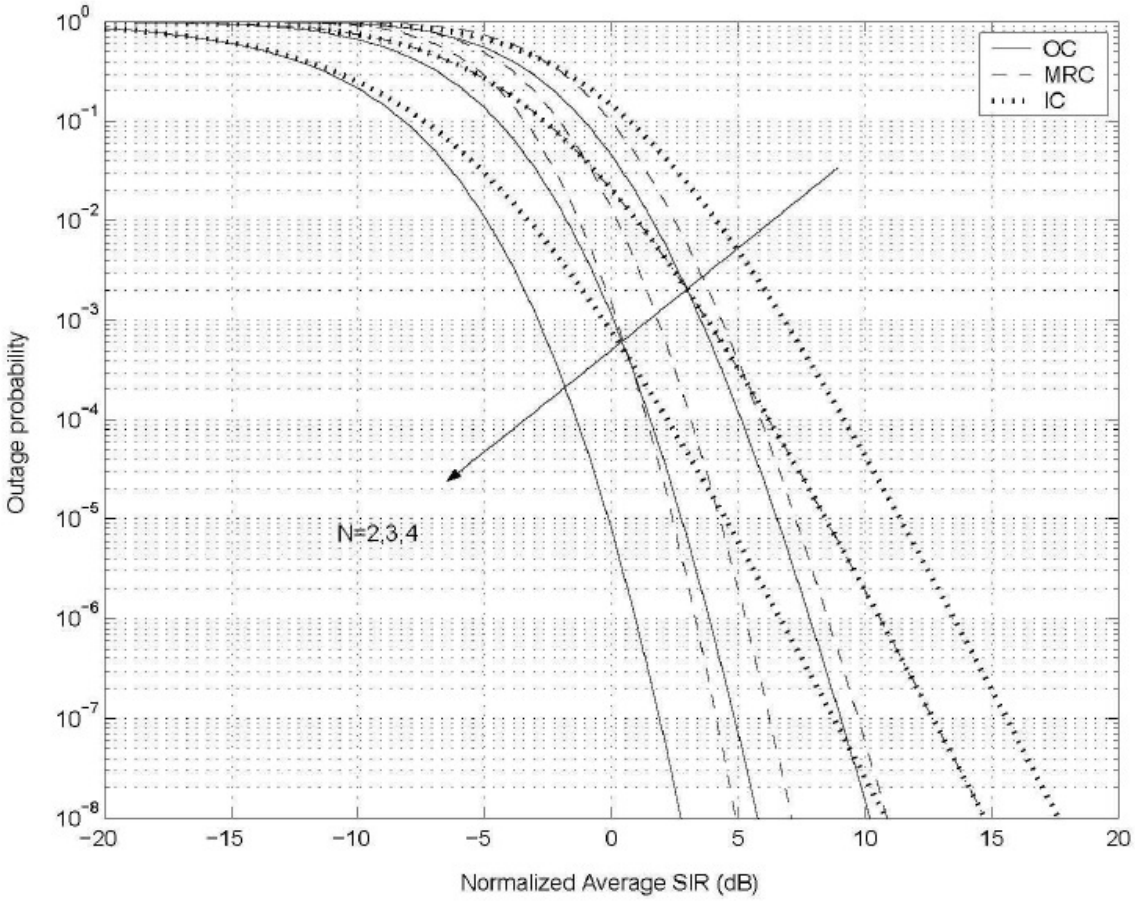

Figure 21: Average SIR vs Outage Probabilty for Optimal Combiner, Maximal Ratio Combiner and Interference Canceller

Receive and Transmit Diversity

When multiple elements are deployed on both sides of the radio link, the systems benefits from both transmit and receive diversity at the same time. The most famous techniques for WiMAX networks are Alamouti scheme in the transmitters side and MRC at the receiver side.

The gain of a NxM system is equal to 10*log(N*M) dB, or in other words equal to the gain of a system with N*M antenna elements at the receiver, with MRC technique implemented.

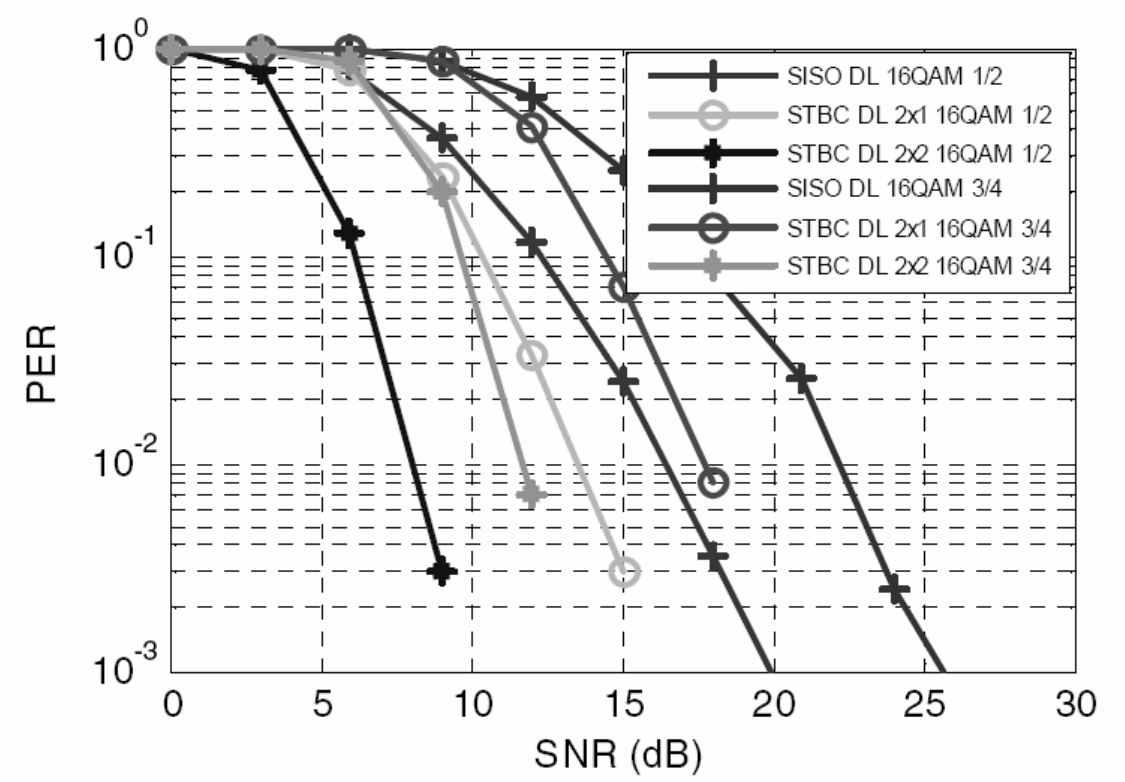

Figure 22: PER vs SNR Comparison of a SISO, a 2x1 Alamouti Scheme and 2x2 Alamouti Scheme for 16 QAM PHY Mode in mobile WiMAX.

The PER vs SNR results for a SISO channel vs. an Alamouti (STBC) 2x1 and 2x2 system in 16 QAM PHY mode is presented in Figure 22, [31], where perfect decorrelation between the different channels is assumed. As it can be seen all the modulation schemes and convolution turbo codes that are used in WiMAX have been measured.

Spatial Multiplexing Gains

When spatial multiplexing is implemented on a system, the gain of the system in means of coverage gain is similar to the gains of a simple SISO system as the N antennas transmit simultaneously. However the fact that different symbols are transmitted from each element, results in N times higher capacity of the system. In Figure 23 the SNR vs Troughput in the DL direction of a WiMAX SISO system is present, while in Figure 24 the corresponding graph for a system with spatial multiplexing (Matrix B) 2x2 is depicted, [31]. As it can be observed, the throughput is doubled in the Matrix B in comparison to the SISO system for a given SNR.

The advantage of Spatial Multiplexing is a linear capacity gain in relation to the number of transmit antennas.

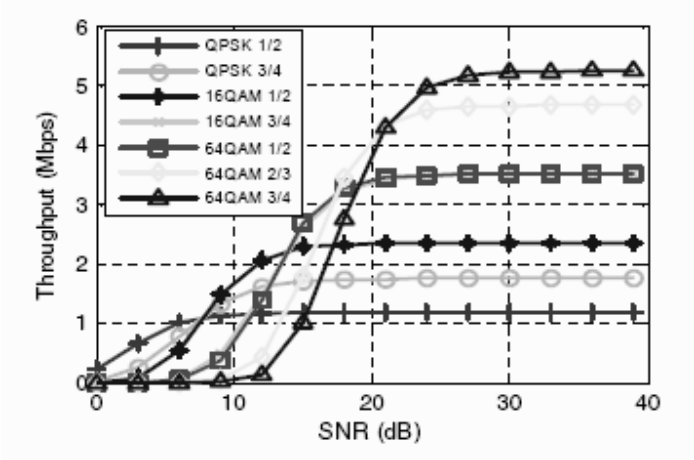

Figure 23: SNR vs Throughput in the DL Direction for a SISO system.

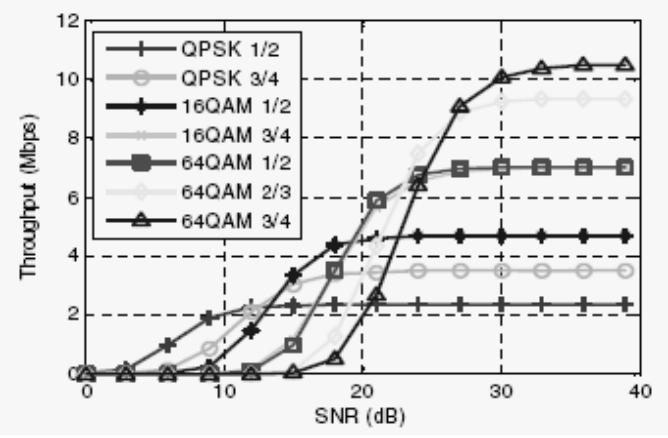

Figure 24: SNR vs Throughput in the DL Direction for a MIMO-B 2x2 system

Adaptive MIMO

Adaptive MIMO technique combines spatial multiplexing, where two parallel data streams are transmitted, with STBC. Spatial multiplexing requires high SINR, when the channel quality is not good enough to maintain the dual stream approach, the transmitter switches to STBC making the signal more robust against fading and interference resulting in an increased data rate by using higher modulation and coding schemes, [28].

Consequently, both spatial multiplexing and STBC gains can be applied to that system based on the channel state. In Figure 25 the capacity versus SNR curves for spatial multiplexing and STBC are presented. At intersection of the two curves corresponds to the SNR where the transmitter switches from the one technique to the other.

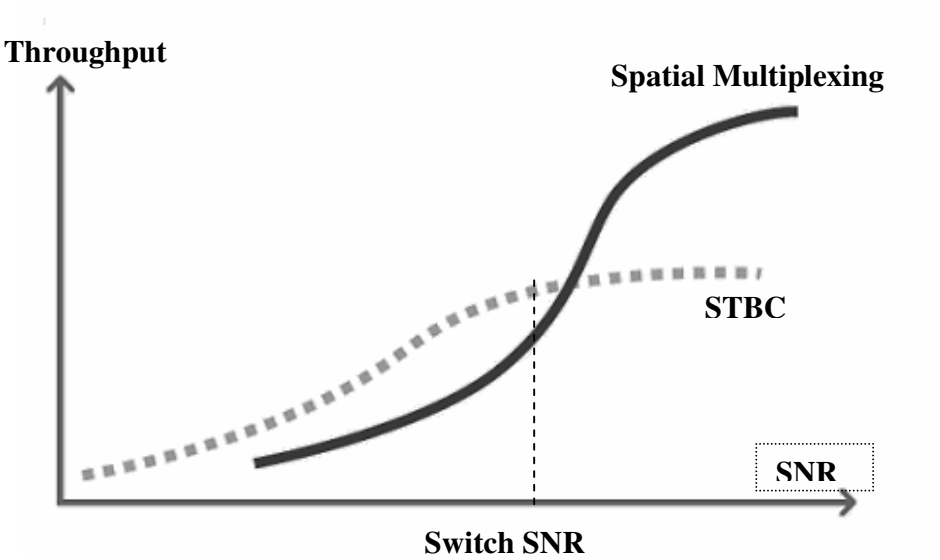

Figure 25: Adaptive MIMO

Beam-forming Gains

The most beneficial technique in means of coverage gain and interference mitigation is Beam-forming technique. In beam-forming the main-lobe of the antenna array becomes to narrow and as a result the energy field is concentrated towards the wanted direction. Moreover the system applies 9 dB additional antenna gain toward the 3dB beam-width direction, known as Beam-forming Gain, [32].

Regarding the interference mitigation issues in beam-forming antenna arrays, taking into account that the side-lobes have about 10 dB lower gain than the main lobe, it is considered that the beam-forming technique can provide a 6dB interference rejection in both directions. This is justified from the fact, that while the beam-former steers its 3-dB beam-width toward

the direction of the wanted TS, the possibility that an interferer is located inside the 3-dB beam-width is reduced.

Improvement Overview

In Table 7 the additional system gains that are applied to the system for each AAS used in WiMAX networks are summarized.

Table 7: Gains Applied to WiMAX System with AAS implementation.

Technique	Algorithm	Gain
Transmit Diversity	Alamouti	3
Receive Diversity	MRC	3
Beam-forming	PAA	9

4.AAS Performance in WiMAX

In this paragraph the 802.16 compliant AAS techniques are investigated in terms of performance improvement. Essentially a basic WiMAX system is compared with different technology profiles such as with MIMO or Beam-forming. As it has been already presented above, the additional gains applied to the system due to advanced techniques, differ from channel to channel for the same system. Prior to determining the impact of the AAS techniques in the performance of a WiMAX system, is to determine the system gain of each channel for the systems presented above.

Impact of AAS Techniques in the System Gain of a WiMAX system

System gain improvement issues are investigated in this paragraph between a basic SISO system, a MIMO Matrix A 2x1 and 2x2 system with Alamouti and MRC implemented in the BS and MRC at the mobile TS for the 2x2 system, a MIMO Matrix B 2x2 system, a Beam-forming system with an 8 elements Beam-forming antenna array implemented at the BS and 2 antenna elements at the mobile TS with MRC technique implemented at the mobile TS with 2 receivers.

Basic SISO & MIMO-B 2x2 System

The reference system is comprised by a single antenna in both the BS and terminal sides; hence no form of AAS is possible. Transceiver structure is based on IEEE 802.16e OFDMA PHY layer, including CTC error coding. The operating frequency is 2.5 GHz and the channel bandwidth is 5 MHz. The BS Tx power is considered 30 dBm while the directional antenna gain of the BS is 16 dBi. Concerning the terminal equipment, realistic product specifications are considered, where the antenna gain is 6 dBi and the uplink power is 24 dBm. The receiver noise figure is selected at 7 dB, including any implementation losses.

The resulting System Gain for the basic system in the DL and UL direction is presented in Table 8. It should be noted that in this table the preamble and the FCH channels are note considered as long as the system gain of these channel is always higher than the system gain of the DL/UL MAP, traffic and ranging channels.

Table 8: System Gain Estimation for the Reference & MIMO-B 2x2 System.

Reference & MIMO-B 2x2 System	DL/UL MAP	DL Traffic	UL Traffic
Tx Power (dBm)	30	30	24
Tx Antenna Gain (dBi)	16	16	6
Subchannelization Gain	0	0	12.4
PCG	0	0	0
EIRP	46	46	42.4
STC Gain	0	0	0
BF (DL) Gain	0	0	0
Rx Antenna Gain (dBi)	6	6	16
BF (UL) Gain	0	0	0
MRC Gain	0	0	0
Sensitivity Threshold (dBm)	-96	-96	-96
Number of Used Subcarriers	420/420	420/420	24
Number of Total Subcarriers	420	420	420
System Gain	148	148	154.4

The parameters presented in Table 8 are described below:

- Tx Power (dBm) refers to the transmit power of the BS in the DL direction or to the transmit power of the TS in the UL direction.

- Tx Antenna Gain (dBi) refers to the gain of the antenna element of the BS in the DL direction or to the gain of the TS in the UL direction.

- Sub-channelization Gain refers to the power gain that is applied to the system due to the fact that the portion of the total used sub-carriers is boosted, i.e. in the Uplink direction 24 sub-carriers are powered out of the 420 available data sub-carriers in one symbol duration in the 5 MHz channel.

.

- Power Combining Gain (PCG) is applied to the system when more than one element is implemented on the transmitter with equal number of Power Amplifiers at the input of each element. The PCG gain of a transmitter with N antenna elements implemented is 10*log(N).

- Equivalent Isotropical Radiated Power (EIRP) arises by the summation of Tx Power, Antenna Gain and PCG.

- Space Time Coding Gain (STC Gain) refers to the gain that is applied to the system through STC when it is implemented on the transmitter.

- Beamforming Downlink Gain (BF (DL) Gain) refers to the gain that is applied to the system when Beam-forming technique is implemented on the transmitter.

- Rx Antenna Gain refers to the gain of the antenna element of the TS in the DL direction or to the gain of the BS in the UL direction.

- Beamforming Uplink Gain (BF (UL) Gain) refers to the gain that is applied to the system when Beam-Forming technique is implemented on the receiver.

- MRC Gain refers to the gain that is applied to the system when Maximal Ratio Combining is implemented on the receiver.

- Sensitivity Threshold (dBm) refers to the lowest signal level that allows the receiver to operate in QPSK ½ PHY mode. The process to estimate the -96 dBm threshold is described below:
- The noise floor of the 5MHz WiMAX system arises from the equation:

$$N = -174 + 10 * \log(5 * 10^6 * {}^{28}\!/_{25} * {}^{420}\!/_{512}) + NF$$

, resulting in -100 dB noise floor foir a given for NF equal to 7 dB for both the BS and TS. The 802.16e certified required SINR threshold are presented in Table 9. Consequently the lowest RSSI for QPSK ½ modulation is calculated to -96dBm. For the DL/UL MAP

where repetition is also applied the term $-10*\log(6)$ has to be added for the estimation of the noise floor.

Table 9: WiMAX Certified Required Thresholds

PHY Mode	SINR Threshold
QPSK-1/2	4
QPSK-3/4	6.8
16 QAM-1/2	10
16 QAM-3/4	13
64 QAM-2/3	17.8
64 QAM-3/4	19

- Number of Elements refers to the number of antenna elements at the transmitter.

- Number of Used Sub-carriers refers to the number of the powered sub-carriers in the channel, i.e. 24 sub-carriers in the UL Traffic, 420 in the DL/UL MAP and DL Traffic.

- Number of Total Subcarriers refers to the number of sub-carriers that are available in the channel for data transmission, i.e. 420 in the 5 MHz channel, 840 in the 10 MHz channel.

Due to the fact that a TDD mode is considered for the system, it is safe to consider that the propagation path is reciprocal for both directions (DL/UL), resulting in equivalent path loss for both directions. Consequently, the maximum path loss that the system will be able to suffer is dictated by the sub-frame with the lowest system gain, thus the reference system is limited in means of system gain by the system gain of the DL sub-frame.

The system gain as calculated above for the reference system is equal to the system gain of a MIMO-B 2x2 system with two 16 dBi antennas implemented at the BS and two 6dBi antennas at the TS, as long as the MIMO-B technique doesn't offer any additional gain at the link budget.

MIMO 1x2 System

The MIMO 1x2 system consists of the BS and the TS as considered for the basic system but at the TS 2 antenna elements are implemented while MRC is applied in the DL direction. The system gain for this system is presented in Table 10, as it can be seen again the system gain of the system is limited by the DL sub-frame.

Table 10: System Gain Estimation for the MIMO 1x2 System

MIMO 1x2 System	DL/UL MAP	DL Traffic	UL Traffic
Tx Power (dBm)	30	30	24
Tx Antenna Gain (dBi)	16	16	6
Subchannelization Gain	0	0	12.4
PCG	0	0	0
EIRP	46	46	42.4
STC Gain	0	0	0
BF (DL) Gain	0	0	0
Rx Antenna Gain (dBi)	6	6	16
BF (UL) Gain	0	0	0
MRC Gain	3	3	0
Sensitivity Threshold (dBm)	-96	-96	-96
Number of Used Subcarriers	420/420	420/420	24
Number of Total Subcarriers	420	420	420
System Gain	151	151	154.4

MIMO-A 2x1 System

The MIMO-A 2x1 system consists of the BS and the TS as considered for the reference system but at the BS 2 antenna elements are implemented while Alamouti/MRC is applied in the DL/UL direction respectively at the BS. The system gain for this system is presented in

Table 11. It should be noted that according to WiMAX standard, [2], the DL/UL MAP is transmitted exclusively by one antenna element, thus the PCG is not applied in the DL/UL MAP transmission.

Table 11: System Gain Estimation for the MIMO-A 2x1 System

MIMO-A 2x1 System	DL/UL MAP	DL Traffic	UL Traffic
Tx Power (dBm)	30	30	24
Tx Antenna Gain (dBi)	16	16	6
Subchannelization Gain	0	0	12.4
PCG	0	3	0
EIRP	46	49	42.4
STC Gain	0	3	0
BF (DL) Gain	0	0	0
Rx Antenna Gain (dBi)	6	6	16
BF (UL) Gain	0	0	0
MRC Gain	0	0	3
Sensitivity Threshold (dBm)	-96	-96	-96
Number of Used Subcarriers	420/420	420/420	24
Number of Total Subcarriers	420	420	420
System Gain	148	154	157.4

MIMO-A 2x2 System

The MIMO-A 2x2 system consists of the BS and the TS as considered for the reference system but at the TS 2 antenna elements are implemented while MRC is applied in the DL direction TS. The System gain for this system is presented in

Table 12.

Table 12: System Gain Estimation for the MIMO-A 2x2 System

MIMO-A 2x2 System	DL/UL MAP	DL Traffic	UL Traffic
Tx Power (dBm)	30	30	24
Tx Antenna Gain (dBi)	16	16	6
Subchannelization Gain	0	0	12.4
PCG	0	3	0
EIRP	46	49	42.4
STC Gain	0	3	0
BF (DL) Gain	0	0	0
Rx Antenna Gain (dBi)	6	6	16
BF (UL) Gain	0	0	0
MRC Gain	3	3	3
Sensitivity Threshold (dBm)	-96	-96	-96
Number of Used Subcarriers	420/420	420/420	24
Number of Total Subcarriers	420	420	420
System Gain	151	157	157.4

Beam-forming 8x2 System

The Beam-forming 8x2 system consists of the BS and the TS described in the reference system, where 8 elements are implemented on the BS and Beam-forming technique is applied and 2 elements implemented on the TS with MRC capability.

In WiMAX Systems, during the preamble, FCH and MAP transmission beamforming gain is not available, because these channels must reach all the TS regardless of where they are in the area. Consequently the Beam-forming gain is applied only in the DL and UL Traffic transmission, [32]. The system gain for the Beam-forming 8x2 system is presented in Table 13. In contrast to the MIMO-A NxM systems where the DL/UL MAP is transmitted by one element, in beam-forming technique it can be transmitted by all the available elements, resulting in $10 * \log(8) = 9$ dB PCG. It should be noted that in order to achieve the 9 dB PCG the elements should have random phases in order to experience artificial multipath and this may slightly affect the original pattern of the elements.

Table 13: System Gain Estimation for the Beam-forming 8x2 System

Beamforming 8x2 System	DL/UL MAP	DL Traffic	UL Traffic
Tx Power (dBm)	30	30	24
Tx Antenna Gain (dBi)	16	16	6
Subchannelization Gain	0	0	12.4
PCG	9	9	0
EIRP	55	55	42.4
STC Gain	0	0	0
BF (DL) Gain	0	9	0
Rx Antenna Gain (dBi)	6	6	16
BF (UL) Gain	0	0	9
MRC Gain	3	3	0
Sensitivity Threshold (dBm)	-96	-96	-96
Number of Used Subcarriers	420/420	420/420	24
Number of Total Subcarriers	420	420	420
System Gain	160	169	163.4

System Gain Overview

In Table 14 the system gain of the systems described above are summarized. As it can be seen the limiting system gain of each system is highlighted in bold format and this limiting value is used in the graph of Figure 26.

Table 14: System Gain Overview

System Gain	DL/UL MAP	DL Traffic	Uplink Traffic
Reference / MIMO-B 2x2	**148**	**148**	154.4
MIMO 1x2	**151**	**151**	154.4
MIMO-A 2x1	**148**	154	157.4
MIMO-A 2x2	**151**	157	157.4
BF 8x2	**160**	169	163.4

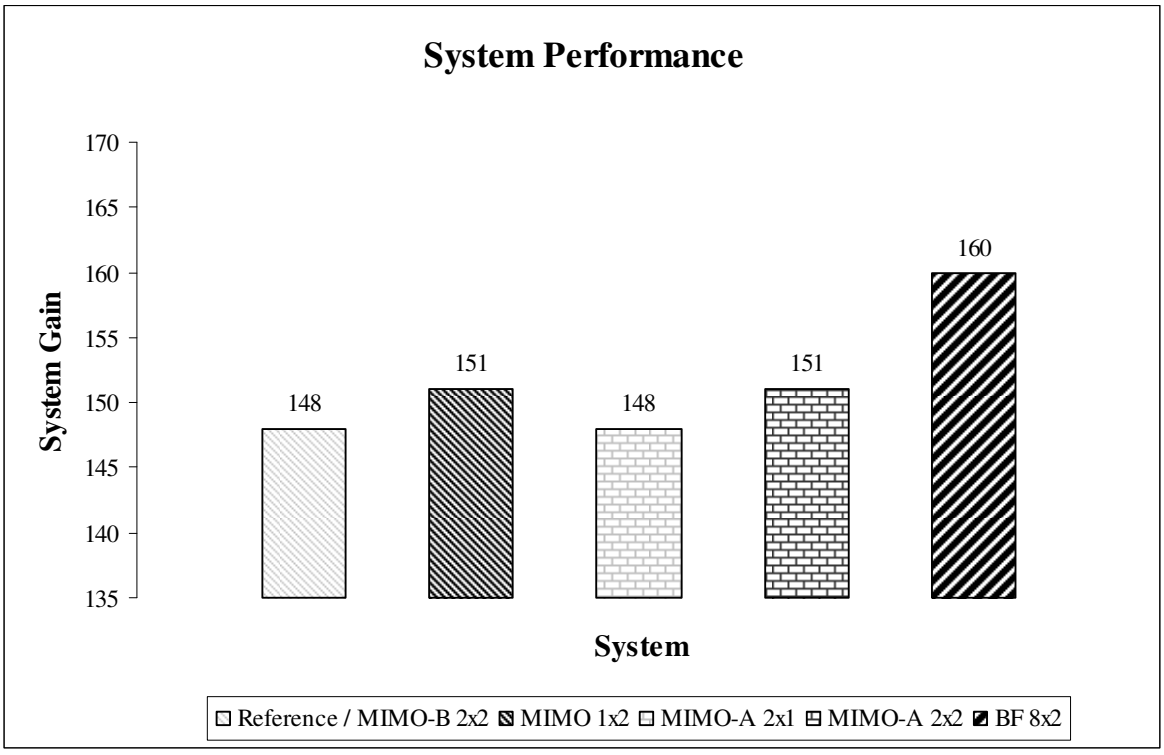

Figure 26: AAS Systems Performance Overview

Impact of AAS Techniques in the Performance of a WiMAX system

In the previous paragraph the system gain improvement has been estimated in a noise dominant environment. In real networks, due to high frequency re-use factors, noise dominant environments are not common. The most usual case, especially when the subscribers use indoor units or PCMCIA cards witch are equipped with omni antenna elements, the environment appears to be interference limited. According to the WiMAX standard a WiMAX certified receiver has significant interference rejection capability which can be improved with AAS techniques. The improved interference rejection that an advanced system is able to offer in contrast to a reference SISO system is investigated in this paragraph.

It should be noted that in the course of this investigation it is considered that the infrastructure and set up of the BSs is common for the wanted BS and the interferer one. For that reason, when i.e. PCG is considered for the wanted BS, the same ability will be assumed for the interferer BS.

MIMO 1X2

In Figure 27, a schematic analysis for the SINR of a MIMO 1x2 system with reference to the Reference SISO or a MIMO-B 2x2 system is presented. The schematic analysis refers to the DL/UL MAP and DL Traffic. The UL Traffic analysis is not presented due to the fact that according to the previous chapter AAS gains are not applied during UL traffic transmission for the MIMO 1x2 system.

As it can be seen in Figure 27, it is considered that the MRC gain is not applied to its maximum (3 dB) at the interferers path. For that reason while the level of the wanted signal is improved by 3 dB, the signal of the interferer is improved by 2 dB, thus the SINR of the MIMO 1x2 system is improved by 1 dB in comparison to the Reference SISO or the MIMO-B 2x2 system.

A numerical estimation of the interference rejection capability of a MIMO 1x2 is presented in Table 15 for the DL/UL MAP and DL Traffic. The level of the wanted signal is considered equal to -60 dBm for the Reference system and 3 dB higher for the MIMO 1x2 system due to MRC, the corresponding values for the interferers signal are considered -80 and -78 dBm respectively while the noise floors for each channels are -108 and -100 for the DL/UL MAP and DL Traffic respectively, resulting in 1 dB additional rejection in the DL sub-frame. It should be noted the interference rejection capability improves as the interference level approaches the level of the noise floor and it is doubled when the interferer's level is equal to the noise floor, while the lowest interference rejection is equal to 1 dB even for an interferer at the same signal level as the wanted signal level.

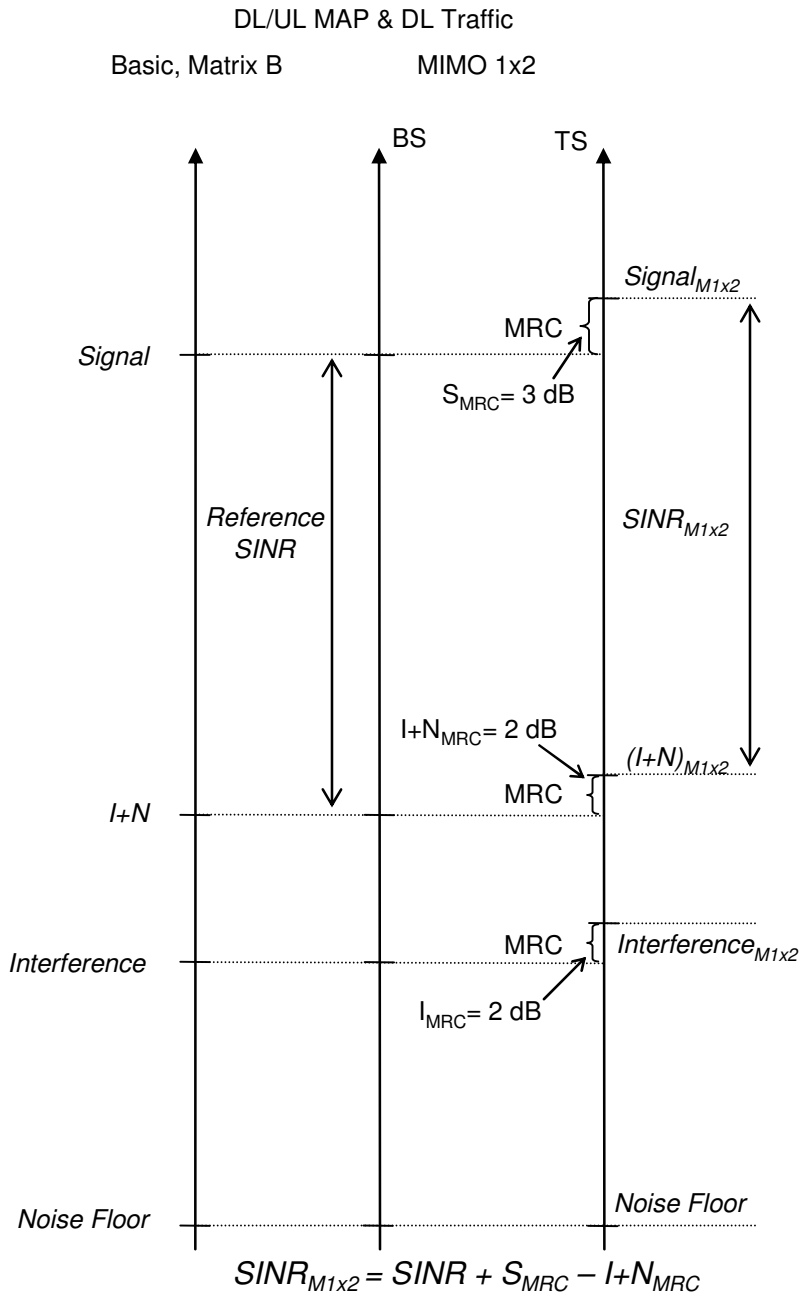

Figure 27: Comparison between a Reference SISO/MIMO-B 2x2 System and a MIMO 1x2 System in means of SINR improvement for DL Traffic and DL/UL MAP.

Table 15: Additional Interference Rejection Estimation of a MIMO 1x2 System for the DL/UL MAP and DL Traffic.

DL Subframe	Basic System	MIMO 1x2	AAS Technique
RSSI	-60	-60	
	-	3 ←	MRC
	-60	***-57***	
Interference Level	-80	-80	
	-	2 ←	MRC
	-80	***-78***	
Noise Floor	***-100***	***-100***	
I+N	***-79.96***	***-77.97***	
SINR	***19.96***	***20.97***	
Interference Rejection	***1.01***		

Regarding the UL Traffic, as it has been mentioned before, no additional gains are applied in the MIMO 1x2 system for that reason the corresponding table is not presented.

MIMO-A 2X1

The schematic analysis for the SINR of a MIMO 2x1 system with reference to a Reference SISO or a MIMO-B 2x2 system is presented in Figure 28 and Figure 29 for the DL Traffic and UL Traffic respectively. Schematic analysis for the DL/UL MAP is not provided as the SINR of the MIMO 2x1 system is equivalent to the SINR of the reference SISO system for the DL/UL MAP.

As it can be seen the PCG is applied in both wanted and interferer signal for those channels. According to the standard the DL/UL MAP is transmitted by only one antenna element thus the PCG is not applied.

Moreover the STC system gain (STCG) improvement is not applied in the DL/UL MAP neither for the wanted signal nor for the interferer as long as all the TS have to receive the DL/UL MAP channel, while it is applied only at the wanted signal in the DL Traffic, due to the fact that the coding technique is readable exclusively by the TS accommodated by each BS.

In the uplink direction the MRC gain is considered equal to 3 dB for the wanted signal and 2 dB for the interferer signal following the same consideration as those made for the MIMO 1x2 system.

According to the numerical analysis provided in Table 16 and Table 17 the additional interference rejection is 3 dB and 1 dB for the DL Traffic and UL Traffic respectively.

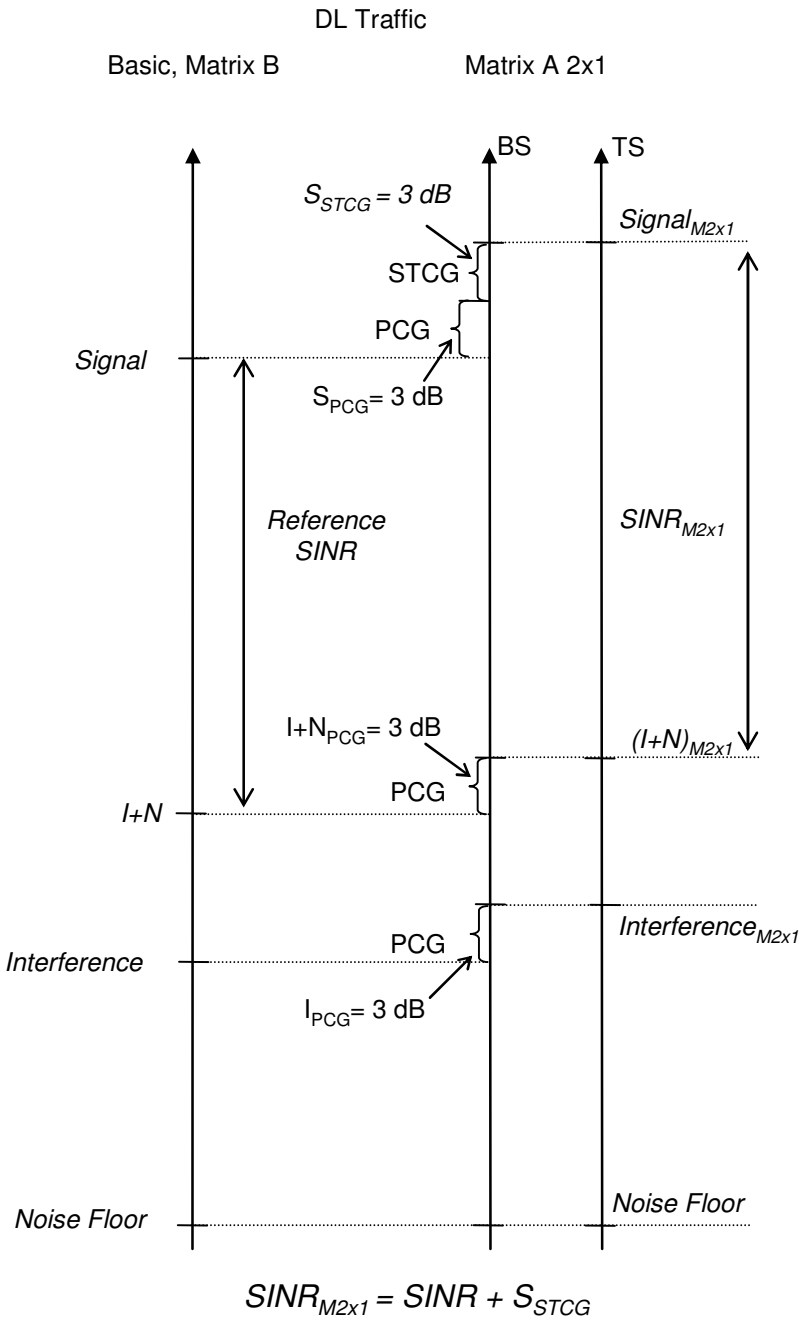

Figure 28: Comparison between a Reference SISO/MIMO-B 2x2 System and a MIMO-A 2x1 System in means of SINR improvement for the DL Traffic.

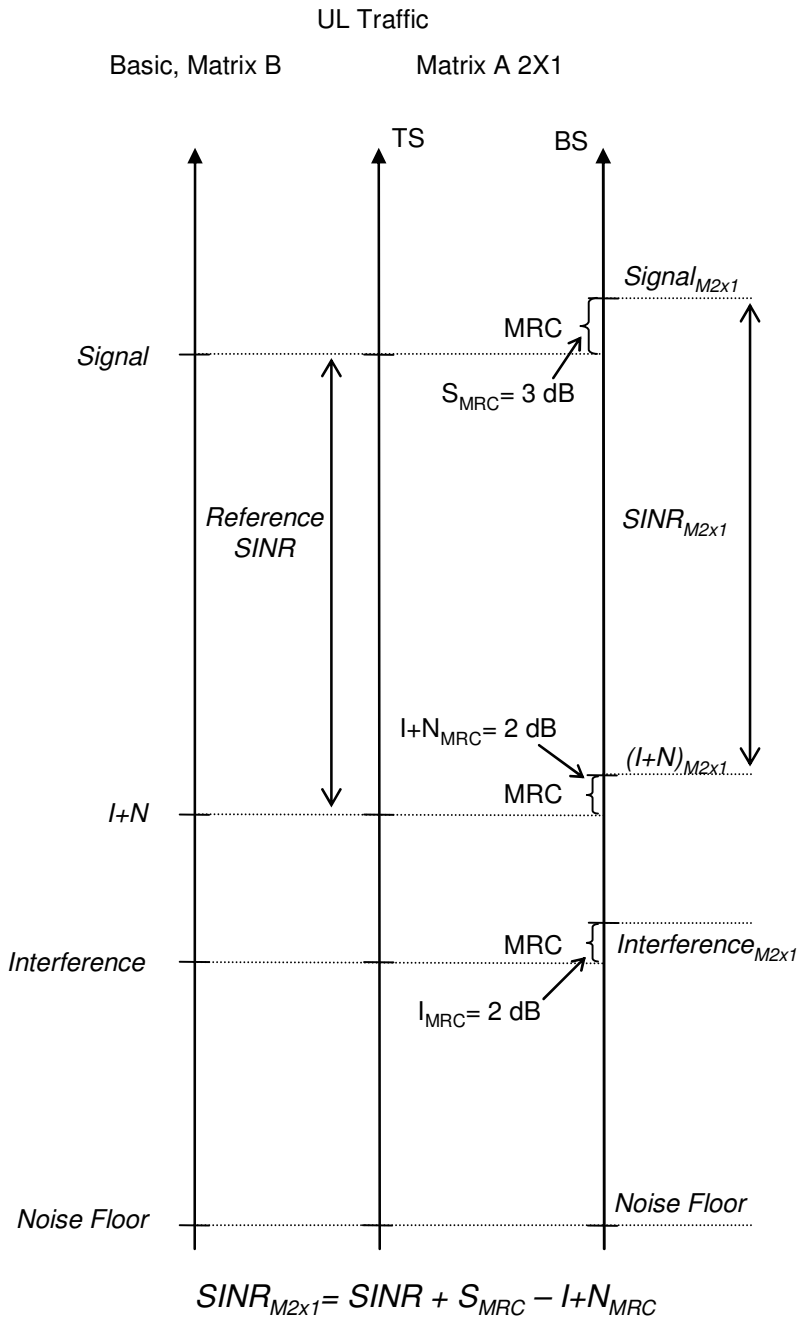

Figure 29: Comparison between a Reference SISO/MIMO-B 2x2 System and a MIMO-A 2x1 System in means of SINR improvement for the UL Traffic.

Table 16: Additional Interference Rejection Estimation of a MIMO-A 2x1 System for the DL Traffic.

DL Traffic	Basic System	MIMO-A 2x1	AAS Technique
RSSI	-60	-60	
	-	3	PCG
	-	3	STCG
	-60	***-54***	
Interference Level	-80	-80	
	-	3	PCG
	-80	***-77***	
Noise Floor	***-100***	***-100***	
I+N	***-79.96***	***-76.98***	
SINR	***19.96***	***22.98***	
Interference Rejection	***3.02***		

Table 17: Additional Interference Rejection Estimation of a MIMO-A 2x1 System for the UL Traffic.

UL Traffic	Basic System	MIMO-A 2x1	AAS Technique
RSSI	-60	-60	
	-	3	MRC
	-60	***-57***	
Interference Level	-80	-80	
	-	2	MRC
	-80	***-78***	
Noise Floor	***-100***	***-100***	
I+N	***-79.96***	***-77.97***	
SINR	***19.96***	***20.97***	
Interference Rejection	***1.01***		

MIMO-A 2X2

The schematic analysis for the MIMO 2x2 system is presented in Figure 30 and Figure 31 for the DL/UL MAP and DL Traffic accompanied by the numerical estimations in Table 18 and Table 19. The corresponding figure and table for the UL Traffic is not presented as long as the AAS technique is the same as in the MIMO-A 2x1 system, resulting in the same analysis presented in Figure 29 and Table 17.

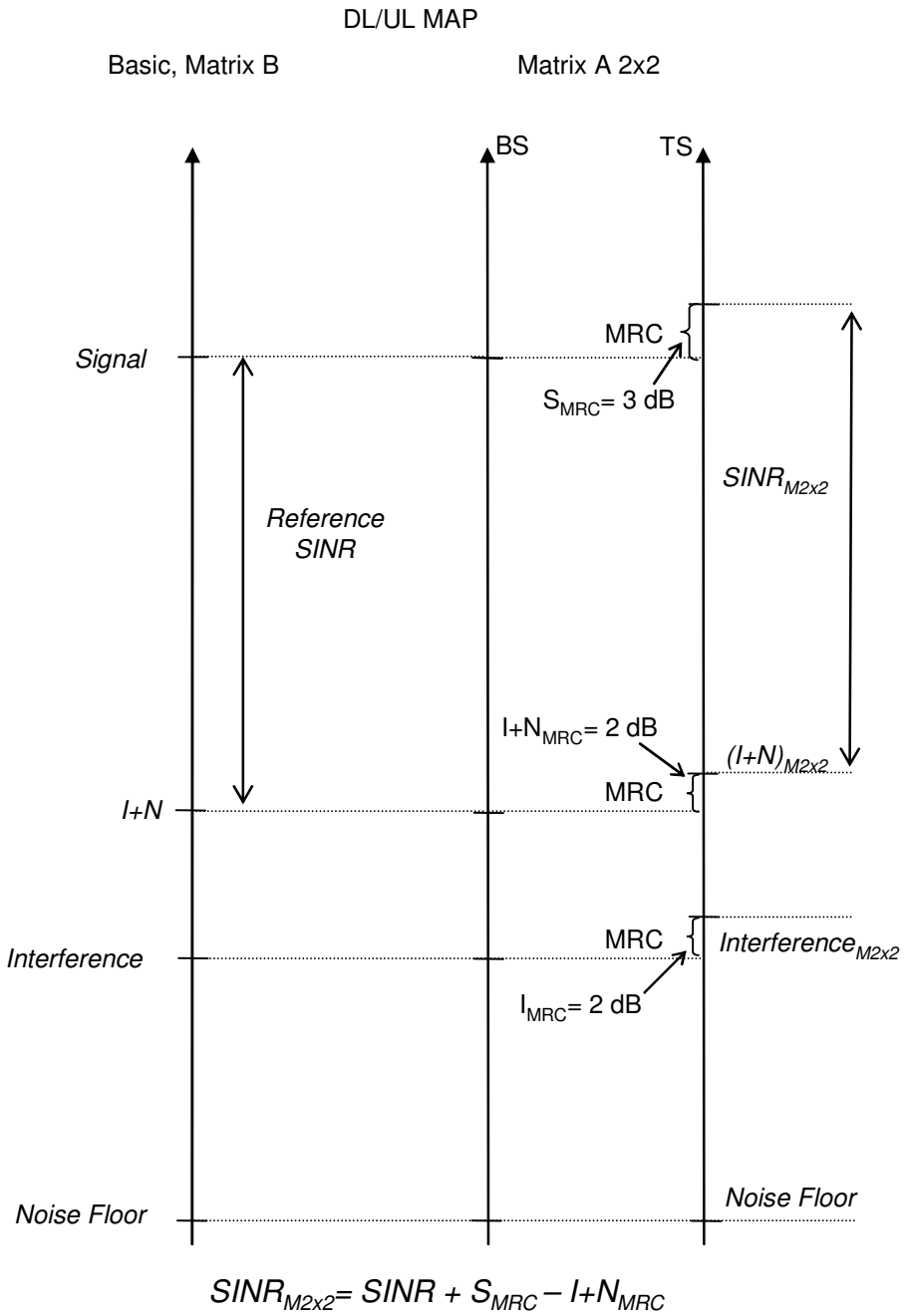

Figure 30: Comparison between a Reference SISO/MIMO-B 2x2 System and a MIMO-A 2x2 System in means of SINR improvement for the DL/UL MAP.

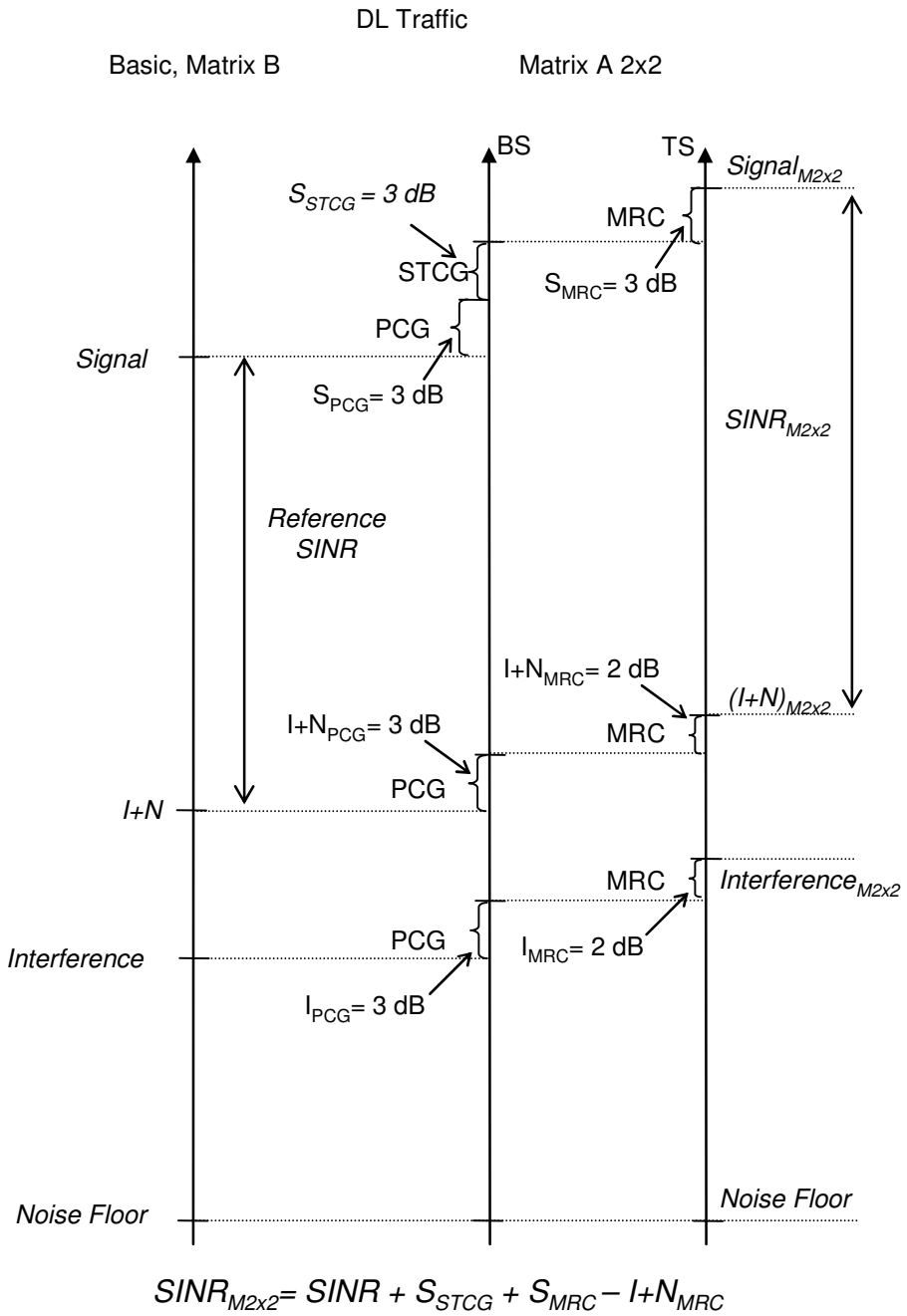

Figure 31: Comparison between a Reference SISO/MIMO-B 2x2 System and a MIMO-A 2x2 System in means of SINR improvement for the DLTraffic.

Table 18: Additional Interference Rejection Estimation of a MIMO-A 2x2 System for the DL/UL MAP.

DL/UL MAP	Basic System	MIMO-A 2x1	AAS Technique
RSSI	-60	-60	
	-	3	MRC
	-60	***-57***	
Interference Level	-80	-80	
	-	2	MRC
	-80	***-78***	
Noise Floor	***-108***	***-108***	
I+N	***-79.99***	***-78***	
SINR	***19.99***	***21***	
Interference Rejection	***1.01***		

Table 19: Additional Interference Rejection Estimation of a MIMO-A 2x2 System for the DL Traffic.

DL Traffic	Basic System	MIMO-A 2x2	AAS Technique
RSSI	-60	-60	
	-	3	PCG
	-	3	STCG
	-	3	MRC
	-60	***-51***	
Interference Level	-80	-80	
	-	3	PCG
	-	2	MRC
	-80	***-75***	
Noise Floor	***-100***	***-100***	
I+N	***-79.96***	***-74.99***	
SINR	***19.96***	***23.99***	
Interference Rejection	***4.03***		

As it can be seen the interference rejection is improved by 1 dB in comparison to the MIMO-A 2x1 system for the DL/UL MAP and DL Traffic, while for the UL Traffic the interference rejection is the same.

BEAM-FORMING 8X2

The Beam-forming technique is considered as the most suitable technique in high interference environments. This can be verified in the schematic and numerical analysis as presented in Figure 32, Figure 33, Table 20 and Table 21.

With the exception of the DL/UL MAP, where the Beam-forming gain cannot be applied as long it has to reach each subscribers wherever it is located inside the service area of the BS, the Beam-forming technique provides significant interference rejection.

The advanced interference rejection capability, is based on the fact that with beamforming the narrow 3-dB beam-width of the wanted BS is steered toward the wanted TS, thus the possibility that an interferer will be at the maximum gain path is reduced. For that reason while the beamforming gain is taken equal to 9 dB for the wanted signal, the corresponding gain for the interferer's signal is considered equal to 3 dB.

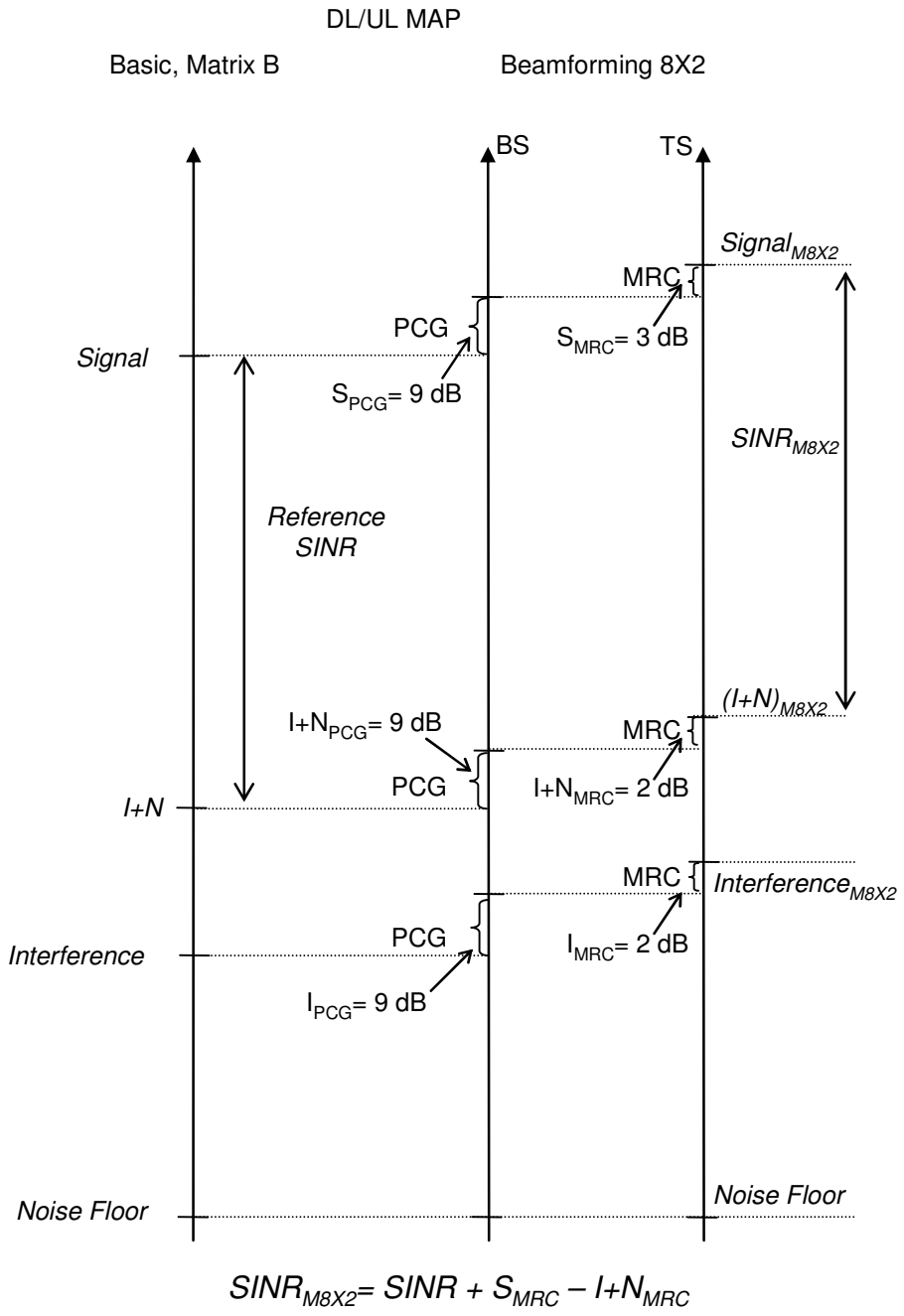

Figure 32: Comparison between a Reference SISO/MIMO-B 2x2 System and a Beam-forming 8x2 System in means of SINR improvement for the DL/UL MAP.

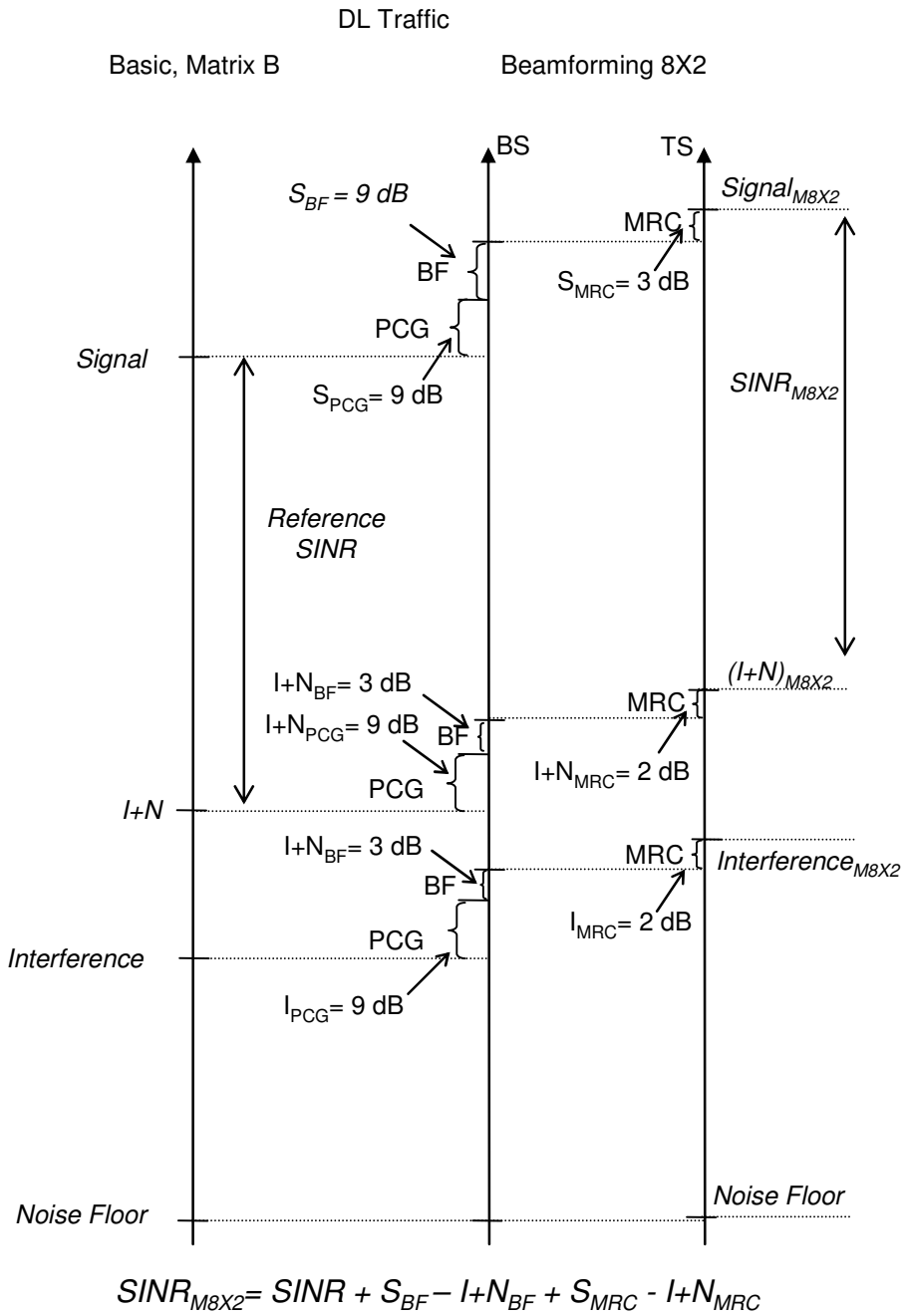

$$SINR_{M8X2} = SINR + S_{BF} - I+N_{BF} + S_{MRC} - I+N_{MRC}$$

Figure 33: Comparison between a Reference SISO/MIMO-B 2x2 System and a Beam-forming 8x2 System in means of SINR improvement for the DL Traffic.

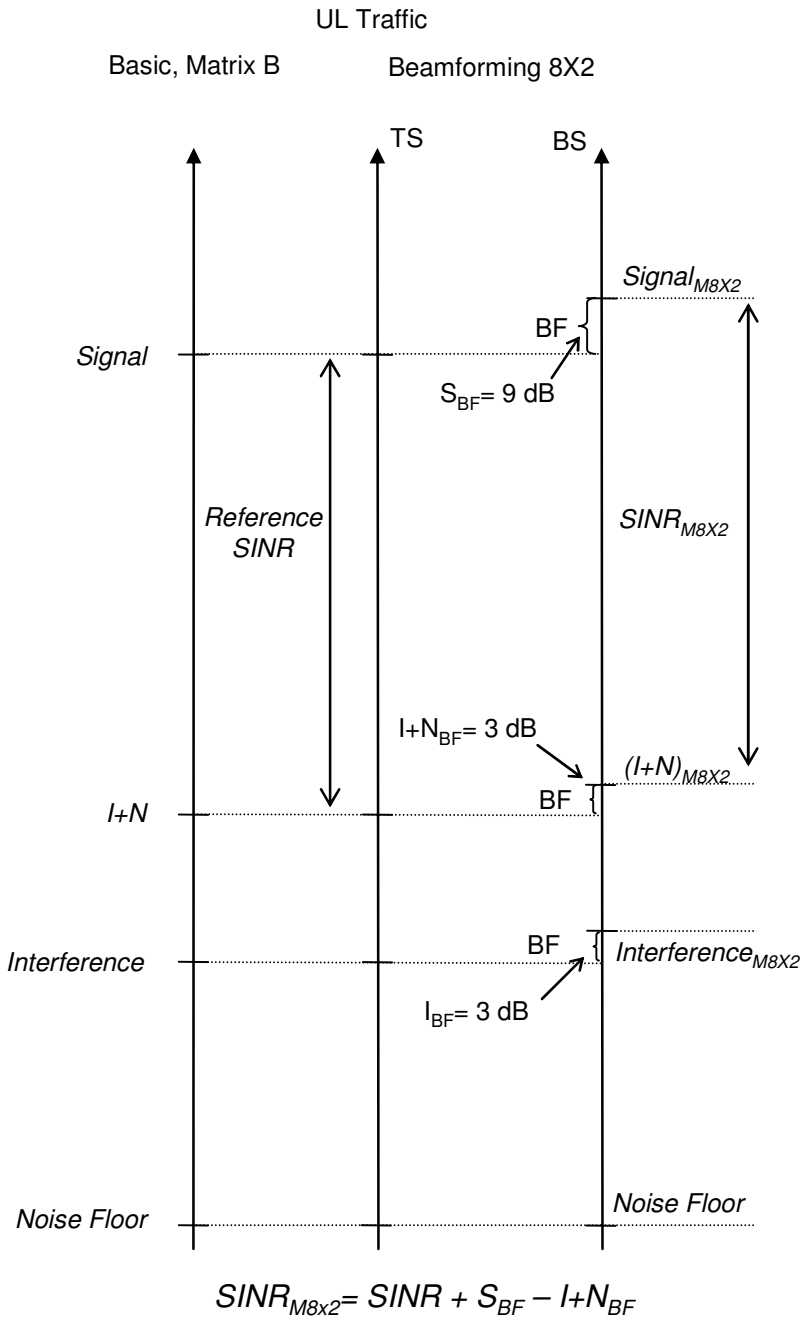

Figure 34: Comparison between a Reference SISO/MIMO-B 2x2 System and a Beam-forming 8x2 System in means of SINR improvement for the UL Traffic.

Table 20: Additional Interference Rejection Estimation of a Beam-forming 8x2 System for the DL/UL MAP.

DL/UL MAP	Basic System	BF 8x2	AAS Technique
RSSI	-60	-60	
	-	9	PCG
	-	3	MRC
	-60	***-48***	
Interference Level	-80	-80	
	-	9	PCG
	-	2	MRC
	-80	***-69***	
Noise Floor	***-108***	***-108***	
I+N	***-79.99***	***-69***	
SINR	***19.99***	***21***	
Interference Rejection	***1.01***		

Table 21: Additional Interference Rejection Estimation of a Beam-forming 8x2 System for the DL Traffic.

DL Traffic	Basic System	MIMO-A 2x2	AAS Technique
RSSI	-60	-60	
	-	9	PCG
	-	9	BF
	-	3	MRC
	-60	***-39***	
Interference Level	-80	-80	
	-	9	PCG
	-	3	BF
	-	2	MRC
	-80	***-66***	
Noise Floor	***-100***	***-100***	
I+N	***-79.96***	***-66***	
SINR	***19.96***	***27***	
Interference Rejection	***7.04***		

Table 22: Additional Interference Rejection Estimation of a Beam-forming 8x2 System for the UL Traffic.

UL Traffic	Basic System	BF 8x2	AAS Technique
RSSI	-60	-60	
	-	9 ←	BF
	-60	***-51***	
Interference Level	-80	-80	
	-	3 ←	BF
	-80	***-77***	
Noise Floor	***-100***	***-100***	
I+N	***-79.96***	***-76.98***	
SINR	***19.96***	***25.98***	
Interference Rejection	***6.02***		

AAS Impact on Performance Overview

In Table 23 the system gain and interference rejection capability of each technique for the are summarized for the DL/UL MAP, DL Traffic and UL Traffic transmission. Those values are utilized for the simulations with the ICS Telecom nG planning tool.

Table 23: System Gain and Interference Rejection for AAS Systems.

System	Sub-frame	Additional Gain (dB) per Technique				Total Gain (dB)	Interfence Rejection
		PCG	STCG	BF	MRC		
MIMO 1X2	DL/UL MAP	-	-	-	3	3	1
	DL Traffic	-	-	-	3	3	1
	UL Traffic	-	-	-	-	0	-
MIMO-A 2X1	DL/UL MAP	-	-	-	-	0	-
	DL Traffic	3	3	-	-	6	3
	UL Traffic	-	-	-	3	3	1
MIMO-A 2X2	DL/UL MAP	-	-	-	3	3	1
	DL Traffic	3	3	-	3	9	4
	UL Traffic	-	-	-	3	3	1
BF 8X2	DL/UL MAP	9	-	-	3	12	1
	DL Traffic	9	-	9	3	21	7
	UL Traffic	-	-	9	-	9	6

5.Simulation Parameters and Configuration

ICS Telecom nG radio planning tool has been utilized in order to perform simulations for evaluation of the performance of the systems presented in the previous section of this study and estimation of the system capacity. ICS telecom nG allows the radio engineer to design WiMAX networks and to analyze what-if scenarios. Among the functionalities used by planners, ICS telecom nG can:

- calculate network coverage taking into account all the aspects of WiMAX networks (adaptive modulation, adaptive antennas, CPE parameters, service flows)
- analyze the coverage over the areas of interest (over a given polygon, over a given clutter class such as urban areas, rooftops, etc…), taking into account the contribution of a subset of stations
- analyze interference

The overall impression is that ICS Telecom nG is a solid tool with infinite capabilities in designing Wireless Networks, which however require extensive configuration. The setup of the simulation parameters as applied in the ICS Telecom nG is discussed in this paragraph.

Propagation Model

The channel models used for the simulations are the Stanford University Interim (SUI) channel models, [33]. The channel parameters are related to terrain type and delay spread. Six channel models are defined for different environments and grouped in 3 categories: SUI-A, SUI-B and SUI-C which are suitable for the terrain categories A B and C defined as:

Category A: Hilly terrain with moderate-to-heavy tree densities (maximum path loss)

Category B: Moderate tree densities (intermediate path loss)

Category C: Mostly flat terrain with light tree densities (low path loss)

The SUI models are based on Hata-Okomura model, which is the most widely used path loss model for signal strength prediction and simulation in macro-cellular environments. Due to the fact that this model is valid for the 500-1500 MHz frequency range and BS antenna heights greater than 30m; frequency and height corrections are applied. Moreover the statistical models proposed by SUI for delay spread and K-factor can be safely used in the 1-4 GHz band.

SUI Models

For a close-in distance of 10m, the median path loss (PL in dB) is given by:

$$PL = A - 10 * \gamma * \log(d) + s$$

The parameter A is defined by $A = 20 * \log(400 * \pi / \lambda)$ where λ is the wavelength in m.

The parameter γ is the path-loss exponent, defined as $\gamma = a - bH_b + c / H_c$ where H_b is the BS antenna height in m and the parameters a, b and c are defined based on the terrain category and consequently on the SUI model that is selected, as presented in Table 24.

Table 24: SUI Propagation Model Components

Parameter	SUI-A	SUI-B	SUI-C
a	4.6	4	3.6
b	0.0075	0.0065	0.005
c	12.6	17.1	20

The parameter s represents the shadowing effect, the values for varying area reliability percentages are presented in Table 25 for the 3 groups of SUI models. The standard deviation is taken equal to 11.8, 11.2 and 9 for SUI-A, SUI-B and SUI-C respectively.

Table 25: Area Reliability Margins for SUI Propagation Models

Area Reliability	Fade Margin		
	SUI-A	SUI-B	SUI-C
99%	26.04	22.57	21.74
98%	19.74	18.66	18.17
95%	14.10	13.52	12.70
93%	11.93	11.45	10.53
90%	8.87	8.87	7.72
85%	5.61	5.45	4.46
80%	2.73	2.73	1.81

This path loss equation is proposed by the Hata-Okomura channel model, as mentioned above this PL equation can be extended by correction factors in order to satisfy frequencies and antenna heights that are not compatible with Hata-Okomura channel model. Two correction factors are applied: the receive antenna height correction factor and the frequency correction factor. The modified pathloss is given by:

$$\Delta PL_M = PL + \Delta PL_H + \Delta PL_F$$

, where ΔPL_H is the receive antenna height correction factor defined as $\Delta PL_H = -10.8 * \log(H_r / 2)$ for SUI-A and SUI-B and $\Delta PL_H = -20 * \log(H_r / 2)$ for SUI-C; and ΔPL_F is the frequency correction factor defined as $\Delta PL_F = 6 * \log(f / 2000)$ where f is the operating frequency in MHz.

In order to satisfy delay spread and K-factor, an additional fast fading margin is introduced to the path loss equation. The values of this margin for varying time availability percentages are presented in Table 26 for the 3 groups of SUI models.

Table 26: Time Availability Margins for SUI Propagation Models.

Time Availability	Fade Margin		
	SUI-A	SUI-B	SUI-C
99.999	50	49	15
99.99	40	39	11
99.9	30	29	8
99	20	19	6
98	17	16	5
95	13	12	4
90	10	9	3

Operating Frequency Band

The WiMAX standard supports the frequency range of 2 to 6 GHz, although other frequency bands can also be accommodated. It is anticipated that additional frequency bands on a regional basis will also be auctioned. WiMAX operates in a mixture of licensed and unlicensed bands. The unlicensed bands are typically the 2.4 GHz and 5.8 GHz bands. Licensed spectrum provides operators control over the usage of the band, allowing them to build a high-quality network. Currently, significant activity is underway in the 2.5 GHz and 3.5 GHz bands, although both those bands are not universally available for wireless access; at least one of them is available in every major country.

System performance varies at different frequencies due to the fact that the path loss is frequency dependent. The parameter A of the path loss equation and also the frequency correction factor ΔPL_F are both frequency dependent. The parameter A is equal to 83 dB for the 3.5 GHz frequency band while for the 2.5 GHz A is equal to 80 dB. The frequency correction factor is around 0.58 dB for 2.5 GHz band while in 3.5 GHz it is around 1.46 dB. Consequently a WiMAX system operating in 3.5 GHz band experiences 4 dB higher path loss in comparison to a similar system operating in 2.5 GHz band, [34].

Moreover, when indoor coverage is required the penetration loss should be taken into account. Penetration throw building walls introduces additional loss to the link budget and this loss depends on the operating frequency. The average penetration loss in dB for the 2.5 and 3.5 GHz band are shown in Table 27,[35].

Table 27: Penetration Loss for 2.5 and 3.5 GHz Band

Frequency Band (GHz)	Penetration Loss (dB)
2.5	10.9
3.5	11.4

Channel Bandwidth

Usually the total available spectrum is limited due to high license costs. For that reason, in order to achieve a more relaxed frequency reuse, 5 MHz channels are used, at the cost of lower per sector throughput. A system that uses a 5 MHz channelization benefits from a lower noise floor level. As it can be evaluated by the noise floor equation the noise floor for a channel of 5 MHz is 3 dB lower than that for 10 MHz channel.

For the simulations with the ATDI ICS Telecom nG, the 2.5 frequency band has been selected, while both 5 and 10 MHz channel have been utilized.

Deployment Scenarios

According to the environment, the customer profile and the offered services, a range of deployment scenarios for WiMAX can be considered:

In urban areas with high population density, a dense network of small cells is necessary to satisfy the requirements for sufficient capacity and NLOS coverage. In addition the cell sizes are further reduced in order to achieve outdoor-to-indoor wireless links feasibility. Given the limited cell edges, the high number of cells and the tight frequency re-use, the system is limited due to co-channel interference rather than the receiver sensitivity. For such scenarios the utilization of licensed spectrum is preferable to minimize the potential for interference among neighboring cells and even among broadband wireless systems from different operators.

A similar approach applies in the WiMAX deployment in suburban areas. Although the population density is moderate, the system is still capacity limited. The cell sizes are a bit larger, however an extended network is necessary since suburban environments usually extend in large geographical areas. Given the limited available spectrum in the licensed bands and the high frequency re-use, the system is considered interference limited. NLOS is a requirement in this scenario also.

In suburban to rural areas, the population density is limited and hence the main deployment objective is to fulfill the coverage requirements, while minimizing the infrastructure costs. The cell sizes are large, typically range or terrain limited and the receiver sensitivity now becomes the restricting factor, as interference is negligible. In the case of rural areas the use of spectrum in the 5 GHz band is also possible, however only for TDD systems according to the standard.

Regarding the cell edges considered above, it should be noted that in all the deployments scenarios the cell edge depends also on the specifications of the subscriber devices. For each different type of access –fixed, portable, mobile- different types of devices are used, and the system performance varies with the type of the device. Consequently, when a network is designed to offer coverage with PCMCIA the cells are reduced in comparison to a network that is designed for indoor terminals for two reasons: system range and spectral efficiency.

For the simulation with the ATDI ICS Telecom nG, two different deployment scenarios have been selected:

- Indoor Scenario: Urban deployment scenario with 500 m distance between the BSs and TS equipped with PCMCIA card, positioned at the 1st floor (5 m AGL) inside the building.

- Outdoor Scenario: Urban deployment scenario with 500 m distance between the BSs and TS equipped with PCMCIA card, positioned at the street level (1.5m AGL).

For the simulations of both scenarios, SUI-B propagation model is selected with 90% area availability and 95% time reliability introducing 8.87 dB and 12 dB additional losses. Moreover for the indoor simulations 11 dB penetration loss is considered by the outer walls of the building, while the additional losses that may be applied from the inner walls of each building cannot be estimated as long as these losses vary with the architecture of the building and the constructive materials as well as by the furniture of each room. For that reason in the outdoor-to-indoor propagation it is considered that the TS is positioned just behind the outer wall of the building.

Sectorization Schemes and Frequency Planning

Due to high deployment cost of WiMAX BSs, omni cells are not usually meet in WiMAX networks. The more cost effective Tri-Sector cells (hexagonal) as well as Quad-Sector cells (square) are usually deployed.. Moreover due to the limited spectrum availability in the licensed bands and the high costs of spectrum renting tight frequency re-use schemes are a common characteristic in real world WiMAX deployments.

In the simulations 2 frequency re-use patterns are considered, the 1x3x1 and 1x3x3 as shown in Figure 35. It should be noted that as long as the PCMCIA cards are equipped with omni-directional antennas, rotation of the frequency plan between neighbor sectors, wouldn't have any positive impact on the network performance.

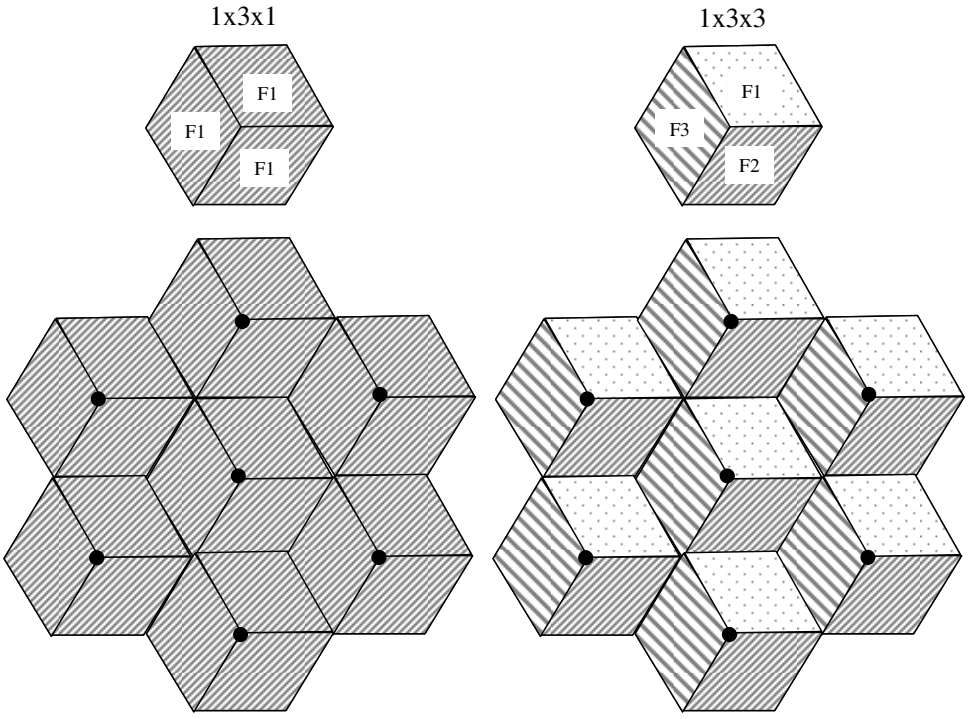

Figure 35: 1x3x1 and 1x3x3 Frequency Re-Use Pattern

Planning Tool Configuration

The parameters used for the configuration of the ICS Telecom nG planning tool are summarized for each system in this paragraph.

Reference System

The simulation parameters for the reference SISO system or the MIMO-B 2x2 system are shown in Table 28. As it can be seen the first simulation considers an outdoor-to-indoor propagation while the second simulation considers an outdoor one. For the outdoor-to-indoor simulation the TS are PCMCIA cards equipped with a 2 dBi omni antenna positioned in the 1st floor of a building (5m AGL). For the outdoor simulation the PCMCIA card is positioned at the street-level (1m). Regarding the BS antenna, a 60o directional antenna with 16 dBi antenna gain is used, at 25m AGL. The values for the propagation parameters have been selected based on the consideration made in the previous chapter.

Table 28: Simulation Parameters for the Reference System

Scenario		Indoor	Outdoor
Base Station Paremeters	Power (dBm) - DL Direction	30	30
	Antenna Gain (dBi)	16	16
	3-dB Beamwidth (^{o})	60	60
	Antenna Elements	1	1
	Antenna Height (m)	25	25
	Downtilt (^{o})	4	4
Terminal Station Parameters	Power (dBm) - UL Direction	24	24
	Antenna Gain (dBi)	2	2
	Antenna Type	Omni	Omni
	Antenna Elements	1	1
	Antenna Height (m)	5	1.5
Propagation Model Paramteres	Model	SUI-B	SUI-B
	Area Availability	90%	90%
	Shadowing Margin (dB)	9	9
	Time Reliability	95%	95%
	Fast Fading Margin (dB)	12	12
	Penetration (dB)	11	-
Channel Parameters	Frequency Band (GHz)	2.5	2.5
	Channel Bandwidth (MHz)	5	5

MIMO 1x2 System

The simulation parameters for the MIMO 1x2 System are shown in Table 29. As it can be seen MRC capability at the TS has been considered and 3dB are added in the DL direction.

Table 29: Simulation Parameters for the MIMO 1x2 System

Scenario		Indoor	Outdoor
Base Station Paremeters	Power (dBm) - DL Direction	30	30
	Antenna Gain (dBi)	16	16
	3-dB Beamwidth (^{o})	60	60
	Antenna Elements	1	1
	Antenna Height (m)	25	25
	Downtilt (^{o})	4	4
Terminal Station Parameters	Power (dBm) - UL Direction	24	24
	Antenna Gain (dBi)	2	2
	Antenna Type	Omni	Omni
	Antenna Elements	2	2
	Antenna Height (m)	5	1.5
	MRC	√	√
Propagation Model Paramteres	Model	SUI-B	SUI-B
	Area Availability	90%	90%
	Shadowing Margin (dB)	9	9
	Time Reliability	95%	95%
	Fast Fading Margin (dB)	12	12
	Penetration (dB)	11	-
Channel Parameters	Frequency Band (GHz)	2.5	2.5
	Channel Bandwidth (MHz)	5	5

MIMO-A 2x1 System

The simulation parameters for the MIMO-A 2x1 System are defined in Table 30. The PC gain is applied only in the traffic transmissions, while STC and MRC capability at the BS has been considered by adding 3 dB gain in DL and UL sub-frame simulations respectively.

Table 30: Simulation Parameters for the MIMO-A 2x1 System

Scenario		Indoor	Outdoor
Base Station Paremeters	Power (dBm) - DL Direction	30	30
	Antenna Gain (dBi)	16	16
	3-dB Beamwidth (^{o})	60	60
	Antenna Elements	2	2
	Antenna Height (m)	25	25
	Downtilt (^{o})	4	4
	PC	√	√
	STC	√	√
	MRC	√	√
Terminal Station Parameters	Power (dBm) - UL Direction	24	24
	Antenna Gain (dBi)	2	2
	Antenna Type	Omni	Omni
	Antenna Elements	1	1
	Antenna Height (m)	5	1.5
Propagation Model Paramteres	Model	SUI-B	SUI-B
	Area Availability	90%	90%
	Shadowing Margin (dB)	9	9
	Time Reliability	95%	95%
	Fast Fading Margin (dB)	12	12
	Penetration (dB)	11	-
Channel Parameters	Frequency Band (GHz)	2.5	2.5
	Channel Bandwidth (MHz)	5	5

MIMO-A 2x2 System

For the simulations of the MIMO-A 2x2 system MRC is considered also in the TS, as it can be seen in Table 31, thus adding 3 more dB in the DL direction in comparison with the MIMO-A 2x1 system configuration.

Table 31: Simulation Parameters for the MIMO-A 2x2 System

Scenario		Indoor	Outdoor
Base Station Paremeters	Power (dBm) - DL Direction	30	30
	Antenna Gain (dBi)	16	16
	3-dB Beamwidth (^{o})	60	60
	Antenna Elements	2	2
	Antenna Height (m)	25	25
	Downtilt (^{o})	4	4
	PC	√	√
	STC	√	√
	MRC	√	√
Terminal Station Parameters	Power (dBm) - UL Direction	24	24
	Antenna Gain (dBi)	2	2
	Antenna Type	Omni	Omni
	Antenna Elements	2	2
	Antenna Height (m)	5	1.5
	MRC	√	√
Propagation Model Paramteres	Model	SUI-B	SUI-B
	Area Availability	90%	90%
	Shadowing Margin (dB)	9	9
	Time Reliability	95%	95%
	Fast Fading Margin (dB)	12	12
	Penetration (dB)	11	-
Channel Parameters	Frequency Band (GHz)	2.5	2.5
	Channel Bandwidth (MHz)	5	5

Beam-forming 8x2 System

In Table 32 the simulation parameters for the Beam-forming 8x2 system are presented, PCG is considered as equal to 9 dB and applied to the entire DL and UL sub-frame, while Beam-forming gain is applied to only to the DL and UL Traffic resulting in 9 dB additional gain for these channels.

It should be noted that 120^o directional antennas are considered for the BSs, as it is common deployment for beam-forming systems due to the fact that the interference rejection of the narrower 60^o directional antenna is not necessary when Beam-forming is implemented.

Table 32: Simulation Parameters for the Beam-forming 8x2 System

Scenario		Indoor	Outdoor
Base Station Paremeters	Power (dBm) - DL Direction	39	39
	Antenna Gain (dBi)	16	16
	3-dB Beamwidth (^{o})	120	120
	Antenna Elements	8	8
	Antenna Height (m)	35	35
	Downtilt (^{o})	4	4
	PC	√	√
	Beam-forming	√	√
Terminal Station Parameters	Power (dBm) - UL Direction	24	22
	Antenna Gain (dBi)	2	2
	Antenna Type	Omni	Omni
	Antenna Elements	2	2
	Antenna Height (m)	5	1.5
	MRC	√	√
Propagation Model Paramteres	Model	SUI-B	SUI-B
	Area Availability	90%	90%
	Shadowing Margin (dB)	9	9
	Time Reliability	95%	95%
	Fast Fading Margin (dB)	12	12
	Penetration (dB)	11	11
Channel Parameters	Frequency Band (GHz)	2.5	2.5
	Channel Bandwidth (MHz)	5	5

6.Simulation Results

The use of AAS Technologies enables the network operator to increase the wireless network performance in means of capacity and coverage. Depending on the demands of each network the appropriate technology can be selected.

In city center deployment scenarios, for example, where the density of users is high, the traffic load will be enormous. In order to meet this high capacity demand, especially in limited available bandwidth occasions, higher frequency re-use will have to be used. This will lead to an interference limited network performance. In order to satisfy the capacity demands of such a network in association with higher frequency re-use schemes that will cause higher interference levels, one of the available AAS technologies can be selected by the network operator.

Scope of this chapter is to identify the exact advantages of each technology in means of coverage in high interference levels environments through simulations with ICS Telecom nG planning tool.

Reference System

As it has been presented in the previous paragraph, for the reference system the lowest system gain appears in the DL sub-frame; for that reason the RSS maps of the DL Traffic is presented in Figure 36 and Figure 37 for the indoor and outdoor scenario respectively. Those maps depict the total area that the system is actually able to cover in an interference free environment for both scenarios.

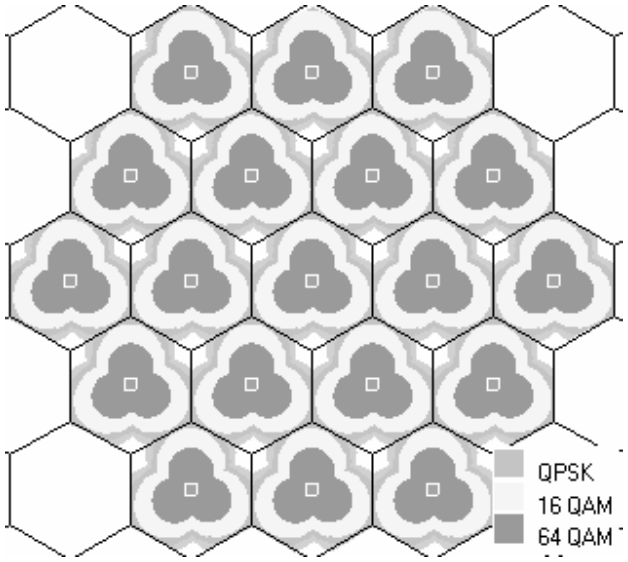

Figure 36: DL Traffic RSS Map for Tri-Sector Cells – Reference System, PCMCIA, Indoor, 1st Floor.

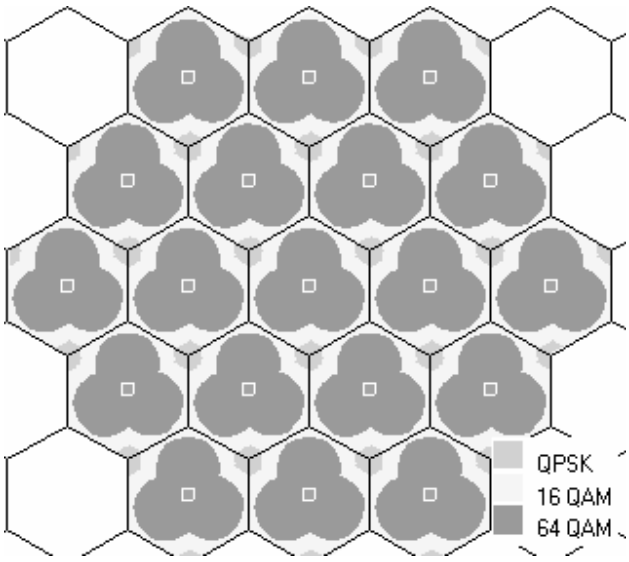

Figure 37: DL Traffic RSS Map for Tri-Sector Cells – Reference System, PCMCIA, Outdoor Street Level.

In urban environments, where dense networks are deployed, the dominant component for PHY mode allocation is the interference. For that reason the SINR maps depict the real PHY mode map for the network. Based on this idea for the course of this document the SINR maps for each system will be presented, for 1x3x1 and 1x3x3 frequency re-use schemes.

Taking into account that a denser network is not easily meet in WiMAX networks due to the high deployment costs, it can be considered that the resulting ranges are the lowest ranges that a system is able to achieve for the scenarios that are investigated.

1x3x1 Scheme

The signaling parts of both the DL and UL sub-frame, have to be received by all the TSs served by each BS. For that reason, the SINR based coverage area is limited by the sub-frame with the shortest SINR based coverage area

For a noise dominant environment it is easy to conclude that the limiting sub-frame is that with the lowest system gain, but in an interference dominant environment the limiting sub-frame arises from a combination of low system gain and low interference rejection capability.

The reference SISO system is limited in means of system gain by the DL/UL MAP and DL Traffic gain, while the interference rejection capability is the same for DL/UL MAP, DL Traffic and UL Traffic: 0 dB for the co-channel, 26 dB for the first adjacent channel and 45 dB for the second adjacent channel.

In Figure 38 the PHY mode map of the central BS for the indoor scenario is presented. In comparison to Figure 36, where the RSSI map is presented, significant degradation can be observed.

It should be noted that 64 QAM PHY mode is not considered for the UL direction and also the ranges for each PHY mode refer to the lowest coding rate for each modulation, i.e. “64 QAM” refers to 64 QAM 2/3.

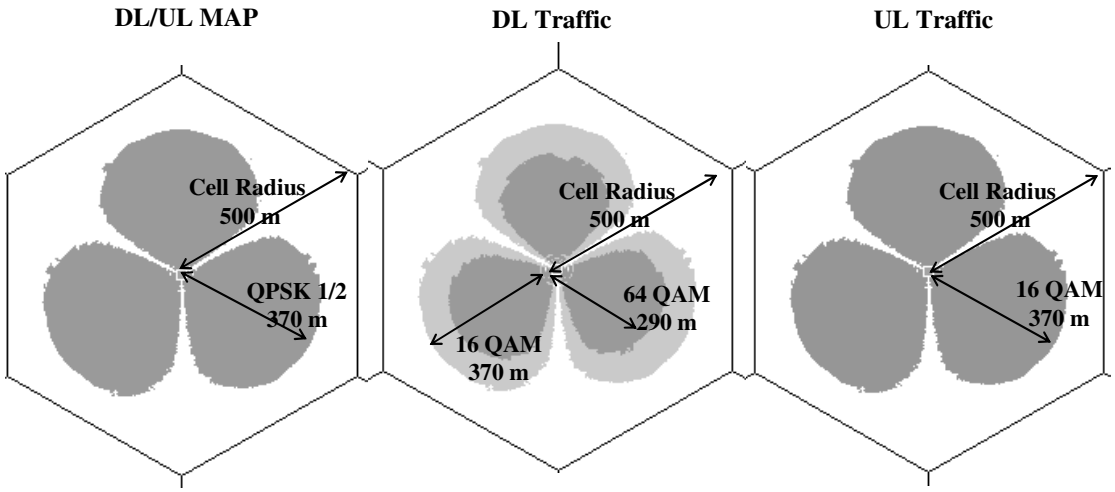

Figure 38: SINR Map for the Central BS – Reference System, PCMCIA, Indoor 1st floor, 1x3x1 Scheme

In Figure 39 the PHY mode regions for the street level coverage are presented.

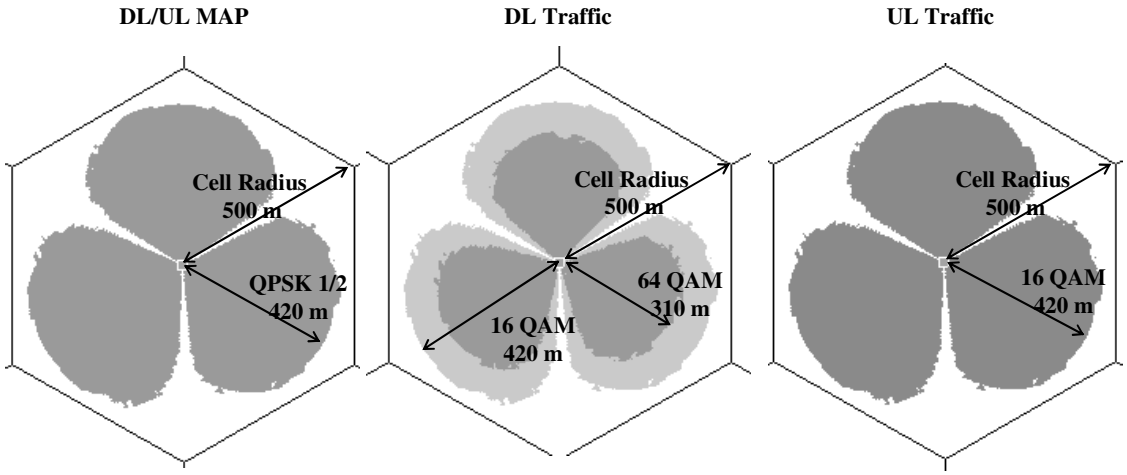

Figure 39: SINR Map for the Central BS – Reference System, PCMCIA, Street Level, 1x3x1 Scheme

As it can be seen, the indoor 1st floor scenario achieves lower ranges than the outdoor street-level scenario due to the fact that that an additional 11 penetration loss is considered.

A more detailed presentation of the PHY mode regions inside the cell area can be seen in Table 33 and Table 34 for the DL and UL Traffic respectively. As it can be observed the performance of the system is better when the TS is positioned in an outdoor environment despite the fact that a lower height for the TS antenna is considered. The factor for the low performance of the indoor scenario is the losses applied from the outer walls of the building (penetration loss).

In specific, the BS is able to achieve 7.4% better coverage in the outdoor scenario in comparison to the indoor, while the area that can be served with the highest PHY mode is

8.5% larger. However, the reference system is not able to achieve blanket coverage in such a dense network where the spacing between the BSs is 500m and only one frequency channel is used (1x3x1 frequency re-use scheme).

Table 33: PHY Mode Regions Percentages Over the Total Cell Area. For the DL Traffic - Reference System, 1x3x1

PHY Mode	Reference 1x3x1 DL	
	Indoor	Outdoor
No Coverage	53.2%	36.9%
QPSK-1/2	0.0%	0.0%
QPSK-3/4	0.0%	0.0%
16 QAM-1/2	4.2%	5.8%
16 QAM-3/4	18.7%	23.7%
64 QAM-2/3	2.8%	3.7%
64 QAM-3/4	21.1%	29.8%

Table 34: PHY Mode Regions Percentages Over the Total Cell Area. For the UL Traffic -Reference System, 1x3x1

PHY Mode	Reference 1x3x1 UL	
	Indoor	Outdoor
No Coverage	53.2%	36.9%
QPSK-1/2	0.0%	0.0%
QPSK-3/4	0.0%	0.0%
16 QAM-1/2	0.2%	0.6%
16 QAM-3/4	46.6%	62.5%

1x3x3 Scheme

The corresponding SINR maps for the 1x3x3 frequency re-use scheme are presented in Figure 40 and Figure 41 for the indoor and the outdoor scenario respectively.

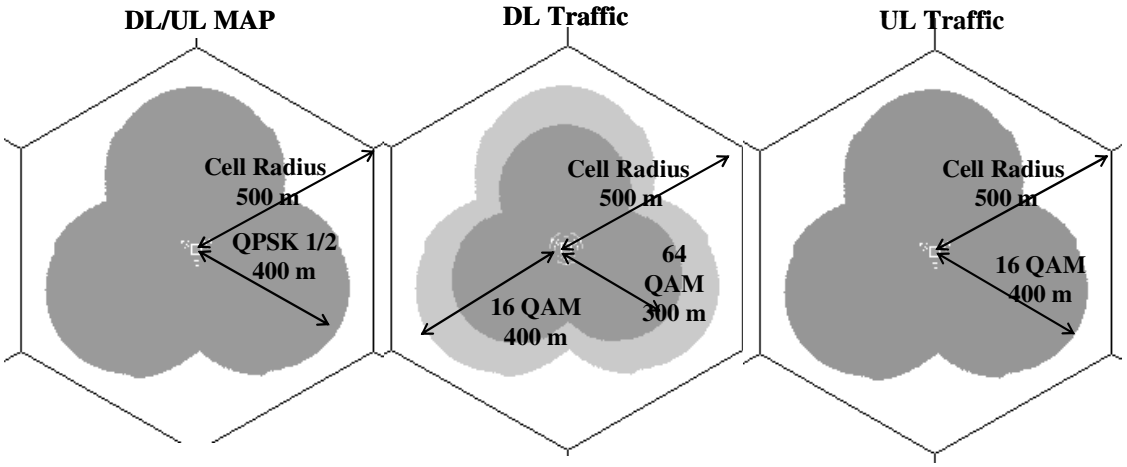

Figure 40: SINR Map for the Central BS – Reference System, PCMCIA, Indoor First floor, 1x3x3 Scheme

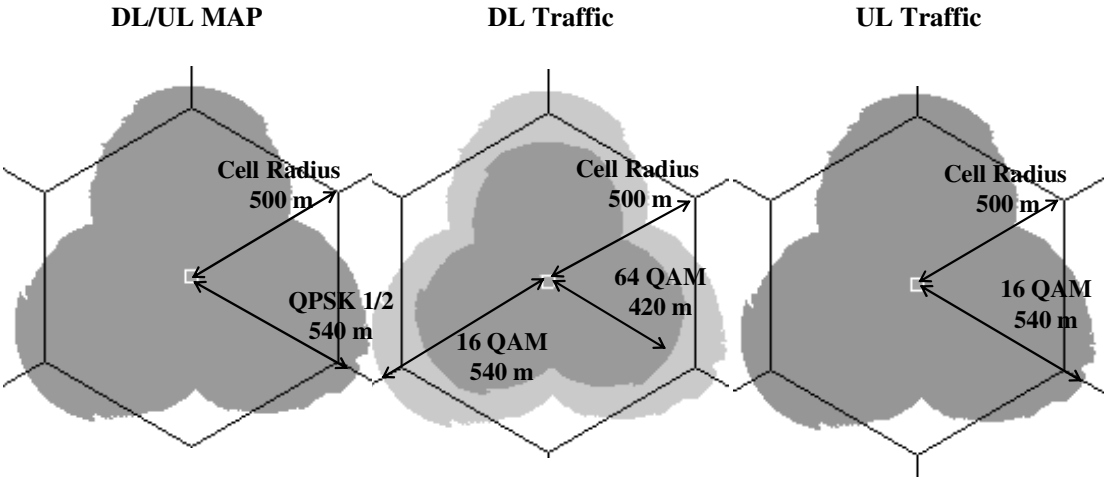

Figure 41: SINR Map for the Central BS – Reference System, PCMCIA, Street Level, 1x3x3 Scheme

As it can be seen, the 1x3x3 schemes achieves better performance in comparison to the 1x3x1, resulting in overlapping cells.

The PHY mode regions percentages are presented in Table 35 and Table 36 for the DL and UL direction respectively. The coverage area of the 1x3x3 scheme is 12.5% higher than that

of the 1x3x1 in the indoor 1st floor scenario while regarding the outdoor street-level coverage, the improvement is 26% of the cell area.

Table 35: PHY Mode Regions Percentages Over the Total Cell Area. For the DL Traffic - Basic System, 1x3x3

PHY Mode	Reference 1x3x3 DL	
	Indoor	Outdoor
No Coverage	40.7%	10.8%
QPSK-1/2	0.0%	0.0%
QPSK-3/4	0.0%	0.0%
16 QAM-1/2	5.4%	2.6%
16 QAM-3/4	20.5%	24.2%
64 QAM-2/3	6.4%	5.0%
64 QAM-3/4	30.0%	57.4%

Table 36: PHY Mode Regions Percentages Over the Total Cell Area. For the UL Traffic -Reference System, 1x3x3

PHY Mode	Reference 1x3x3 UL	
	Indoor	Outdoor
No Coverage	40.7%	10.8%
QPSK-1/2	0.0%	0.0%
QPSK-3/4	0.0%	0.0%
16 QAM-1/2	1.5%	4.2%
16 QAM-3/4	57.8%	85.0%

MIMO 1x2 System

According to the previous paragraph where the performance improvement of each system is presented the limiting sub-frame for the MIMO 1x2 system regarding the system gain is the DL sub-frame and an 1 dB interference rejection is introduced to the system in the DL/UL MAP and the DL Traffic. In contrast to the reference system where it was easy to conclude that the system is limited by the DL sub-frame; in the MIMO 1x2 system where the interference rejection capability varies with the sub-frame, simulations have to be performed in order to identify the limiting sub-frame, as long as the system gain of the UL sub-frame is higher than that of the DL sub-frame but the absence of additional interference rejection capability may render it the limiting sub-frame.

1x3x1 Scheme

In Figure 42 and Figure 43 the SINR maps for the indoor and outdoor scenario in 1x3x1 frequency re-use are presented.

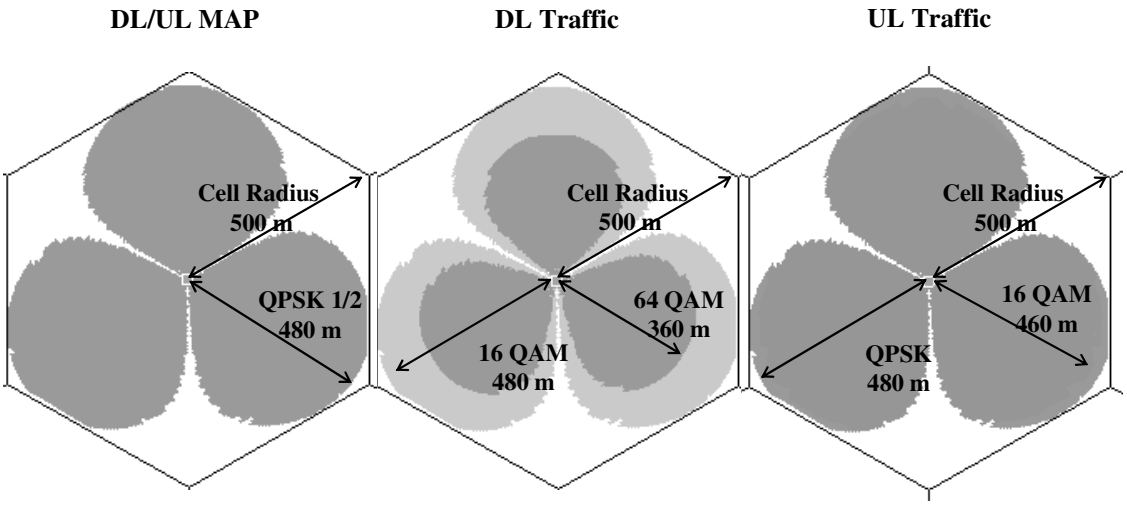

Figure 42: SINR Map for the Central BS – MIMO 1x2, PCMCIA, Indoor 1st Floor, 1x3x1 Scheme

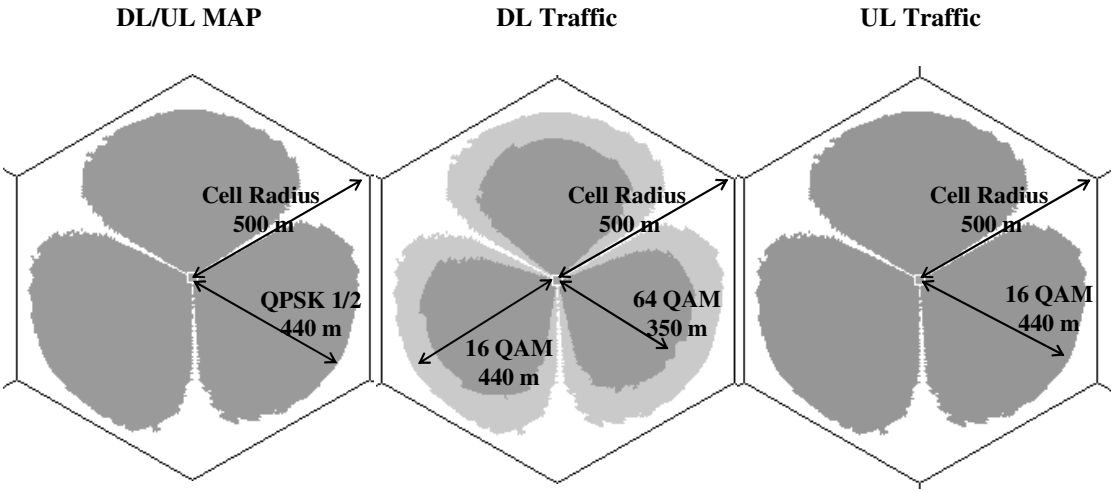

Figure 43: SINR Map for the Central BS – MIMO 1x2, PCMCIA, Street Level, 1x3x1 Scheme

An interesting observation that can be made is that the range of the outdoor scenario is lower than that of the indoor scenario. This is due to the fact that in the indoor scenario the TS is positioned at 5m resulting in lower path-loss. However, the total covered area is larger for the outdoor scenario and higher spectral efficiency is observed too.

The PHY mode regions percentages for the 1x3x1 scheme are presented in Table 37 and Table 38.

Table 37: PHY Mode Regions Percentages Over the Total Cell Area. For the DL Traffic - MIMO 1x2, 1x3x1

PHY Mode	MIMO 1x2 1X3X1 DL	
	Indoor	Outdoor
No Coverage	25.99%	29.5%
QPSK-1/2	0.00%	0.0%
QPSK-3/4	0.00%	0.0%
16 QAM-1/2	7.63%	5.1%
16 QAM-3/4	28.93%	25.2%
64 QAM-2/3	4.51%	4.0%
64 QAM-3/4	32.94%	36.2%

Table 38: PHY Mode Regions Percentages Over the Total Cell Area. For the UL Traffic - MIMO 1x2, 1x3x1

PHY Mode	MIMO 1x2 1X3X1 UL	
	Indoor	Outdoor
No Coverage	25.99%	29.5%
QPSK-1/2	0.0%	0.00%
QPSK-3/4	5.2%	0.00%
16 QAM-1/2	14.0%	6.91%
16 QAM-3/4	54.77%	63.60%

1x3x3 Scheme

In Figure 44 and Figure 45 the SINR maps for the two scenarios are presented when 1x3x3 frequency re-use scheme is applied.

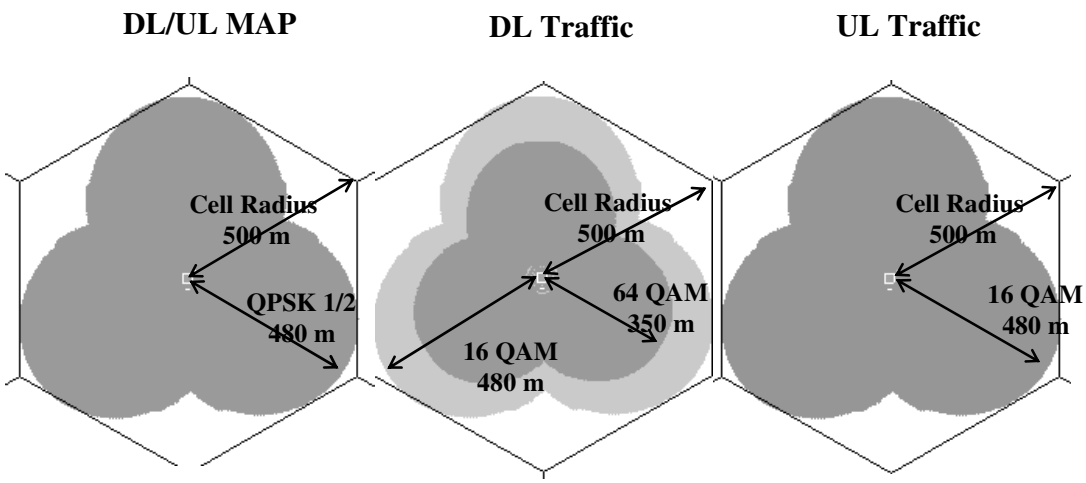

Figure 44: SINR Map for the Central BS – MIMO 1x2, PCMCIA, Indoor 1st Floor, 1x3x3 Scheme

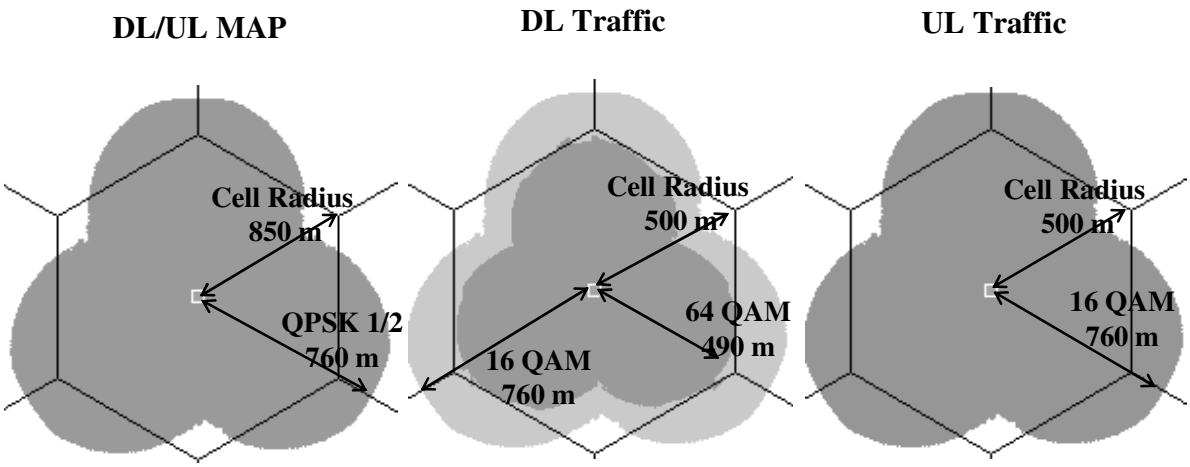

Figure 45: SINR Map for the Central BS – MIMO 1x2, PCMCIA, Street Level, 1x3x3 Scheme

The percentages of each PHY mode region over the total cell area are presented in Table 39 and Table 40 . As it can be seen, the uncovered cell area is greater for this

Table 39: PHY Mode Regions Percentages Over the Total Cell Area. For the DL Traffic - MIMO 1x2, 1x3x3

PHY Mode	MIMO 1x2 1X3X3 DL	
	Indoor	Outdoor
No Coverage	21.01%	5.3%
QPSK-1/2	0.00%	0.0%
QPSK-3/4	0.00%	0.0%
16 QAM-1/2	7.00%	1.4%
16 QAM-3/4	26.61%	14.8%
64 QAM-2/3	4.32%	6.7%
64 QAM-3/4	41.06%	71.7%

Table 40: PHY Mode Regions Percentages Over the Total Cell Area. For the UL Traffic - MIMO 1x2, 1x3x3

PHY Mode	MIMO 1x2 1X3X3 UL	
	Indoor	Outdoor
No Coverage	21.0%	5.3%
QPSK-1/2	0.0%	0.0%
QPSK-3/4	0.0%	0.0%
16 QAM-1/2	0.0%	0.0%
16 QAM-3/4	79.0%	94.7%

Due to the fact that the DL sub-frame is the limiting factor of the system, the interference rejection of the DL/UL MAP sub-frame results in coverage extension for the total frame. For

that reason the resulting uncovered area of both scenarios and frequency reuse patterns is decreased in contrast to the reference system.

MIMO-A 2x1 System

The MIMO-A 2x1 system is limited in means of system gain by the signaling part of the DL sub-frame. Through the fact that no additional interference rejection is applied to the DL/UL MAP in MIMO-A 2x1 system, it can be concluded that the coverage remains limited of the DL sub-frame transmission in an interference dominant environment.

1x3x1 Scheme

The SINR maps for all the DL and UL sub-frame of the indoor and outdoor scenario are presented in Figure 46 and Figure 47.

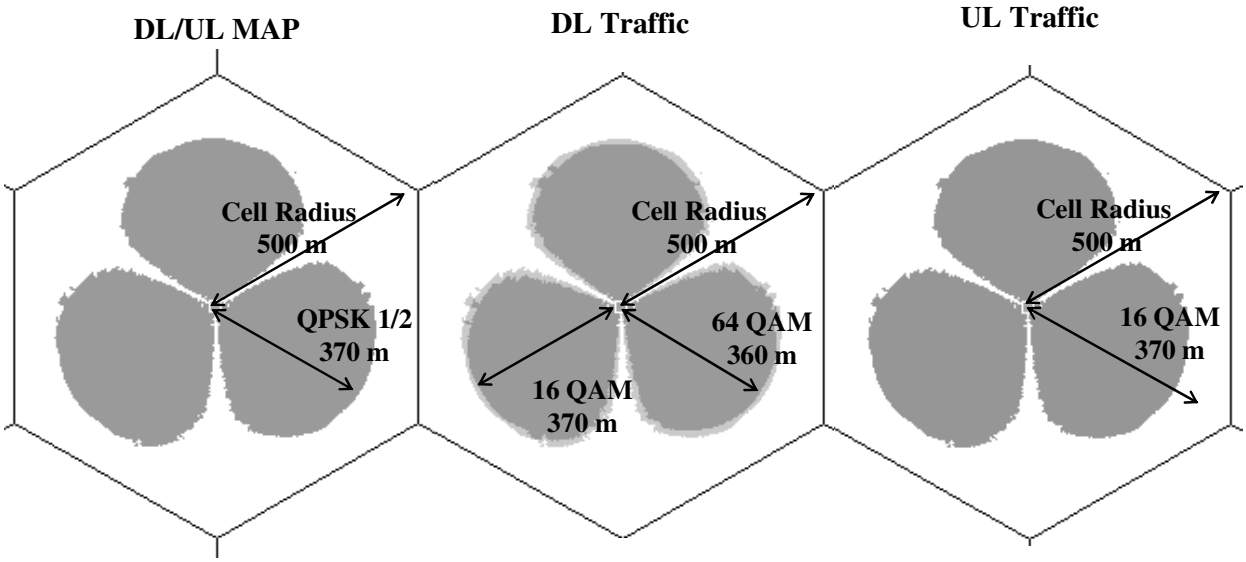

Figure 46: SINR Map for the Central BS – MIMO-A 2x1, PCMCIA, Indoor 1st Floor, 1x3x1 Scheme

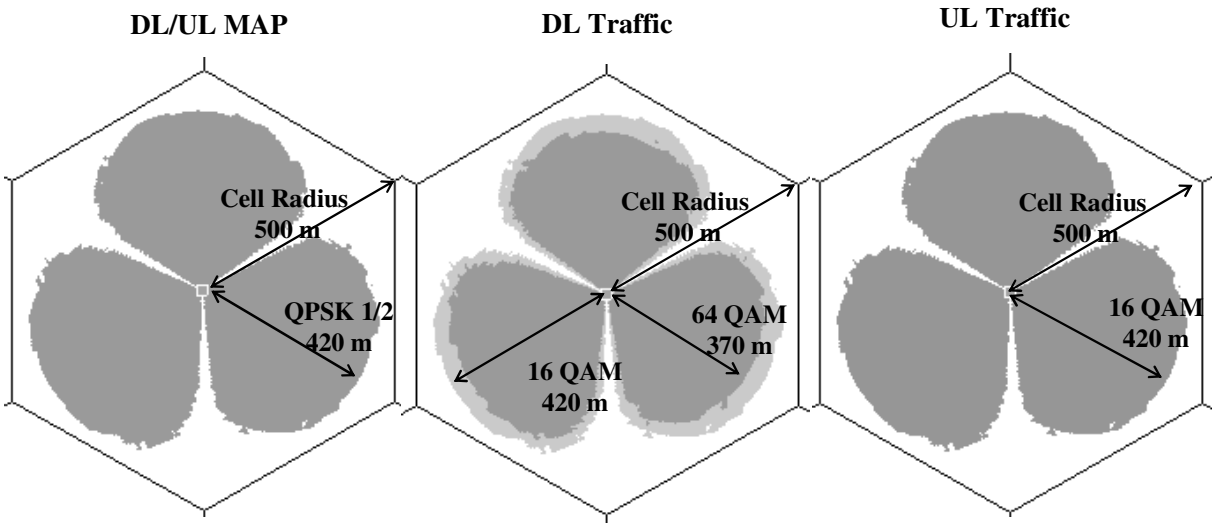

Figure 47: SINR Map for the Central BS – MIMO-A 2x1, PCMCIA, Street Level, 1x3x1 Scheme

The PHY mode regions percentages are presented in Table 41 and Table 42 for the 1x3x1 frequency re-use scheme.

Table 41: PHY Mode Regions Percentages Over the Total Cell Area. For the DL Traffic Channel- MIMO-A 2x1, 1x3x1

PHY Mode	MIMO-A 2x1 1X3X1 DL	
	Indoor	Outdoor
No Coverage	53.2%	36.9%
QPSK-1/2	0.0%	0.0%
QPSK-3/4	0.0%	0.0%
16 QAM-1/2	0.0%	0.0%
16 QAM-3/4	5.4%	13.9%
64 QAM-2/3	4.5%	4.3%
64 QAM-3/4	36.9%	44.9%

Table 42: PHY Mode Regions Percentages Over the Total Cell Area. For the UL Traffic Channel- MIMO-A 2x1, 1x3x1

PHY Mode	MIMO-A 2x1 1X3X1 UL	
	Indoor	Outdoor
No Coverage	53.2%	36.9%
QPSK-1/2	0.0%	0.0%
QPSK-3/4	0.0%	0.0%
16 QAM-1/2	0.0%	0.0%
16 QAM-3/4	46.8%	63.1%

According to the system gain and interference rejection analysis the DL/UL MAP of the MIMO-A 2x1 system has the same system gain improvement and interference rejection analysis as the reference system. Consequently, the covered area of the two systems is the same. However, this system is able to achieve higher spectral efficiency due to improved interference rejection in the Traffic transmission.

1x3x3 Scheme

In the 1x3x3 frequency re-use scheme the limiting channel is the DL/UL MAP channel for the outdoor scenario but for the indoor scenario the DL Traffic is the limiting one. In Figure 48 and Figure 49 the SINR maps for the two scenarios are presented.

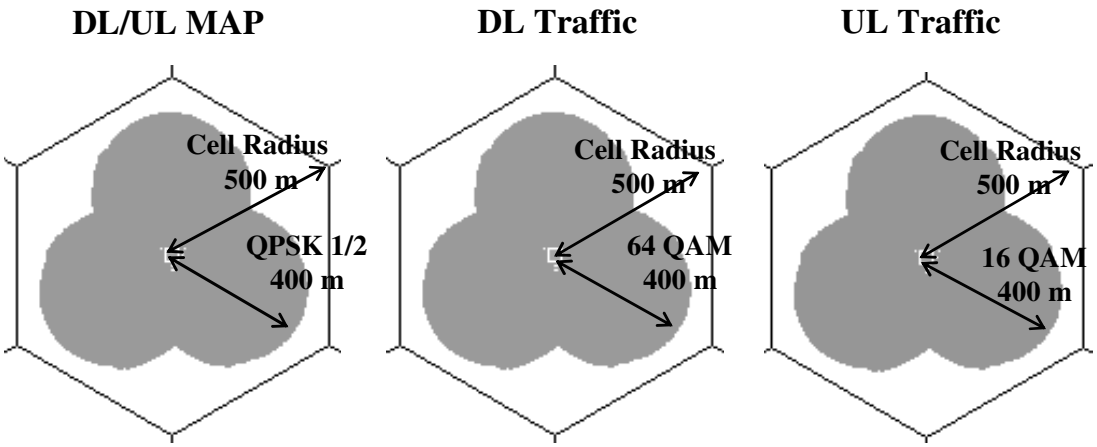

Figure 48: SINR Map for the Central BS – MIMO-A 2x1, PCMCIA, Indoor 1st Floor, 1x3x3 Scheme

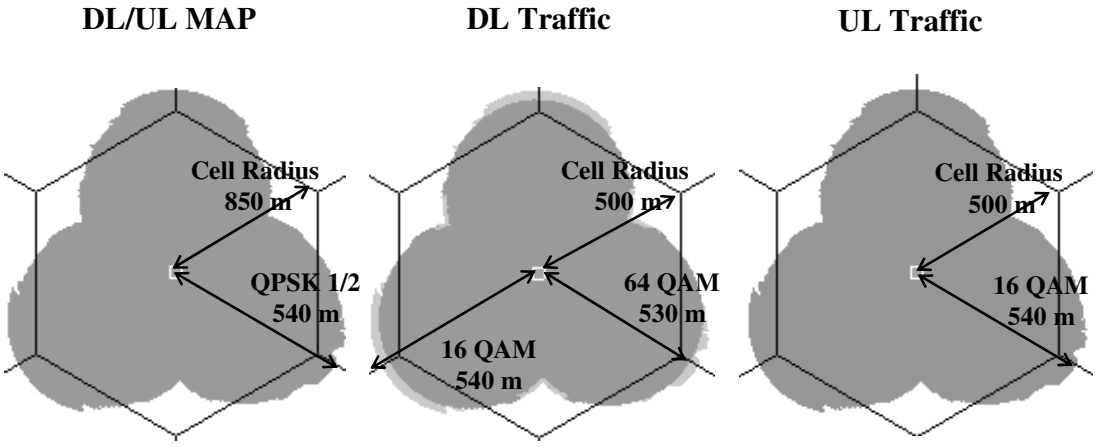

Figure 49: SINR Map for the Central BS – MIMO-A 2x1, PCMCIA, Street Level, 1x3x3 Scheme

The PHY mode regions percentages are presented in Table 43 and Table 44.

Table 43: PHY Mode Regions Percentages Over the Total Cell Area. For the DL Traffic Channel- MIMO-A 2x1, 1x3x3

PHY Mode	MIMO-A 2x1 1X3X3 DL	
	Indoor	Outdoor
No Coverage	40.7%	10.8%
QPSK-1/2	0.0%	0.0%
QPSK-3/4	0.0%	0.0%
16 QAM-1/2	0.0%	0.0%
16 QAM-3/4	0.0%	1.0%
64 QAM-2/3	5.3%	2.5%
64 QAM-3/4	54.0%	85.7%

Table 44: PHY Mode Regions Percentages Over the Total Cell Area. For the UL Traffic Channel- MIMO-A 2x1, 1x3x3

PHY Mode	MIMO-A 2x1 1X3X3 UL	
	Indoor	Outdoor
No Coverage	40.7%	10.8%
QPSK-1/2	0.0%	0.0%
QPSK-3/4	0.0%	0.0%
16 QAM-1/2	0.0%	0.0%
16 QAM-3/4	59.3%	89.2%

The comparison of the figures and the percentages tables for this system with the corresponding figures and tables for the two systems investigated before shows that the this system offers better link quality and spectral efficiency under the same conditions despite the fact that the MIMO 1x2 can cover greater percentage of the cell area.

Moreover, another advantage of that system in comparison to the MIMO 1x2 system is that implementation of multiple antennas at the BSs base stations is a more attractive technique especially in mobile networks where the TSs are limited from size and battery life.

MIMO-A 2x2 System

The MIMO-A 2x2 combines the advantages of the two AAS systems investigated before, while the signaling part of the DL sub-frame limits the SINR based coverage for this system for this scenario too.

1x3x1 Scheme

The SINR maps for the DL and UL sub-frame of the indoor and outdoor scenario are presented in Figure 50 and Figure 51.

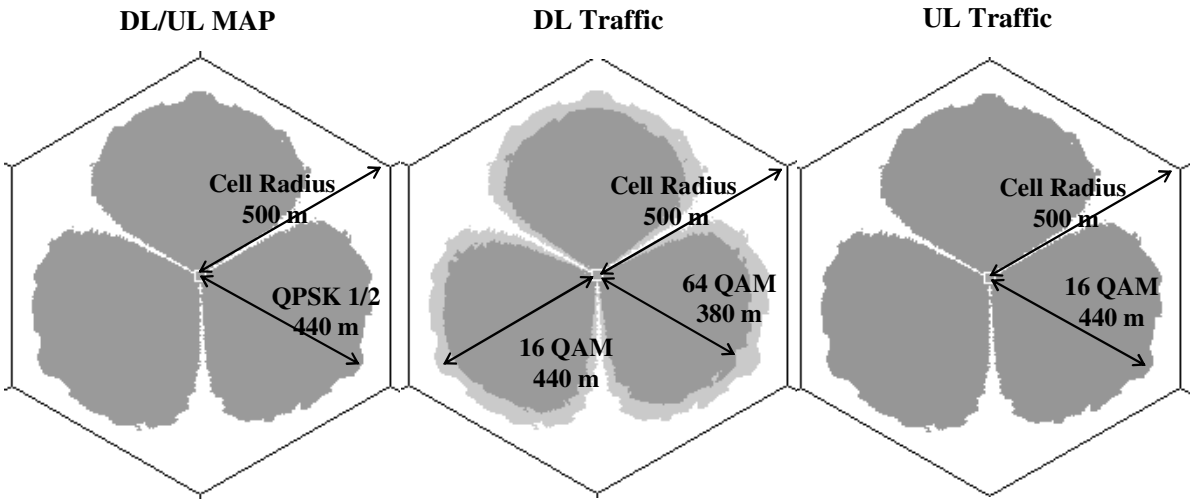

Figure 50: SINR Map for the Central BS – MIMO-A 2x2, PCMCIA, Indoor 1st Floor, 1x3x1 Scheme

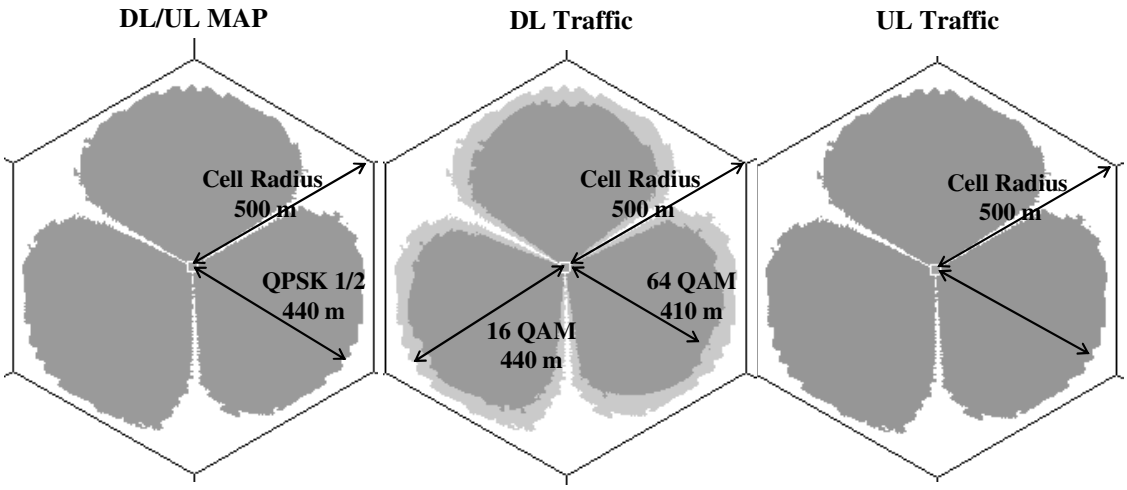

Figure 51: SINR Map for the Central BS – MIMO-A 2x2, PCMCIA, Street Level, 1x3x1 Scheme

The PHY mode regions percentages for the simulation results presented above are provided in Table 45 and Table 46.

Table 45: PHY Mode Regions Percentages Over the Total Cell Area. For the DL Traffic Channel- MIMO-A 2x2, 1x3x1

PHY Mode	MIMO-A 2x2 1X3X1 DL	
	Indoor	Outdoor
No Coverage	35.9%	26.3%
QPSK-1/2	0.0%	0.0%
QPSK-3/4	0.0%	0.0%
16 QAM-1/2	0.0%	0.0%
16 QAM-3/4	14.7%	17.1%
64 QAM-2/3	4.7%	5.5%
64 QAM-3/4	44.8%	51.2%

Table 46: PHY Mode Regions Percentages Over the Total Cell Area. For the UL Traffic Channel- MIMO-A 2x2, 1x3x1

PHY Mode	MIMO-A 2x2 1X3X1 UL	
	Indoor	Outdoor
No Coverage	35.9%	26.3%
QPSK-1/2	0.0%	0.0%
QPSK-3/4	0.0%	0.0%
16 QAM-1/2	0.8%	3.9%
16 QAM-3/4	63.3%	69.8%

The system gain of this system is improved in comparison to the MIMO 1x2. However, the fact that the interference rejection capability is the same for both systems, results in higher interference levels. For that reason the covered cell area is reduced for this system in comparison to the 1x2 system.

On the other hand the combination of higher system gain and interference rejection capability during the DL Traffic transmission results in high spectral efficiency for the 1x3x1 frequency re-use scheme, almost equivalent to the reference system when 1x3x3 scheme is applied.

1x3x3 Scheme

In Figure 52 and Figure 53 the SINR maps for the indoor and outdoor scenario in the 1x3x3 frequency re-use scheme are presented.

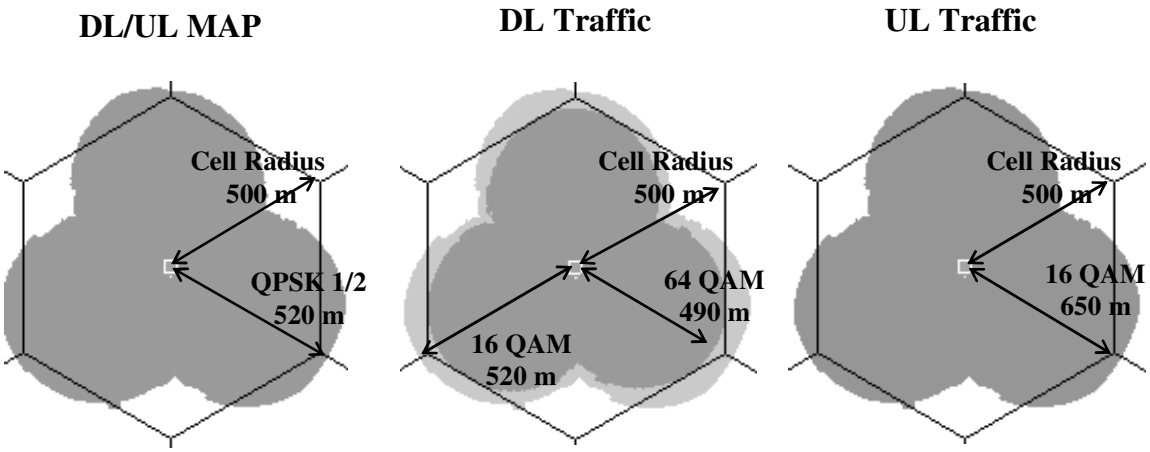

Figure 52: SINR Map for the Central BS – MIMO-A 2x2, PCMCIA, Indoor 1st Floor, 1x3x3 Scheme

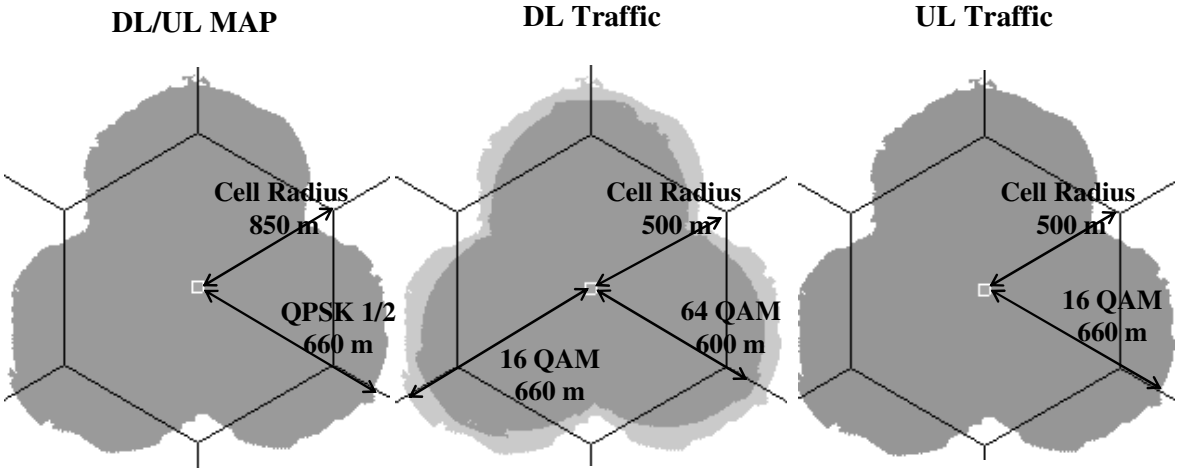

Figure 53: SINR Map for the Central BS – MIMO-A 2x2, PCMCIA, Street Level, 1x3x3 Scheme

The PHY mode regions percentages for the 1x3x3 frequency re-use scheme are presented in Table 47 and Table 48. As it can be seen, almost the entire cell area can be covered for the outdoor scenario, while the percentage of the uncovered area for the indoor scenario is significantly reduced. Moreover, the spectral efficiency of both scenarios is significantly improved, while for the outdoor scenario it is also maximized.

Table 47: PHY Mode Regions Percentages Over the Total Cell Area. For the DL Traffic Channel- MIMO-A 2x2, 1x3x3

PHY Mode	MIMO-A 2x2 1X3X3 DL	
	Indoor	Outdoor
No Coverage	12.4%	3.4%
QPSK-1/2	0	0.0%
QPSK-3/4	0.0%	0.0%
16 QAM-1/2	0.0%	0.0%
16 QAM-3/4	9.2%	3.4%
64 QAM-2/3	7.0%	1.8%
64 QAM-3/4	71.5%	91.4%

Table 48: PHY Mode Regions Percentages Over the Total Cell Area. For the UL Traffic Channel- MIMO-A 2x2, 1x3x3

PHY Mode	MIMO-A 2x2 1X3X3 UL	
	Indoor	Outdoor
No Coverage	12.4%	3.4%
QPSK-1/2	0.0%	0.0%
QPSK-3/4	0.0%	0.0%
16 QAM-1/2	0.0%	0.0%
16 QAM-3/4	87.6%	96.6%

MIMO-A 2x2 is the most advantageous system between the MIMO-A system that are investigated in this study. This can be evaluated through the simulation results too. Due to the enhanced system gain of this system and the significant interference rejection capability of it, the system can achieve high coverage range and also utilize the entire additional system gain provided to the WiMAX systems through the sub-channelization technique.

Beam-forming 8x2 System

Beam-forming 8x2 system combines beam-forming technique with receive diversity at the BS and TS respectively. According to simulation results the limiting channel for this system is the DL/UL MAP channel for both scenarios and frequency re-use schemes.

1x3x1 Scheme

The SINR maps for the DL and UL sub-frame of the indoor and outdoor scenario are presented in Figure 54 and Figure 55.

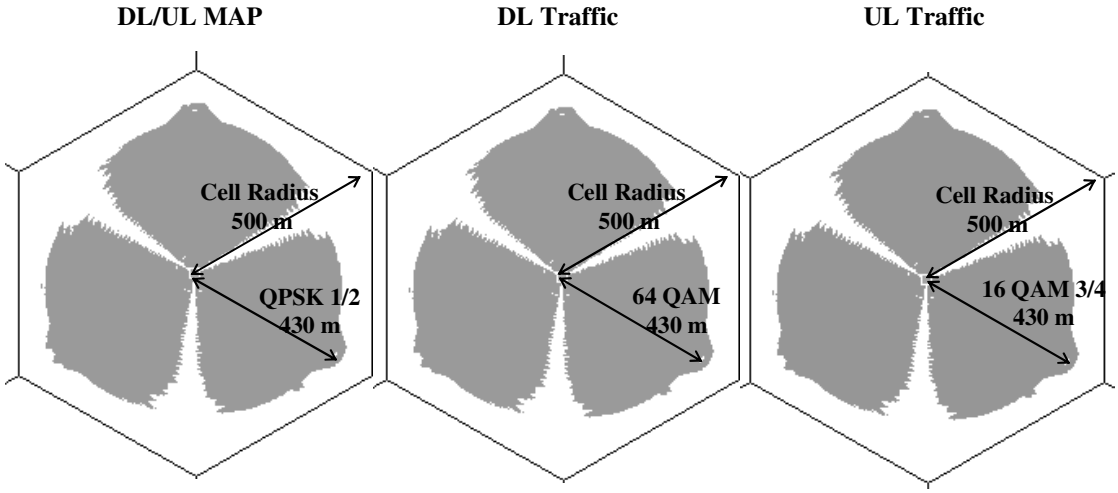

Figure 54: SINR Map for the Central BS – Beam-forming 8x2, PCMCIA, Indoor 1st Floor, 1x3x1 Scheme

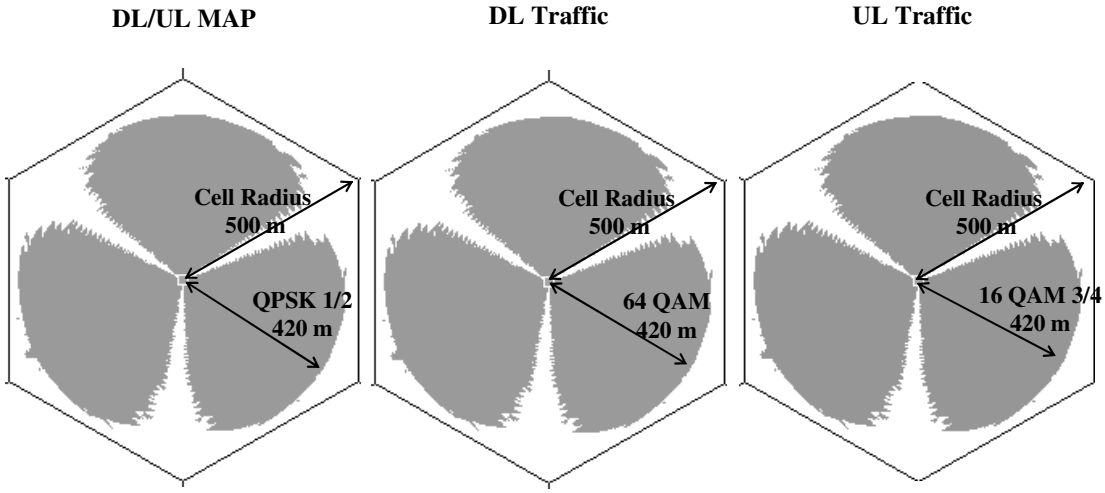

Figure 55: SINR Map for the Central BS – Beam-forming 8x2, PCMCIA, Street Level, 1x3x1 Scheme

The PHY mode regions percentages are presented in Table 49 and Table 50. Comparing the simulation results of this system with the MIMO-A 2x2 system in the 1x3x1 frequency re-use scheme, it can be seen that the uncovered area is larger for the BF 8x2 system. This is justified by the fact that in beam-forming systems the DL/UL MAP is transmitted without beam-forming, while the 120^{o} antennas implemented at the BSs provide less interference

rejection to the BS, in comparison to the more 60^{o} antennas of the MIMO-A systems. However, the high interference rejection capability during the DL and UL Traffic transmission, allows almost all the TSs to operate in the highest PHY mode.

Table 49: PHY Mode Regions Percentages Over the Total Cell Area. For the DL Traffic Channel- Beamforming 8x2, 1x3x1

PHY Mode	Beamforming 8x2 1X3X1 DL	
	Indoor	Outdoor
No Coverage	42.4%	32.0%
QPSK-1/2	0.0%	0.0%
QPSK-3/4	0.0%	0.0%
16 QAM-1/2	0.0%	0.0%
16 QAM-3/4	0.0%	0.0%
64 QAM-2/3	4.0%	7.4%
64 QAM-3/4	53.6%	60.6%

Table 50: PHY Mode Regions Percentages Over the Total Cell Area. For the UL Traffic Channel- Beamforming 8x2, 1x3x1

PHY Mode	Beamforming 8x2 1X3X1 UL	
	Indoor	Outdoor
No Coverage	42.4%	32.0%
QPSK-1/2	0.0%	0.0%
QPSK-3/4	0.0%	0.0%
16 QAM-1/2	0.0%	0.0%
16 QAM-3/4	57.6%	68.0%

1x3x3 Scheme

In Figure 56 and Figure 57the SINR maps for the indoor and outdoor scenario in the 1x3x3 frequency re-use scheme are presented.

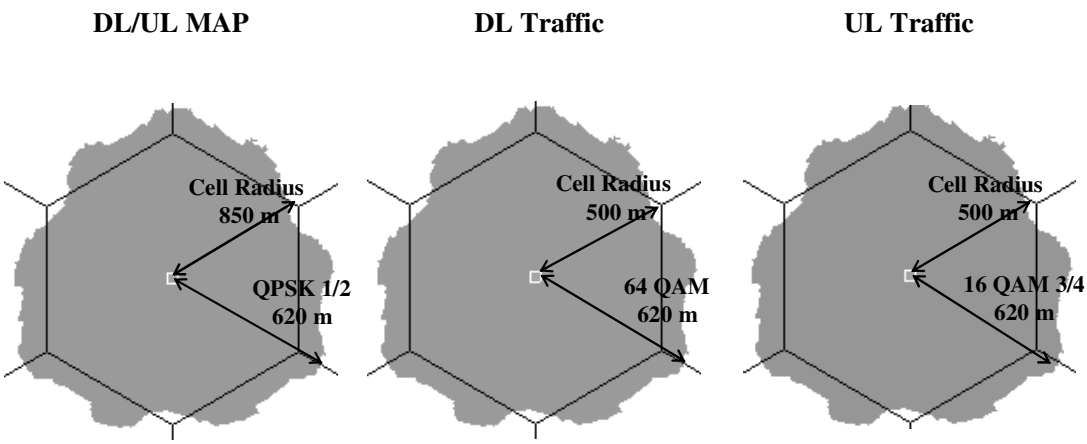

Figure 56: SINR Map for the Central BS – Beam-forming 8x2, PCMCIA, Indoor 1st Floor, 1x3x3 Scheme

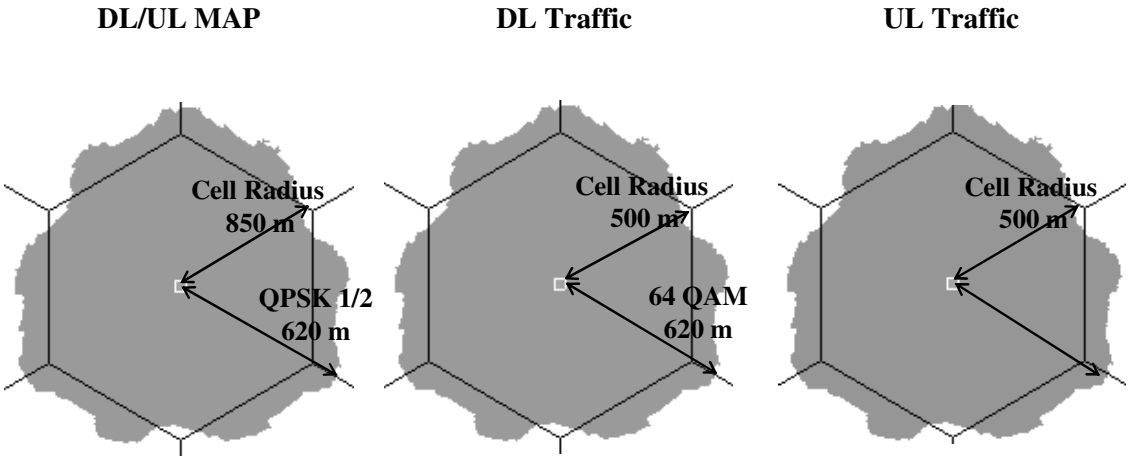

Figure 57: SINR Map for the Central BS – Beam-forming 8x2, PCMCIA, Street Level, 1x3x3 Scheme

The PHY mode regions percentages are presented in Table 51 and Table 52. As it can be seen, the entire cell area can be covered for both scenarios while the TSs operate in the highest PHY modes, resulting in high spectral efficiency.

Table 51: PHY Mode Regions Percentages over the Total Cell Area. For the DL Traffic Channel- Beamforming 8x2, 1x3x3

PHY Mode	Beamforming 8x2 1X3X3 DL	
	Indoor	Outdoor
No Coverage	4.2%	1.1%
QPSK-1/2	0.0%	0.0%
QPSK-3/4	0.0%	0.0%
16 QAM-1/2	0.0%	0.0%
16 QAM-3/4	0.0%	0.0%
64 QAM-2/3	0.0%	0.1%
64 QAM-3/4	95.8%	98.8%

Table 52: PHY Mode Regions Percentages over the Total Cell Area. For the UL Traffic Channel- Beamforming 8x2, 1x3x3

PHY Mode	Beamforming 8x2 1X3X3 UL	
	Indoor	Outdoor
No Coverage	4.2%	1.1%
QPSK-1/2	0.0%	0.0%
QPSK-3/4	0.0%	0.0%
16 QAM-1/2	0.0%	0.0%
16 QAM-3/4	95.8%	98.9%

7.Capacity Estimations

The challenge for modern real world WiMAX deployments is to increase the wireless network capacity, where an enormous increase in traffic is expected such as in the city center with limited available bandwidth and interference composing the most limiting factor for the whole system performance. This chapter focuses on the performance of each advanced antenna technique in means of capacity based on the simulation results.

Capacity Estimations

For the capacity estimation of each system, it is considered that the mobile stations are normally distributed inside the cell area; consequently, the coverage percentage of each PHY mode, P_{MCS}^{A}, depicts the percentage of users inside the cell that operate with the corresponding PHY mode. Those percentages can be utilized for the estimation of average sector throughput.

As it can be seen in the tables provided in the previous chapter, the "no coverage" area is also included in the percentages. Due to the fact that any subscriber positioned in this area will not be accommodated by the BS, this area has to be excluded. Conclusively, for the capacity estimation of the Tri-Sector cell, the percentages over the total cell area, P_{MCS}^{A}, are converted to percentages of the covered area, P_{MCS}^{C}:

$$P_{MCS}^{C} = \frac{P_{MCS}^{A}}{\sum_{i \in E} P_{i}^{A}}$$

,where E={QPSK ½, QPSK ¾, 16 QAM ½, 16 QAM ¾, 64 QAM $^{2}/_{3}$, 64 QAM ¾}.

Afterwards those percentages are utilized as weighted factors of the throughput performance per PHY mode. Once each weighted factor is multiplied by the average throughput per MCS, R_i for $i \in E$, the summation of those products provides the average BS throughput, R_{AVG}^{BS}:

$$R_{AVG}^{BS} = \sum_{i \in E} P_i^C * R_i$$

The average throughput of the tri-sector cell, R_{AVG}^{C}, arises by multiplying the R_{AVG}^{BS} by 3:

$$R_{AVG}^{C} = 3 * R_{AVG}^{BS}$$

Reference System

The resulting average BS and Tri-Sector Cell throughputs per direction for the Reference system are presented in Table 53 to Table 56.

Table 53: Tri – Sector Cell DL Throughput for Scenario A, Reference System 1x3x1

PHY Mode	Sector Data Rate (Mbps)	Reference 1x3x1 DL	
		Indoor	Outdoor
QPSK-1/2	1.584	0.00%	0.00%
QPSK-3/4	2.376	0.00%	0.00%
16 QAM-1/2	3.168	8.90%	9.20%
16 QAM-3/4	4.752	39.89%	37.65%
64 QAM-2/3	6.336	6.05%	5.86%
64 QAM-3/4	7.128	45.16%	47.30%
Average BS Throughput		5.780	5.823
Tri-Sector Cell Throughput		17.340	17.469

Table 54: Tri – Sector Cell UL Throughput for Scenario A, Reference System 1x3x1

PHY Mode	Sector Data Rate (Mbps)	Reference 1x3x1 UL	
		Indoor	Outdoor
QPSK-1/2	0.72	0.00%	0.00%
QPSK-3/4	1.08	0.00%	0.00%
16 QAM-1/2	1.44	0.42%	0.94%
16 QAM-3/4	2.16	99.58%	99.06%
Average BS Throughput		2.157	2.153
Tri-Sector Cell Throughput		6.471	6.460

Table 55: Tri – Sector Cell DL Throughput for Scenario A, Reference System 1x3x3

PHY Mode	Sector Data Rate (Mbps)	Reference 1x3x3 DL	
		Indoor	Outdoor
QPSK-1/2	1.584	0.00%	0.00%
QPSK-3/4	2.376	0.00%	0.00%
16 QAM-1/2	3.168	8.60%	2.90%
16 QAM-3/4	4.752	32.95%	27.09%
64 QAM-2/3	6.336	10.26%	5.64%
64 QAM-3/4	7.128	48.19%	64.36%
Average BS Throughput		5.923	6.325
Tri-Sector Cell Throughput		17.770	18.974

Table 56: Tri – Sector Cell UL Throughput for Scenario A, Reference System 1x3x3

PHY Mode	Sector Data Rate (Mbps)	Reference 1x3x3 UL	
		Indoor	Outdoor
QPSK-1/2	0.72	0.00%	0.00%
QPSK-3/4	1.08	0.00%	0.00%
16 QAM-1/2	1.44	2.60%	4.69%
16 QAM-3/4	2.16	97.40%	95.31%
Average BS Throughput		2.141	2.126
Tri-Sector Cell Throughput		6.424	6.379

As it can be seen the TDD capacity (DL and UL) of the reference system provided by a single BS does not exceed the 8.5 Mbps for the best scenario (outdoor street-level 1x3x3). In the case that 64 QAM modulation was also considered in the UL direction, the total capacity would be significantly increased. However, it is not supported by the WiMAX forum certified products that have been released by now.

MIMO-B 2x2

The performance of the MIMO-B 2x2 system is equivalent to that of a reference system in means of coverage and interference rejection but the spatial multiplexing offers the capability of doubling the throughput under good SINR conditions and with the precondition that the two available paths are completely uncorrelated. The average throughputs for the MIMO-B 2x2 system are presented in Table 57 to Table 60.

Table 57: Tri – Sector Cell DL Throughput for Scenario A, MIMO-B 2x2 1x3x1

PHY Mode	Sector Data Rate (Mbps)	MIMO-B 2x2 1x3x1 DL	
		Indoor	Outdoor
QPSK-1/2	3.17	16.31%	7.34%
QPSK-3/4	4.75	19.13%	16.62%
16 QAM-1/2	6.34	16.95%	17.44%
16 QAM-3/4	9.50	20.85%	24.25%
64 QAM-2/3	12.67	3.16%	3.77%
64 QAM-3/4	14.26	23.60%	30.58%
Average BS Throughput		8.247	9.270
Tri-Sector Cell Throughput		24.740	27.810

Table 58: Tri – Sector Cell UL Throughput for Scenario A, MIMO-B 2x2 1x3x1

PHY Mode	Sector Data Rate (Mbps)	MIMO-B 2x2 1x3x1 UL	
		Indoor	Outdoor
QPSK-1/2	1.44	1.15%	3.48%
QPSK-3/4	2.16	16.98%	13.86%
16 QAM-1/2	2.88	20.68%	17.05%
16 QAM-3/4	4.32	61.19%	65.62%
Average BS Throughput		3.622	3.675
Tri-Sector Cell Throughput		10.867	11.025

Table 59: Tri – Sector Cell DL Throughput for Scenario A, MIMO-B 2x2 1x3x3

PHY Mode	Sector Data Rate (Mbps)	MIMO-B 2x2 1x3x3 DL	
		Indoor	Outdoor
QPSK-1/2	3.17	7.26%	2.04%
QPSK-3/4	4.75	15.43%	4.33%
16 QAM-1/2	6.34	19.16%	6.82%
16 QAM-3/4	9.50	21.77%	24.22%
64 QAM-2/3	12.67	3.56%	5.04%
64 QAM-3/4	14.26	32.82%	57.54%
Average BS Throughput		9.376	11.847
Tri-Sector Cell Throughput		28.129	35.542

Table 60: Tri – Sector Cell UL Throughput for Scenario A, MIMO-B 2x2 1x3x3

PHY Mode	Sector Data Rate (Mbps)	MIMO-B 2x2 1x3x3 UL	
		Indoor	Outdoor
QPSK-1/2	1.44	0.00%	0.00%
QPSK-3/4	2.16	2.09%	1.41%
16 QAM-1/2	2.88	7.77%	3.30%
16 QAM-3/4	4.32	90.14%	95.30%
Average BS Throughput		4.163	4.242
Tri-Sector Cell Throughput		12.489	12.726

MIMO 1x2

The main advantage of MIMO-A 1x3 against the reference system, is the extended coverage that it can achieve and not the accomplishment of higher spectral efficiency. For that reason, there is not great differentiation between the average throughputs for the MIMO 1x2 system, presented in Table 61 to Table 64, and the reference system.

Table 61: Tri – Sector Cell DL Throughput for Scenario A, MIMO 1x2 1x3x1

PHY Mode	Sector Data Rate (Mbps)	MIMO 1x2 1X3X1 DL	
		Indoor	Outdoor
QPSK-1/2	1.584	0.00%	0.00%
QPSK-3/4	2.376	0.00%	0.00%
16 QAM-1/2	3.168	10.31%	7.28%
16 QAM-3/4	4.752	39.09%	35.74%
64 QAM-2/3	6.336	6.09%	5.65%
64 QAM-3/4	7.128	44.51%	51.33%
Average BS Throughput		5.743	5.946
Tri-Sector Cell Throughput		17.228	17.837

Table 62: Tri – Sector Cell UL Throughput for Scenario A, MIMO 1x2 1x3x1

PHY Mode	MIMO 1x2 1X3X1 UL		
	Sector Data Rate (Mbps)	Indoor	Outdoor
QPSK-1/2	0.72	0.00%	0.00%
QPSK-3/4	1.08	7.06%	0.00%
16 QAM-1/2	1.44	18.94%	9.80%
16 QAM-3/4	2.16	74.01%	90.20%
Average BS Throughput		1.947	2.089
Tri-Sector Cell Throughput		5.842	6.268

Table 63: Tri – Sector Cell DL Throughput for Scenario A, MIMO 1x2 1x3x3

PHY Mode	MIMO 1x2 1X3X3 DL		
	Sector Data Rate (Mbps)	Indoor	Outdoor
QPSK-1/2	1.584	0.00%	0.00%
QPSK-3/4	2.376	0.00%	0.00%
16 QAM-1/2	3.168	8.86%	1.52%
16 QAM-3/4	4.752	33.69%	15.64%
64 QAM-2/3	6.336	5.47%	7.10%
64 QAM-3/4	7.128	51.99%	75.75%
Average BS Throughput		5.933	6.640
Tri-Sector Cell Throughput		17.800	19.920

Table 64: Tri – Sector Cell UL Throughput for Scenario A, MIMO 1x2 1x3x3

PHY Mode	MIMO 1x2 1X3X3 UL		
	Sector Data Rate (Mbps)	Indoor	Outdoor
QPSK-1/2	0.72	0.00%	0.00%
QPSK-3/4	1.08	0.00%	0.00%
16 QAM-1/2	1.44	0.00%	0.00%
16 QAM-3/4	2.16	100.00%	100.00%
Average BS Throughput		2.160	2.160
Tri-Sector Cell Throughput		6.480	6.480

MIMO-A 2x1

According to the simulation results, the MIMO-A system is able to achieve higher spectral efficiency than that of the reference and the MIMO 1x2 system, especially in the 1x3x3 frequency re-use scheme. This can be verified in Table 65 to Table 68, where the average throughputs of the MIMO-A 2x1 system are presented.

Table 65: Tri – Sector Cell DL Throughput for Scenario A, MIMO-A 2x1 1x3x1

PHY Mode	MIMO-A 2x1 1X3X1 DL		
	Sector Data Rate (Mbps)	Indoor	Outdoor
QPSK-1/2	1.584	0.00%	0.00%
QPSK-3/4	2.376	0.00%	0.00%
16 QAM-1/2	3.168	0.00%	0.00%
16 QAM-3/4	4.752	11.45%	21.99%
64 QAM-2/3	6.336	9.64%	6.81%
64 QAM-3/4	7.128	78.91%	71.20%
Average BS Throughput		6.780	6.552
Tri-Sector Cell Throughput		20.339	19.655

Table 66: Tri – Sector Cell UL Throughput for Scenario A, MIMO-A 2x1 1x3x1

PHY Mode	MIMO-A 2x1 1X3X1 UL		
	Sector Data Rate (Mbps)	Indoor	Outdoor
QPSK-1/2	0.72	0.00%	0.00%
QPSK-3/4	1.08	0.00%	0.00%
16 QAM-1/2	1.44	0.00%	0.00%
16 QAM-3/4	2.16	100.00%	100.00%
Average BS Throughput		2.160	2.160
Tri-Sector Cell Throughput		6.480	6.480

Table 67: Tri – Sector Cell DL Throughput for Scenario A, MIMO-A 2x1 1x3x3

PHY Mode	Sector Data Rate (Mbps)	MIMO-A 2x1 1X3X3 DL	
		Indoor	Outdoor
QPSK-1/2	1.584	0.00%	0.00%
QPSK-3/4	2.376	0.00%	0.00%
16 QAM-1/2	3.168	0.00%	0.00%
16 QAM-3/4	4.752	0.00%	1.09%
64 QAM-2/3	6.336	8.94%	2.83%
64 QAM-3/4	7.128	91.06%	96.08%
Average BS Throughput		7.057	7.080
Tri-Sector Cell Throughput		21.171	21.239

Table 68: Tri – Sector Cell UL Throughput for Scenario A, MIMO-A 2x1 1x3x3

PHY Mode	Sector Data Rate (Mbps)	MIMO-A 2x1 1X3X3 UL	
		Indoor	Outdoor
QPSK-1/2	0.72	0.00%	0.00%
QPSK-3/4	1.08	0.00%	0.00%
16 QAM-1/2	1.44	0.00%	0.00%
16 QAM-3/4	2.16	100.00%	100.00%
Average BS Throughput		2.160	2.160
Tri-Sector Cell Throughput		6.480	6.480

MIMO-A 2x2

The higher system gain and interference rejection capability of the MIMO-A 2x2, allows the TSs of this system to operate in high PHY modes. As a result the average throughputs of this system are significantly higher than the corresponding throughputs of the other MIMO-A system investigated in this study. As it can be seen in Table 69 to Table 72, where the average BS and tri-sector cells throughputs for the MIMO-A 2x2 system are presented, the throughput of the system is almost maximized in both scenarios and frequency schemes in the UL direction, while the same observation can be made for the DL direction of the 1x3x3 frequency re-use scheme.

Table 69: Tri – Sector Cell DL Throughput for Scenario A, MIMO-A 2x2 1x3x1

PHY Mode	Sector Data Rate (Mbps)	MIMO-A 2x2 1X3X1 DL	
		Indoor	Outdoor
QPSK-1/2	1.584	0.00%	0.00%
QPSK-3/4	2.376	0.00%	0.00%
16 QAM-1/2	3.168	0.00%	0.00%
16 QAM-3/4	4.752	22.91%	23.16%
64 QAM-2/3	6.336	7.27%	7.45%
64 QAM-3/4	7.128	69.82%	69.39%
Average BS Throughput		6.526	6.519
Tri-Sector Cell Throughput		19.578	19.556

Table 70: Tri – Sector Cell UL Throughput for Scenario A, MIMO-A 2x2 1x3x1

PHY Mode	Sector Data Rate (Mbps)	MIMO-A 2x2 1X3X1 UL	
		Indoor	Outdoor
QPSK-1/2	0.72	0.00%	0.00%
QPSK-3/4	1.08	0.00%	0.00%
16 QAM-1/2	1.44	1.28%	5.29%
16 QAM-3/4	2.16	98.72%	94.71%
Average BS Throughput		2.151	2.122
Tri-Sector Cell Throughput		6.452	6.366

Table 71: Tri – Sector Cell DL Throughput for Scenario A, MIMO-A 2x2 1x3x3

PHY Mode	Sector Data Rate (Mbps)	MIMO-A 2x2 1X3x3 DL	
		Indoor	Outdoor
QPSK-1/2	1.584	10.45%	0.00%
QPSK-3/4	2.376	0.00%	0.00%
16 QAM-1/2	3.168	0.00%	0.00%
16 QAM-3/4	4.752	10.45%	3.52%
64 QAM-2/3	6.336	7.99%	1.88%
64 QAM-3/4	7.128	81.57%	94.59%
Average BS Throughput		6.982	7.029
Tri-Sector Cell Throughput		20.946	21.088

Table 72: Tri – Sector Cell UL Throughput for Scenario A, MIMO-A 2x2 1x3x3

PHY Mode	Sector Data Rate (Mbps)	MIMO-A 2x2 1X3X3 UL	
		Indoor	Outdoor
QPSK-1/2	0.72	0.00%	0.00%
QPSK-3/4	1.08	0.00%	0.00%
16 QAM-1/2	1.44	0.00%	0.00%
16 QAM-3/4	2.16	100.00%	100.00%
Average BS Throughput		2.160	2.160
Tri-Sector Cell Throughput		6.480	6.480

Beam-forming 8x2

The average BS and tri-sector cell throughputs based on the simulation results for the indoor 1st floor and the outdoor street-level scenario are presented in Table 73 to Table 76. As it can be seen the average throughput is almost maximized even for the 1x3x1 frequency re-use scheme in both scenarios.

Table 73: Tri – Sector Cell DL Throughput for Scenario A, Beam-forming 8x2 1x3x1

PHY Mode	Sector Data Rate (Mbps)	Beamforming 8x2 1X3X1 DL	
		Indoor	Outdoor
QPSK-1/2	1.584	0.00%	0.00%
QPSK-3/4	2.376	0.00%	0.00%
16 QAM-1/2	3.168	0.00%	0.00%
16 QAM-3/4	4.752	0.00%	0.00%
64 QAM-2/3	6.336	7.02%	10.86%
64 QAM-3/4	7.128	92.98%	89.14%
Average BS Throughput		7.072	7.042
Tri-Sector Cell Throughput		21.217	21.126

Table 74: Tri – Sector Cell UL Throughput for Scenario A, Beam-forming 8x2 1x3x1

PHY Mode	Sector Data Rate (Mbps)	Beamforming 8x2 1X3X1 UL	
		Indoor	Outdoor
QPSK-1/2	0.72	0.00%	0.00%
QPSK-3/4	1.08	0.00%	0.00%
16 QAM-1/2	1.44	0.00%	0.00%
16 QAM-3/4	2.16	100.00%	100.00%
Average BS Throughput		2.160	2.160
Tri-Sector Cell Throughput		6.480	6.480

Table 75: Tri – Sector Cell DL Throughput for Scenario A, Beam-forming 8x2 1x3x3

PHY Mode	Sector Data Rate (Mbps)	Beamforming 8x2 1X3X3 DL	
		Indoor	Outdoor
QPSK-1/2	1.584	0.00%	0.00%
QPSK-3/4	2.376	0.00%	0.00%
16 QAM-1/2	3.168	0.00%	0.00%
16 QAM-3/4	4.752	0.00%	0.00%
64 QAM-2/3	6.336	0.00%	0.10%
64 QAM-3/4	7.128	100.00%	99.90%
Average BS Throughput		7.128	7.127
Tri-Sector Cell Throughput		21.384	21.382

Table 76: Tri – Sector Cell UL Throughput for Scenario A, Beam-forming 8x2 1x3x3

PHY Mode	Sector Data Rate (Mbps)	Beamforming 8x2 1X3X3 UL	
		Indoor	Outdoor
QPSK-1/2	0.72	0.00%	0.00%
QPSK-3/4	1.08	0.00%	0.00%
16 QAM-1/2	1.44	0.00%	0.00%
16 QAM-3/4	2.16	100.00%	100.00%
Average BS Throughput		2.160	2.160
Tri-Sector Cell Throughput		6.480	6.480

8.Conclusions

The impact of the Advanced Antenna Systems on the performance of wireless networks was investigated in this study. The most important AAS techniques and algorithms were analyzed in a theoretical basis, with utilization of bibliographical resources and product specifications. The analysis was mainly focused on the AAS proposed by the IEEE 802.16e, widely known as WiMAX.

Based on the features of WiMAX, the MIMO Matrix A, B and Beam-forming systems were considered. Scope of this investigation was to perform a comparative analysis between those systems and at the same time to compare the performance of each one of them with the performance of a SISO system.

In specific, the systems considered in this study were: MIMO 1x2, MIMO-A 2x1, MIMO-A 2x2, MIMO-B 2x2 and Beamforming 8x1. Based on the technique implemented on each one of the systems, specific system gain improvements are achieved. Another significant characteristic of the AAS techniques and algorithms is that they can provide significant interference rejection to the system. The analysis on the impact of each technique to the received signal strength of the wanted and the interfering signals resulted in specific interference rejection capabilities for each system.

The resultant system gain and interference rejection improvements were utilized in order to investigate the performance of each system through simulations with the ICS Telecom nG radio planning tool, in an urban environment with tight frequency re-use schemes.

The simulation results indicated that the most important characteristic of the techniques investigated in this study is the improved interference rejection, which results in high link quality and spectral efficiency. In specific the following observations were made:

- The covered area of the MIMO-A 2x1 is equivalent to that of the reference system as long as both of these systems have the same system gain and interference rejection. However the MIMO-A 2x1 system achieves higher spectral efficiency than that achieved by the reference system due to higher interference rejection capability during the DL and UL Traffic transmission.

- The MIMO-A 2x2 provides better coverage and spectral efficiency in comparison to the MIMO-A 2x1. Moreover, in the extreme case where only one frequency channel is available, this system can cover higher percentage of the cell area than the Beam-forming 8x2 system.

- The Beam-forming 8x2 system provides the highest spectral efficiency between the systems which were simulated. Regarding the area that can be covered, the high system gain provides extended coverage in comparison to the other systems, with the exception of the MIMO-A 2x2 system for the 1x3x1 frequency re-use scheme.

References:

[1] IEEE. Standard 802.16-2004. Part16: Air interface for fixed broadband wireless access systems. October 2004.

[2] IEEE. Standard 802.16e-2005. Part16: Air interface for fixed and mobile broadband wireless access systems—Amendment for physical and medium access control layers for combined fixed and mobile operation in licensed band. December 2005.

[3] Jeffrey G. Andrews, Arunabha Ghosh and Rias Muhamed. Fundamentals of WiMAX-Understanding Broadband Wireless Networking. Prentice Hall, 2007.

[4] David Tse and Pramod Viswanath. Fundamentals of Wireless Communication. Cambridge University Press, September 2004.

[5] Intel.Scalable OFDMA Physical Layer in IEEE 802.16 WirelessMAN. Intel Technology Journal, August 2004.

[6] WiMAX Forum. Fixed, nomadic, portable and mobile applications for 802.16-2004 and 802.16e WiMAX networks. White Paper, November 2005.

[7] WiMAX Forum. Mobile WiMAX – Part I:A Technical Overview and Performance Evaluation. White Paper, April 2006.

[8] WiMAX Forum. WiMAX's technology for LOS and NLOS environments. White Paper.

[9] Redline Communications, Technical Advisory-Link Budget Analysis. Redline, April 2007.

[10] Raviraj Adve. Smart Antennas, January 2007. http://www.comm.utoronto.ca

[11] WiMAX Forum. A Comparative Analysis of Mobile WiMAX™ Deployment Alternatives in the Access Network.White Paper, May 2007

[12] Airspan. Multiple Antenna Systems in WiMAX. White Paper, 2007.

[13] Sophocles J.Orfanidis. Electromagnetic Waves and Antennas.Rutgers University, February,2008. www.ece.rutgers.edu/~orfanidi/ewa

[14] Cisco-Navini. WiMAX RF Planning Guide. Navini, September 2007.

[15] Frank Gross. Smart Antennas for Wireless Communications. Mc-Graw Hill,2005.

[16] Ta-Sung Lee. MIMO Techniques for Wireless Communications. National Chiao Tung University.

[17] Yi Hong and Zhao Yang Dong. Performance Analysis of Space-Time Trellis Coded OFDM System. International Journal of Applied Mathematics and Computer.

[18] Zhuo Chen, B. Vucetic and Jinhong Yuan. Space-time trellis codes with transmit antenna selection. Electronic Letters, May 2003

[19]

[20] Markus Rupp and Christoph F. Mecklenbrauker. On Extended Alamouti Schemes for SpaceTime Coding. International Symposium on Wireless Personal Multimedia Communications, October 2002.

[21] Rohde & Schwarz. Introduction to MIMO Systems. Rohde & Schwarz, June 2006.

[22] Armin Dammann, Ronald Raulefs and Gunther Auer, Gerhard Bauch. Comparison of Space-Time Block Coding and Cyclic Delay Diversity for a Broadband Mobile Radio Air Interface.

[23] Amin Shokrollahi. LDPC Codes: An Introduction. Digital Fountain, Inc., April 2003.

[24] Olav Tirkkonen and Ari Hottinen. Improved MIMO Performance with Non-Orthogonal Space-Time Block Codes. Nokia Research Center, November 2001.

[25] Mohinder Jankiraman. Space-Time Codes and MIMO Systems. Artech House, 2004.

[26] J P. Burke, J R. Zeidler and B D. Rao. CINR difference analysis of optimal combining versus maximal ratio combining. Univesity of California,2005.

[27] Ranjan K. Mallik. Effect of Channel Correlation on the Performance of Diversity Receivers. Indian Institute of Technology – Delhi.

[28] Motorola. A Practical Guide to WiMAX Antennas: MIMO and Beamforming Technical Overview. White Paper ,2007.

[29] Konstantinos Ntagkounakis, Bayan Sharif and Panagiotis Dallas. Novel Channel and Polarization Assignment Schemes for 2–11 GHz Fixed–Broadband Wireless Access Networks. Wireless Personal Communications, December 2005.

[30] E. Biglieri, A. Goldsmith, B. Muquet and H. Sari. Diversity, Interference Cancellation and Spatial Multiplexing in MIMO Mobile WiMAX Systems.

[31] Mai Tran, Angela Doufexi and Andrew Nix. Mobile WiMAX MIMO Performance Analysis: Downlink and Uplink. University of Bristol, 2008.

[32] Cisco-Navini. Delivering personal broadband. Navini, July 2007.

[33] IEEE 802.16 Broadband Wireless Access Working Group.Channel Models for Fixed Wireless Applications. IEEE, July 2001.

[34] WiMAX Forum. WiMAX Deployment Considerations for Fixed Wireless Access in the 2.5 GHz and 3.5 GHz Licensed Bands. White Paper, June 2005.

[35] João Pedro Eira, António J. Rodrigues. Analysis of WiMAX data rate performance. Technical University of Lisbon, February 2009.